THE INTEGRATED MANUAL AND AUTOMATIC CONTROL OF COMPLEX FLIGHT SYSTEMS

Semi-Annual Status Report

July 1984 - March 1985

Principal Investigator: Dr. David K. Schmidt
School of Aeronautics & Astronautics
Purdue University
West Lafayette, IN 47907

NASA Technical Officer: Mr. Donald T. Berry
Vehicle Dynamics and Control Division
Ames Research Center
Dryden Flight Research Facility
P.O. Box 273
Edwards, CA 93523

Grant No. NAG4-1

April 12, 1985

Table of Contents

INTRODUCTION

This constitutes a status report on the research being performed by Purdue University's School of Aeronautics and Astronautics for NASA Ames/Dryden, under grant number NAG4-1. The topics of research in this program include pilot/vehicle analysis techniques, identification of pilot dynamics, and control synthesis techniques for optimizing aircraft handling qualities. The project activities for the period of July 1, 1984 through March 31, 1985, will be discussed herein.

PUBLICATIONS RELATED TO GRANT ACTIVITIES

The following paper was presented at the 1984 AIAA Guidance and Control Conference, held in Seattle, WA, in August 1984.

> Biegad, D. and Schmidt, D. K., "Time Series Modeling of Human Operator Dynamics in Manual Control Tasks."

Recently, notification was received that this paper was also accepted for publication in the Journal of Guidance, Control, and Dynamics later in this year (1985).

An abstract for a paper entitled

> "Closed-Loop Pilot/Vehicle Analysis of the Approach and Landing Task"

was authored by Mr. Mark Anderson and the grant principle investigator and was submitted for possible presentation at the 1985 AIAA Guidance and Control Conference, to be held in August 1985. Notification of acceptance of this paper is expected shortly. A copy of the extended abstract was previously forwarded to the technical monitor (Mr. D. T. Berry, DFRF), and a copy is attached as an appendix to this report.

CURRENT TECHNICAL ACTIVITY

During the current project period, an analysis has been underway of the flight-test results obtained recently (1984) by CALSPAN on "Pitch-Rate Flight Control Systems in the Flared Landing Task," (Ref. 1), obtained with the Total In-Flight Simulator (TIFS). The analysis approach considered here is based on the Optimal Control/Frequency Domain (OC/FD) techniques developed under this grant at Purdue. These techniques originally stem from an optimal-control approach to perform a Neal-Smith-like analysis on aircraft attitude dynamics, (see Ref. 2), but have recently been extended and used successfully to analyse the flared landing task. This extended analysis method will be reported in the (1985 Guidance and Control Conference) paper to be presented this year, as cited above, and is further documented in Ref. 3.

Attitude Analysis

An additional modification of the method of Ref. 2 provided a technique independent of one of the parameters that previously had to be emperically adjusted (namely, closed-loop "droop"). The results from this revised analysis of the Neal-Smith data base are shown in Figure 1. The sensitivity parameter (SP) is defined as

$$SP = (\text{Droop, dB}) \times [\Delta(\theta/\theta c)\max/\Delta\text{DC Gain, dB}]$$

or the "droop" in the closed-loop frequency response obtain from the OC/FD analysis, multiplied by the change in closed-loop resonance peak per unit change in (pilot) DC gain. This (SP) parameter has the same interpretation as the original "Resonace Peak," in terms of oscillatory tendency, but it also reflects the sensitivity of the closed-loop dynamics to slight

variations in pilot aggressiveness. Finally, as mentioned above, it does not require a priori selection of any parameters like the allowable droop or closed-loop bandwidth. The total pilot phase compensation (see Fig. 1) includes the effects of 0.2 sec. observation time delay and 0.1 sec. neurometer lag of the pilot.

Next, an analysis of the LAHOS data base, using this method, was performed to determine if any coorelation existed between those quantities (SP and Phase, dependent only on vehicle attitude dynamics) and the pilot ratings of the aircraft in the landing task. Since T_{θ_2} is constant in this data base, the flight-path response is determined uniquely by the aircraft attitude dynamics. The results from this analysis are given in Figure 2. Notice that these results group nicely into Level 1, 2, and 3 regions, with the same general "shape" of the boundaries as shown in Fig. 1. The primary difference between the Neal-Smith results (Fig. 1) and the LAHOS results (Fig. 2) is the increase in required, and acceptable, pilot phase compensation in this landing task (Fig. 2). This is consistent with the aircraft dynamics being more sluggish at the lower (landing) speed, and perhaps implies pilot acceptance of higher workload (phase) being required for landing. That is, configurations rated Level 1 in the landing task (Fig. 2) would have received Level 2 ratings in the precision attitude control task evaluated by Neal and Smith (Fig. 1). Put still another way, Level 2 attitude dynamics here (in this data base) may be sufficient to obtain a Level 1 rating in the landing task.

An analysis of the attitude dynamics of some of the TIFS "Pitch-Rate" configurations yields the results summarized in Table 1. Listed are the ratings from the two pilots, closed-loop $\theta/\theta c$ bandwidth, pilot phase

compensation (2 values) and sensitivity parameter SP. Note that all closed-loop bandwidths are very close (2.7 - 2.9 rad/sec), and are lower than the bandwidths for configurations rated Level 1 in the LAHOS data base (shown in Fig. 3, corresponding to the results in Fig. 2). The lower bandwidths are consistent with the TIFS configurations representing larger aircraft.

The two values for pilot phase compensations reflect the phase at the closed-loop bandwidth frequency, and the peak phase compensation, which occurred for these cases at 4.0 - 4.5 rad/sec. A plot of pilot-model frequency response is shown in Fig. 4, for Config. 7-1, for example. This configuration reflected "conventional" aircraft dynamics. The open- and closed-loop frequency responses and pilot-model compensation for these configurations and for this (θ-tracking) task are given in Appendix B.

Note that for Config. 1-1 to 1-3, the SP, pilot phase, and bandwidth are essentially constant. This is consistent with the fact that although T_{θ_2} is being varied in these configurations, the attitude dynamics are invariant with T_{θ_2}. This is a result of high-gain feedback action (e.g., rate command systems) yielding dynamics that are insensitive to variations in plant parameters (i.e., T_{θ_2}). Note that all three of these configurations were rated consistently poorly, with Pilot B's ratings all between 5.5 - 7.0 Cooper-Harper.

In contrast, Config. 7-1 received a solid Level 1 rating (3. and 2.5, Cooper-Harper). Note that for this configuration, the pilot phase compensation is 15 degrees less than for Config. 1-1 to 1-3, although the sensitivity parameter is higher.

Finally, consider Config. 4-1 to 4-3 and Config. 4-3-1. Config. 4-1 to 4-3 dynamics are the same as Config. 1-1 to 1-3, except a prefilter has been added, which restores the attitude dependence on T_{θ_2}. Consequently, we see a monotonic increase in the pilot phase compensation as T_{θ_2} is decreased. This is to be expected since as $1/T_{\theta_2}$ gets larger, the aircraft-attitude frequency response exhibits less lead below the short-period frequency. Although the ratings show some variation for Config. 4-1, and only one rating was obtained for 4-3, it is clear that 4-2 was rated better than 4-1 or 4-3, and was rated comparable to 7-1. When comparing pilot phase and SP between Config. 4-2 and 7-1, one sees they are very close. Finally, it is possible that Config. 4-3 was rated worse than 4-2 because of the increased phase lead required, but this will be re-examined below.

Regarding Config. 4-3-1 (4-3 plus a wash-out), it is noted that it was rated worse than Config. 4-2, but better than Config. 4-3. Note that both the SP and pilot phase for 4-3-1 are between the respective values for 4-2 and 4-3 consistent with the rating.

Flight-Path Analysis

The above analysis was aimed at exploring correlation between ratings of the configurations in the landing task and the important measures of (closed-loop) attitude dynamics. It is clear that for precise flare and landing, precision flight path control is required and this will now be considered.

In VFR landings, attitude, n_z, and sink rate (γ) information is available to the pilot. Consequently, a multi-loop analysis is considered essential. Such an analysis is in fact developed in Ref. 3, cited previously, based on an analysis of the LAHOS data base. However, care is required in the analysis of the TIFS "Pitch-Rate" results because there are several difference between the two experiments that may be significant. The differences and/or key issues are

1. Cockpit location/pilot's objective
2. n_z transfer function numerators (dynamics)
3. Variable T_{θ_2}
4. $T_{\theta_2} - T_q$ prefilter
5. Time delay
6. Wash out filter

In the LAHOS experiment, the cockpit, aircraft c.g., and center of rotation (percussion) were very closely located along the longitudinal axis. The aircraft had conventional aircraft dynamics, plus leads and lags, T_{θ_2} was constant, and there was essentially no additional time delay. Finally, the two real (airframe) zeros (one + and one -) in the n_z/F_s transfer functions are large in magnitude (10-20 1/sec). In the TIFS Pitch-Rate experiment, none of the above was true.

As a result of the dynamics and geometry in the LAHOS experiment, the pilot could fly as aggressively as possible, constrained by stability of the closed-loop ($\gamma/\gamma c$) system and his limitations. Equivalent pilot phase compensation in this loop, after performing block diagram reduction of the

multi-loop system, correlated strongly with pilot ratings. In addition, the deviation from the desired -20dB/decade characteristic of the pilot/vehicle open-loop Bode magnitude, expressed in terms of an "open-loop peak" was used to indicate loop "quality," or desirability. Again, only two closed-loop parameters (phase and "peak") were necessary to evaluate the LAHOS configurations. Those results are shown in Figure 5.

Analysis 1

In any event, the results from the same analysis procedure, applied to some of the TIFS "pitch-rate" results are given in Table 2. The equivalent phase compensation is the phase of $P_{eq}(j\omega)$, evaluated at open-loop ($\gamma/\gamma_\varepsilon$) phase crossover. P_{eq} is obtained from block diagram reduction, as shown in Fig. 6, where P_θ, P_γ, and $P_\varepsilon(s)$ are all obtained from the optimal-control modeling of the human operator - as in the analysis summarized in Fig. 5 above.

Unlike the results from the attitude analysis, the closed-loop bandwidths in this flight-path analysis now increase with increasing $1/T_{\theta_2}$, both with and without the prefilter (i.e., Config. 1-1 to 1-3 and Config. 4-1 to 4-3). These bandwidths are only slightly lower than those from the LAHOS analysis (not given here).

Also unlike the attitude analysis results, a monotonic reduction in pilot phase compensation is noted for Config. 1-1 to 1-3, or as T_{θ_2} is reduced. For these three rate-command configurations, although the attitude response is independent of T_{θ_2}, the flight path response is not. Clearly, the flight path response is "quickened" for these configurations (1-1 to 1-3) as $1/T_{\theta_2}$ increases, so required pilot phase lead

diminishes. In addition, the open-loop peak has the same trend, decreasing as $1/T_{\theta_2}$ increases. Hence the flight-path closed-loop dynamics are improving, along with a reduction in workload (phase lead).

A different situation arises with Config. 4-1 to 4-3. Now note that for these configurations, the flight-path (γ/F_{st}) response is independent of T_{θ_2} (while it is the attitude response that has this property for Config. 1-1 to 1-3). Therefore, a single-loop analysis would not be sensitive to T_{θ_2} variations. But in this multi-loop analysis, the results in Table 2 reveal increased pilot phase is again required as $1/T_{\theta_2}$ increases. This is related to the attitude response exhibiting less lead as $1/T_{\theta_2}$ decreases. Note that the ratings, however, do not follow this same monotonic trend.

But an opposite trend is noted in the open-loop-peak parameter. That is, as $1/T_{\theta_2}$ increases this peak decreases, or stability robustness of the loop improves. It is possible an "optimum" exists, or a trade between pilot phase versus open-loop peak, somewhat consistent with the LAHOS results in Fig. 5, except that the open-loop peaks in the (TIFS) data are too high to be compatible with Fig. 5. This open-loop peak can be shown to depend strongly on the numerators in the n_z/F transfer function. Because these two real (+ and -) numerators for the large vehicles simulated on the TIFS are smaller in magnitude than for LAHOS (1.5-3.0 1/sec compared to 10.-20. 1/sec for LAHOS), higher open loop peaks result here. Although these (open-loop peak) results cannot be compared directly between experiments, the trends appear consistent, however.

This consistency is further reinforced when Config. 4-3-1 (4-3 plus wash out) and 7-1 (conventional) are considered. Config. 4-3-1 requires less phase compensation than 4-3 (33° versus 37°), and exhibits a lower open-loop peak. The improved rating on 4-3-1, therefore, appears warrented on the basis of these results, along with the attitude analysis discussed previously. Finally, the solid Level 1 rating of Config. 7-1 is also compatible with the pilot phase and open-loop peak associated with this configuration.

The final topic of discussion regarding the results in Table 2 is the important effect the time delay of 170 ms has on these results. Given in the table are the results from the analysis both with and without the delay. Without the delay, the required pilot phase is much lower, and are not compatible at all with the LAHOS results in Fig. 5. The phases in Table 2 in this case are far too low. However, with the time delay included, the pilot phase and the ratings are much more consistent with those obtained for LAHOS. For the remainder of the discussion, the time delay is included in the analysis.

Analysis 2

Although the above analysis is sensitive to five of the six key experimental variables cited at the outset (time delay, T_{θ_2}, prefilters, etc.), it is not sensitive to the pilot location relative to the c.g. or to the center of rotation (c.r.). This area has been a primary focus in this study for the current project period.

The location of the pilot is considered to affect two key aspects of closed-loop flight-path control. If the pilot is far removed from the c.g. and the c.r., his acceleration cues (n_z) are significantly altered.

Also, if the pilot is remote from the c.g. and c.r., the appropriate control objective may need further definition. (Note: this problem does not arise in the attitude control task, in which the vehicle attitude perceived is independent of pilot location, as long as the pilot is located on the longitudinal axis.)

With the optimal-control modeling technique, both the pilot objective and available cues may be evaluated analytically through adjustments in the objective function (J_p) and in the selection of system responses in the vector of pilot observations (y_p). In all the analysis performed on the precision control of flight path (LAHOS and this analysis), the pilot is considered to be observing attitude, sink rate (or γ), and the flight path error ($\gamma - \gamma_{command}$) reflected at the cockpit, in addition to the rate of change of these variables, consistent with the assumption that the pilot derives rate information from the observed angles (e.g., $\dot{\theta}$ from θ observation).

We will now consider the results from an analysis based on the assumption that fundamentally, the pilot must be able to control the flight path, and perhaps more importantly the path rate (proportioned to n_z) that he senses at the cockpit. His ability to do this is analyzed by modeling the situation as precision control of flight path at the cockpit, defined by

$$\dot{\gamma}_{c.p.} = V_o n_z \Big|_{c.p.}$$

With this modeling assumption, the relevant dynamics, pilot observations and control objective (cost function) are now defined.

The open- and closed-loop ($\gamma_{c.p.}/\gamma_{com}$) frequency responses from this analysis approach are shown in Figs. 7-14. These figures are shown rather than one point tabulated (e.g., open-loop peak) from the plot, to reveal the dramatic differences in both the open- and closed-loop Bode plots. As $1/T_{\theta_2}$ increases, both for Config. 1-1 to 1-3 and for Config. 4-1 to 4-3, the closed-loop, as well as the open-loop frequency responses clearly reveal improved closed-loop dynamics. The closed-loop magnitude, recall, should be "flat" for perfect tracking performance in this case, and the open-loop Bode magnitude should exhibit the desirable -20dB/decade constant slope, especially near crossover, for good stability robustness. As $1/T_{\theta_2}$ is increased, these configurations clearly improve in both these areas.

Note, furthermore, that there is virtually no difference in these results between configurations with and without prefilter. That is, Config. 1-1 Bode results are the same as Config. 4-1, performance and stability here are independent of the presence of the prefilter. (The significance of the prefilter will become more apparent later, when pilot phase compensation is considered. The pilot essentially compensates for the lack of this prefilter in Config. 1-1 to 1-3, to keep the performance and stability essentially the same as Config. 4-1 to 4-3.) Likewise, the Config. 4-3-1 results are identical to those of Config. 4-3 (no difference due to the washout filter). Finally, the Bode characteristics for Config. 7-1 appear very similar to Config. 4-2, both rated virtually the same.

For reference now, consider the information in Table 3. Given are the relations between the $\gamma_{c.p.}$ and the $\gamma_{c.r.}$ to the $\gamma_{c.g.}$, in terms of the ratio of the numerators of their transfer functions (from stick input, for example). The relations reveal three things: 1) the key numerator zeros of the $\gamma_{c.g.}/F_{st}$ transfer functions are small in magnitude, as noted previously; 2) the analogous numerator zeros for $\gamma_{c.p.}/F_{st}$ are both minimum phase, but lightly damped; and 3) the prefilter is not a factor in these relations. Point 1) explains the larger open-loop peaks in the $\gamma_{c.g.}$- analysis discussed previously. More importantly, the "notches" in the Bode plots in Figs. 7-14 are clearly due to the two lightly-damped zeros in $\gamma_{c.p.}/F_{st}$.

With regard to pilot phase compensation required, the results are equally interesting. These results, tabulated in Table 4, are extremely consistent with the ratings. Configs. 1-1 to 1-3 require the highest phase compensation, due to the pilot having to adjust for the lack of the "lead" prefilter. Equally significant is the fact that the configuration requiring the lowest pilot phase compensation is Config. 4-2, precisely the configuration receiving the best ratings (2 and 3, compared even to 2.5 and 3 for Config 7-1). Furthermore, these phase results reveal that Config. 4-3 requires more pilot lead than Config. 4-2, while Config. 4-3-1 requires a phase lead between that of Config. 4-2 and Config. 4-3. These results are also consistent with the ratings! (Note that the poor rating for Config. 4-3 has been questioned, but these results indicate that a rating worse than that for 4-2 is justifiable.)

A final point deals with the frequency at which the peak pilot phase compensation occurs. The location of this peak, in relation to open-loop bandwidth, may be used to determine the limiting factors in the closed-loop dynamics. In the case of the analysis of the LAHOS data. This peak was seen to occur near the open-loop phase crossover, and above the closed-loop bandwidth frequency. This indicates that the limiting factor is closed-loop stability, or phase margin. On the other hand, the results in Table 4 reveal that these peaks in phase compensation occur well below phase crossover (see Figs. 7-14), and essentially at the closed-loop bandwidth frequency. This indicates the limiting factor is more one of performance (ability to track) than of stability. This is due, again to the lightly-damped zeros in the $\gamma_{c.p.}$ transfer functions, making the task essentially more difficult. This is further indicated in the frequency response of the pilot's P_{eq} dynamics.

Shown in Fig. 15 is the P_{eq} for Config. 7-1. Note that the peak "compensation" in both magnitude and phase occurs near 3 rad/sec., where the two zeros in $\gamma_{c.p.}/F_{st}$ occur (see Table 3). This is in contrast to this peak occurring near 10 rad/sec in the LAHOS results. The 10 rad/sec value is near the limit of pilot capability since the minimum neromuscular lag time constant is around 0.1 sec.

Analysis 3

Even more vivid are the results of an analysis which treats the pilot's control objective as one of ultimately controlling the flight-path at the c.g. or at the center of rotation. At the current time, the preferred approach is to analyze the response most difficult to control, and

that is the response of the center of rotation. This point has the property that it does not accelerate directly due to control surface deflection, but only as a result of a change in vehicle angle of attack. Also, selecting the c.r. eliminates the kinematic effect of the rotational motion and tends to focus on the "point-mass" performance of the flight vehicle. In any event, this may all be academic in the results now to be discussed, because the trends are the same if the c.g. is chosen instead.

Shown in Fig. 16-23 are the open-loop and closed-loop Bodes, for the modeled situation, attempting to control the flight path at the c.r. based on sensed information at the cockpit. But these Bodes are still open- and closed-loop frequency responses for $\gamma_{c.p.}/F_{st}$! In other words, they are comparable to the results in Figs. 7-14, in terms of their relation to performance, and stability, but the desirable closed-loop frequency response is no longer flat. It should now have a "notch," depending on the $\gamma_{c.r.}/\gamma_{c.p.}$ dynamics.

To explain, consider Fig. 24. The pilot closes the loop around the $\gamma_{c.p.}/F_{st}$, but the final response controlled is $\gamma_{c.r.}$ Reversing the order of the block diagram reveals that the situation is equivalent to that in the $\gamma_{c.p.}$ analysis, with the commanded response "shaped" by the $\gamma_{c.r.}/\gamma_{c.p.}$ characteristics. So the optimum ($\gamma_{c.p.}$) closed-loop Bode response is no longer flat, but should have a "notch" to compensate for the difference in the characteristics of the commanded $\gamma_{c.p.}$ response.

More importantly, however, in that the open-loop Bodes in Figs. 16-23 still determine the closed-loop stability, and the desired characteristic is still that of -20 dB/decade slope of the magnitude curve, especially

near crossover. Note the drastic improvement in this characteristic as $1/T_{\theta_2}$ increases, and for Config. 7-1 as well, compared to Config. 1-1 and 4-1. From consideration of these Figures, it is clear that the pilot's ability to obtain a stable, robust loop closure is nil for Config. 1-1 and 4-1, with monotonic improvement as $1/T_{\theta_2}$ is increased. Taken along with the pilot phase compensation results, given in Table 5, these results are all compatible with the ratings.

Shown in Fig. 25, is a plot that is comparable to Fig. 2. In Fig. 25, the pilot phase compensation is shown, versus the open-loop peak obtained from Figs. 16-23. The grouping of the configuration is similar to that in Fig. 2, a situation to be considered further as the remainder of the TIFS "Pitch Rate" configurations are evaluated.

REFERENCES

1. Berthe, C. J., Chalk, C. R., and Sarrafian, S.: Pitch Rate Flight Control Systems in the Flared Landing Task and Design Criteria Development. Calspan Report No. 7205-6 (Preliminary), June 1984.

2. Bacon, B., and Schmidt, D. K: An Optimal-Control Approach to Pilot/Vehicle Analysis and the Neal/Smith Criteria. Journal of Guidance, Control, and Dynamics, Vol. 6, No. 5, September-October 1983.

3. Anderson, M: An Optimal Control Approach to Pilot/Vehicle Analysis of the Flared Landing Task. M.S. Thesis, School of Aeronautics and Astronautics, Purdue University, December 1984.

Table 1.- Attitude Analysis Results

	CONFIGURATION							
	1-1	1-2	1-3	4-1	4-2	4-3	4-3-1	7-1
Pilot Rating (Pilot A / Pilot B)	5/7	8,7/5.5	3,4/7	2.5/5	2/3	-/7	4/-	3/2.5
Closed-loop Bandwith (rad/s)	2.7	2.7	2.7	2.9	2.8	2.7	2.7	2.8
Pilot Phase Compensation at B.W. (deg)	0.4	0.3	0.2	-19.7	-15.0	-6.1	-9.7	-16.8
Max. Pilot Phase Compensation (deg)	6.3	6.4	6.4	-11.2	-6.4	1.2	-1.2	-8.6
Frequency for Max. Pilot Phase (rad/sec)	4.0	4.0	4.3	4.8	4.5	4.3	4.5	4.5
Sensitivity Parameter, SP (dB)	1.3	1.3	1.3	2.6	1.9	2.6	2.1	2.3

Table 2.- Flight Path (c.g.) Analysis Results

	CONFIGURATION							
	1-1	1-2	1-3	4-1	4-2	4-3	4-3-1	7-1
Pilot Rating (Pilot A / Pilot B)	5/7	8,7/5.5	3,4/7	2.5/5	2/3	-/7	4/-	3/2.5
Closed-loop Bandwith (rad/s)	1.7	1.8	1.9	1.7	1.8	1.9	1.9	1.8
Pilot Phase Compensation (deg) (no time delay)	28.	25.	23.	2.	7.	17.	13.	4.
Open-Loop Peak (dB) (no time delay)	4.5	3.6	2.2	2.9	2.9	2.6	2.2	1.1
Pilot Phase Compensation (deg) (with 170ms delay)	46.	45.	44.	23.	29.	37.	33.	25.
Open-Loop Peak (dB) (with 170ms delay)	20.	19.	18.	19.	18.	17.	16.	15.

Table 3.- Flight Path Numerator Relationships

Configurations	c.g./Cockpit	Center of Rotation/Cockpit
1-1 and 4-1	$\frac{-.0085\ (S-1.9)(S+2.4)}{.052\ (S+0.2\pm2.7j)}$	$\frac{-.0016\ (S-13.5)(S+17.)}{.052\ (S+0.2\pm2.7j)}$
1-2 and 4-2	$\frac{-.009\ (S-2.6)\ (S+3.1)}{.06\ (S+0.6\pm3.43j)}$	$\frac{-.0016\ (S-27.)\ (S+16.)}{.06\ (S+0.6\pm3.43j)}$
1-3 and 4-3 4-3-1	$\frac{-.01\ (S-3.1)\ (S+3.6)}{.06\ (S+0.9\pm4.j)}$	$\frac{-.002\ (S-40.)\ (S+14.2)}{.06\ (S+0.9\pm4.j)}$
7-1	$\frac{-.007\ (S-2.6)\ (S+3.1)}{.043\ (S+0.6\pm3.4j)}$	$\frac{-.0012\ (S-27.)\ (S+15.5)}{.043\ (S+0.6\pm3.4j)}$

Table 4.- Flight Path (c.p.) Pilot Phase Compensation

	CONFIGURATION							
	1-1	1-2	1-3	4-1	4-2	4-3	4-3-1	7-1
Closed-loop Bandwith (rad/s)	1.7	2.0	2.1	1.6	2.0	2.1	2.1	1.9
Max. Pilot Phase Compensation (deg)	56.	39.	33.	23.	18.	26.	21.	18.
Frequency for Max. Pilot Phase (rad/sec)	2.3	2.5	2.7	2.5	2.8	3.0	3.0	2.8
Pilot Rating (Pilot A / Pilot B)	5/7	8,7/5.5	3,4/7	2.5/5	2/3	-/7	4/-	3/2.5

Table 5.- Flight Path (c.p./c.r.) Pilot Phase Compensation

	CONFIGURATION							
	1-1	1-2	1-3	4-1	4-2	4-3	4-3-1	7-1
Closed-loop Bandwith (rad/s)	1.7	2.0	2.1	1.6	2.0	2.1	2.1	1.9
Max. Pilot Phase Compensation (deg)	63.	45.	4.1	3 2,	27.	34.	31.	28.
Frequency for Max. Pilot Phase (rad/sec)	2.3	2.5	2.8	2.5	2.8	3.0	3.0	2.8
Pilot Rating (Pilot A / Pilot B)	5/7	8,7/5.5	3,4/7	2.5/5	2/3	-/7	4/-	3/2.5

OC/FD ATTITUDE TRACKING ANALYSIS

Neal-Smith Data

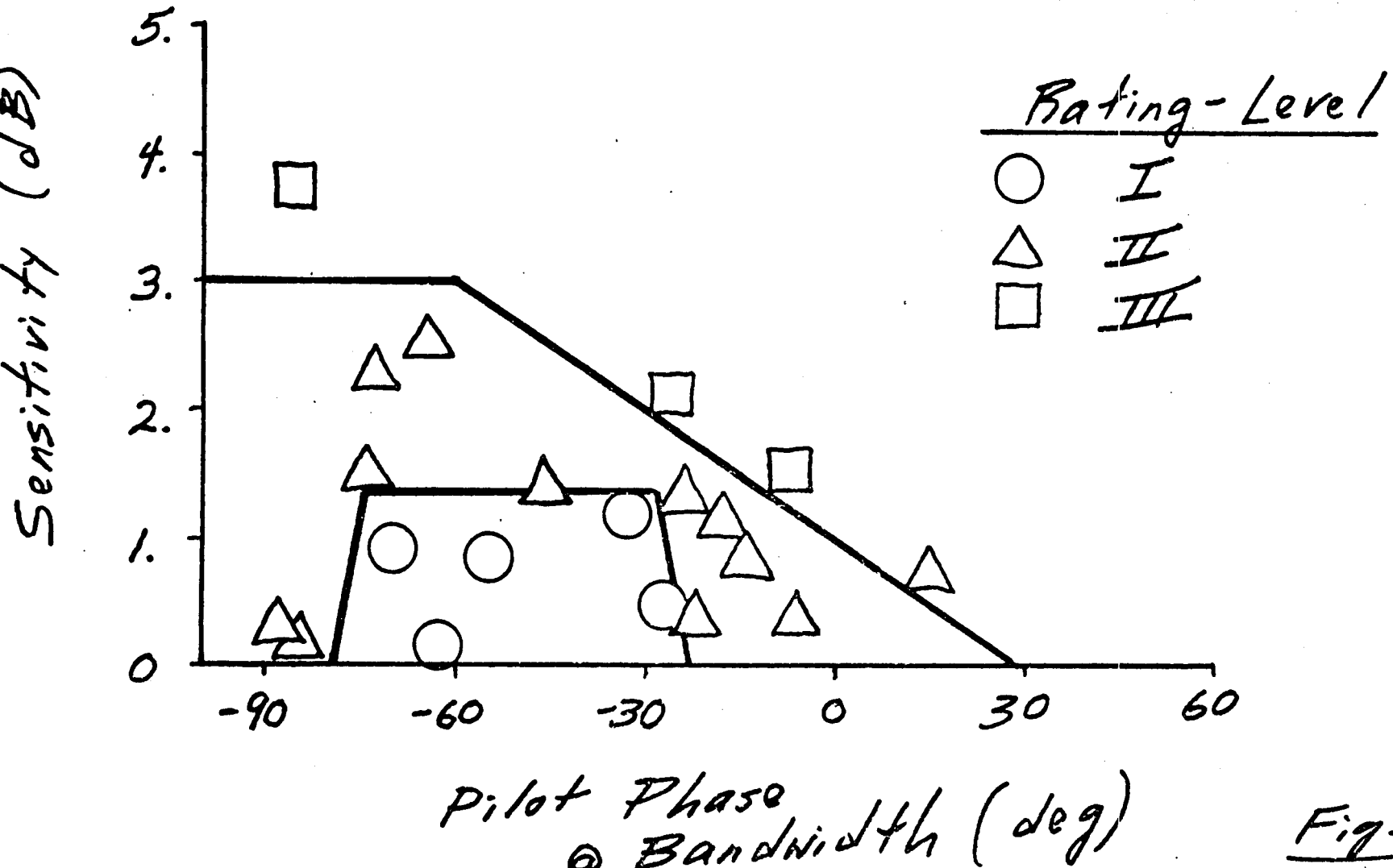

Fig. 1

OC/FD ATTITUDE ANALYSIS OF LANDING TASK

LAHOS DATA

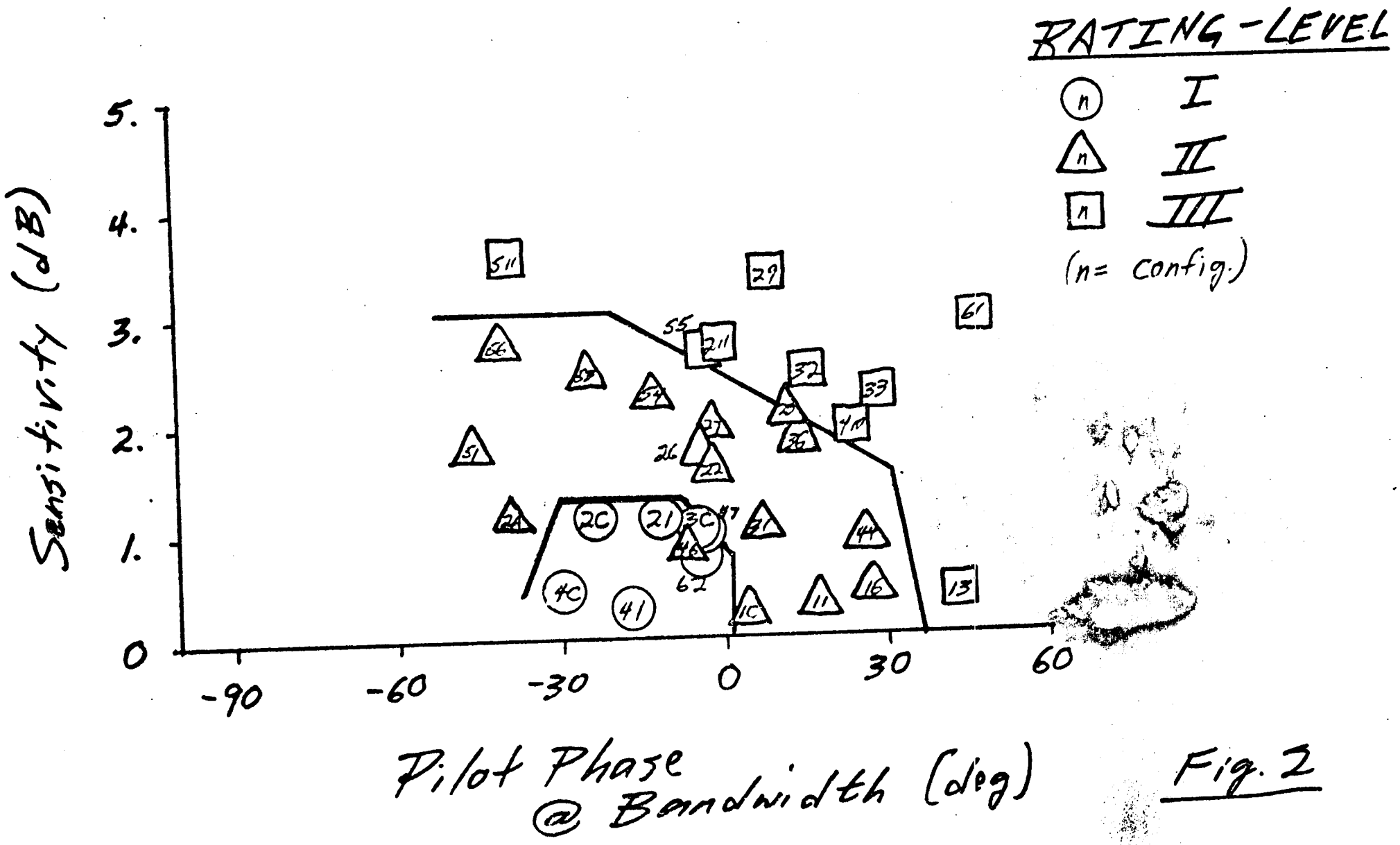

Fig. 2

OC/FD ATTITUDE ANALYSIS

LAHOS Data

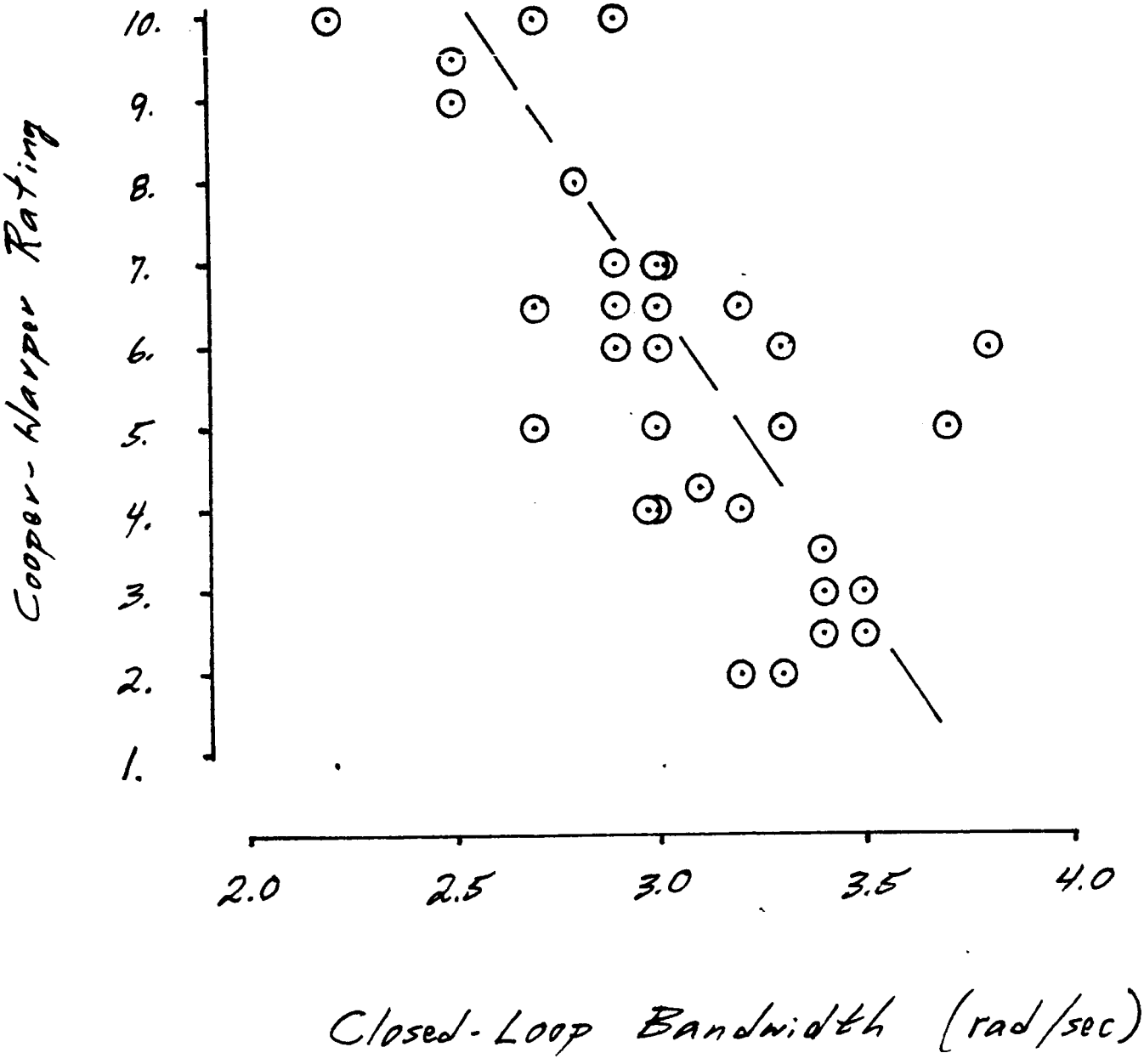

Fig. 3

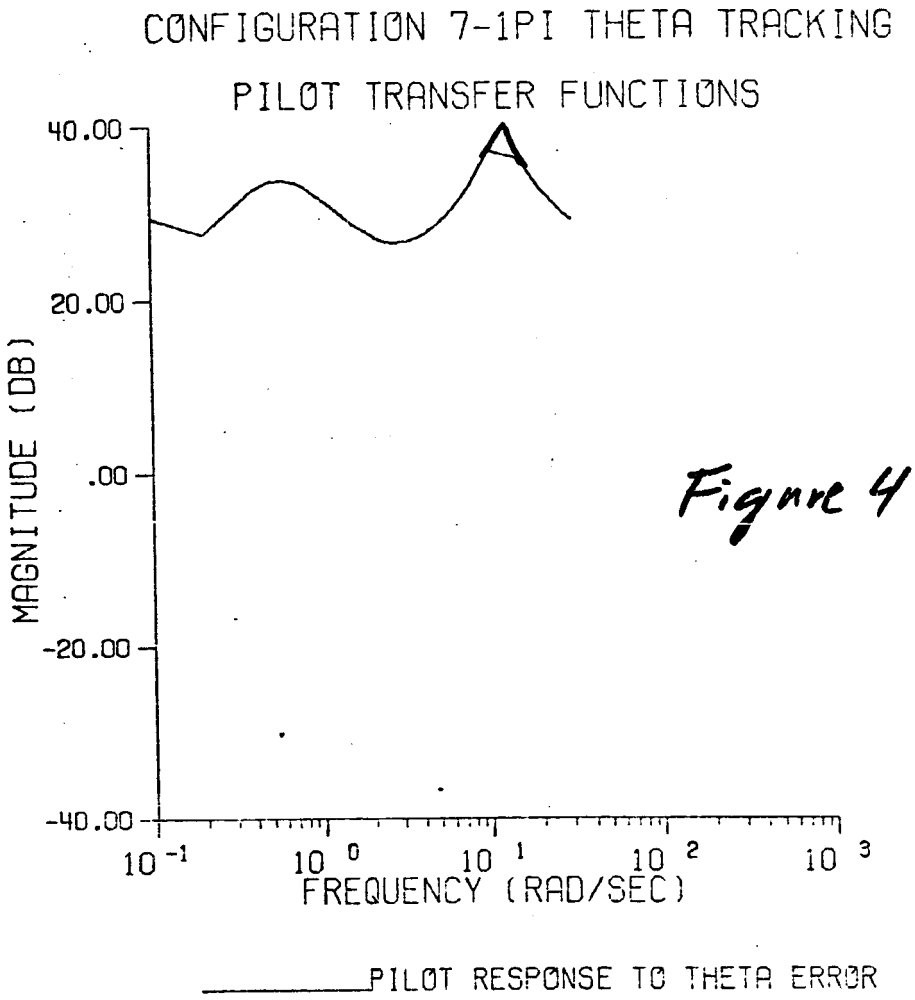
CONFIGURATION 7-1PI THETA TRACKING
PILOT TRANSFER FUNCTIONS
40.00
20.00
.00
-20.00
-40.00
MAGNITUDE (DB)
10 -1
10 0
10 1
10 2
10 3
FREQUENCY (RAD/SEC)
PILOT RESPONSE TO THETA ERROR

Figure 4

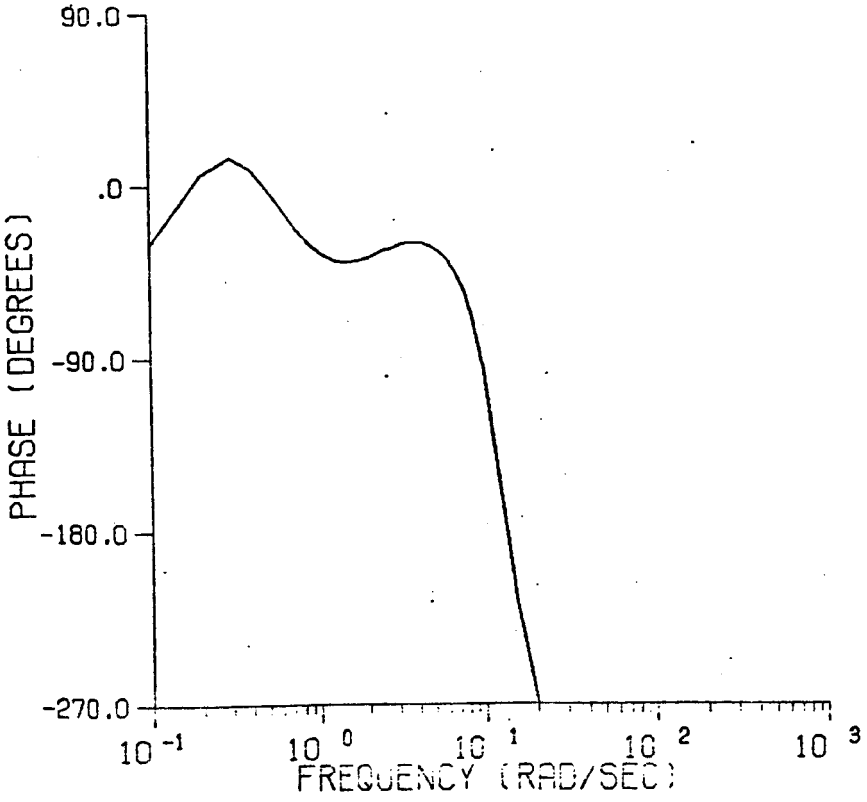
90.0
.0
-90.0
-180.0
-270.0
PHASE (DEGREES)
10 -1
10 0
10 1
10 2
10 3
FREQUENCY (RAD/SEC)

OC/FD FLIGHT-PATH ANALYSIS

Landing Task
LAHOS Data

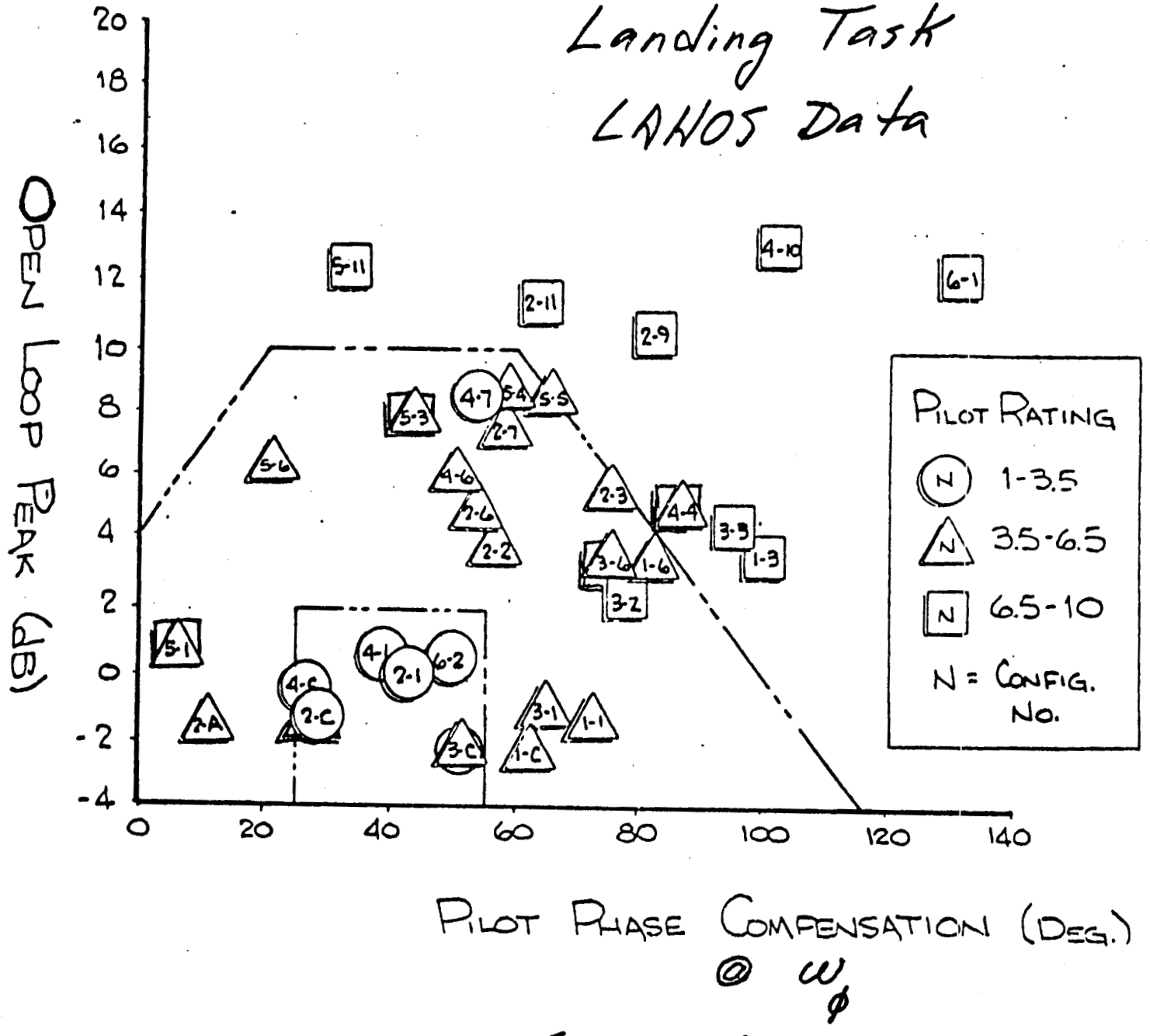

Figure 5.

PRECISION FLIGHT-PATH MODEL

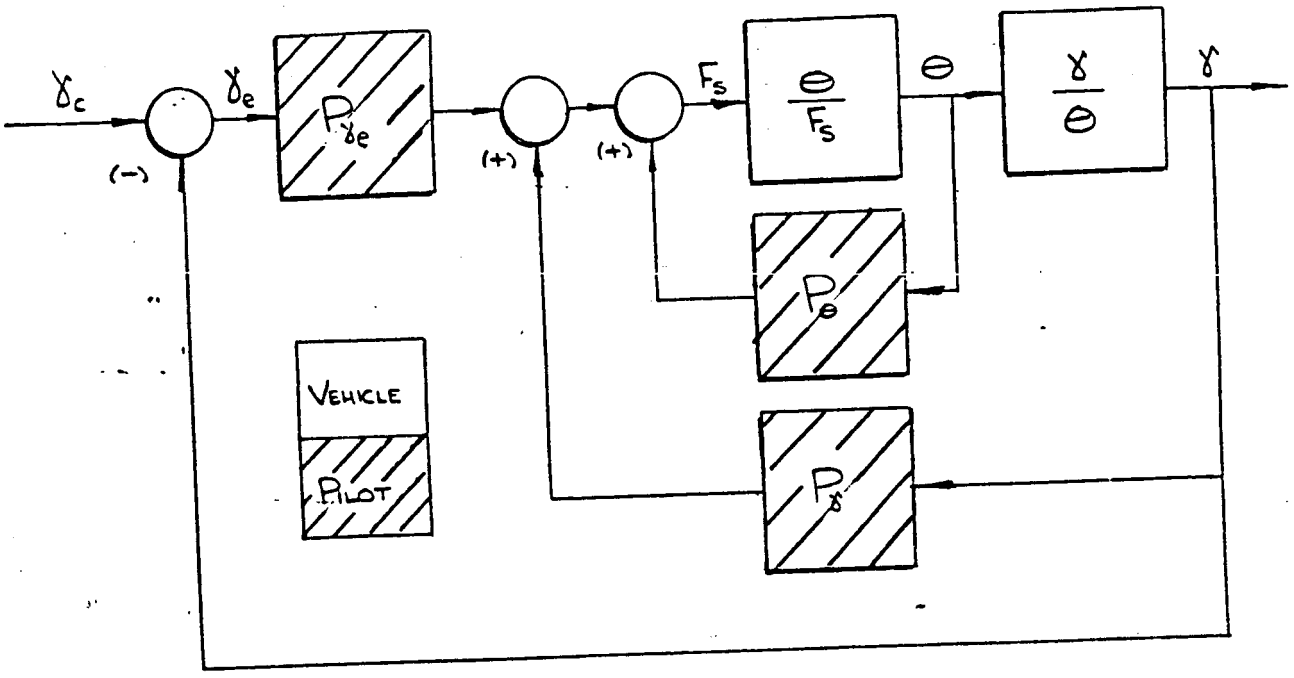

EQUIVALENT PRECISION FLIGHT-PATH MODEL

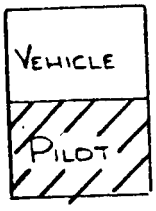

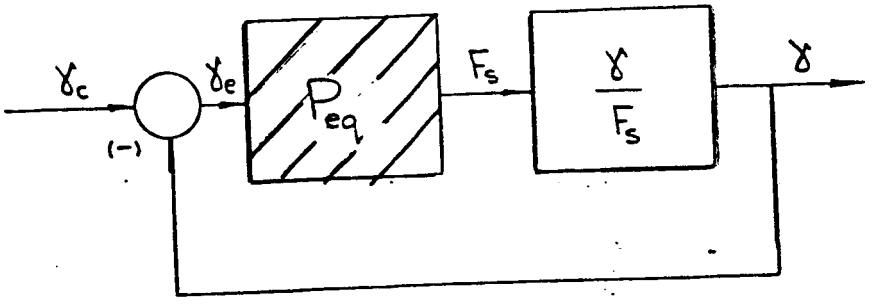

Figure 6.

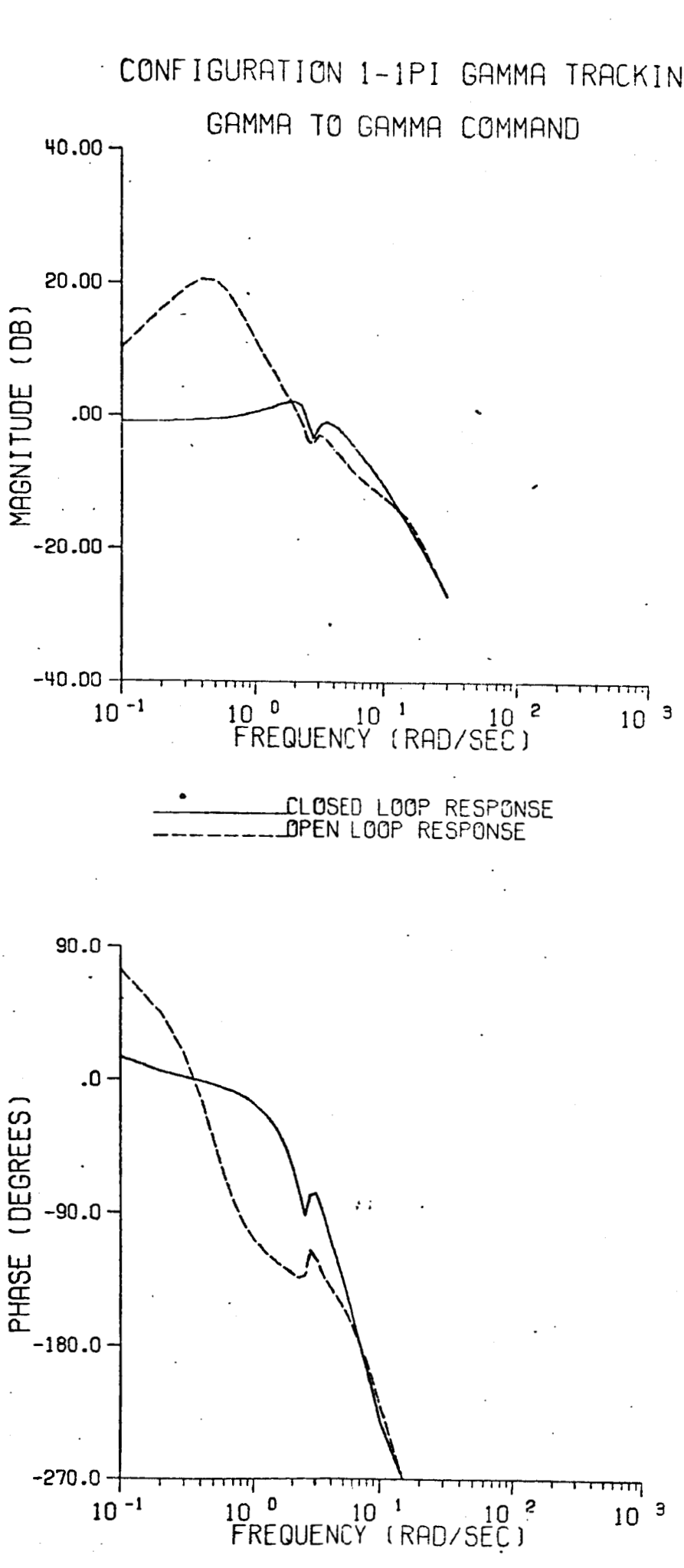
CONFIGURATION 1-1PI GAMMA TRACKING
GAMMA TO GAMMA COMMAND
40.00
20.00
.00
-20.00
-40.00
MAGNITUDE (DB)
10 -1
10 0
10 1
10 2
10 3
FREQUENCY (RAD/SEC)
CLOSED LOOP RESPONSE
OPEN LOOP RESPONSE
90.0
.0
-90.0
-180.0
-270.0
PHASE (DEGREES)
10 -1
10 0
10 1
10 2
10 3
FREQUENCY (RAD/SEC)

POR: 5.17.

Fig. 7

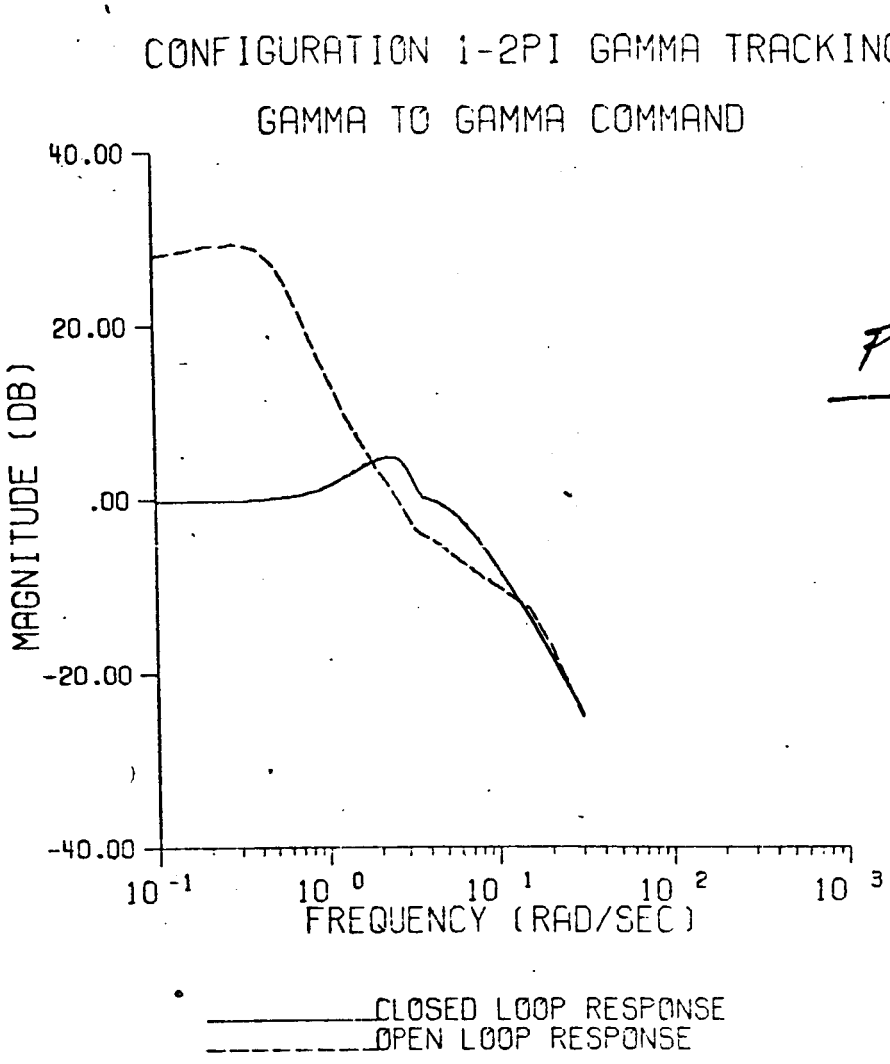

POR: 8,7/5.5

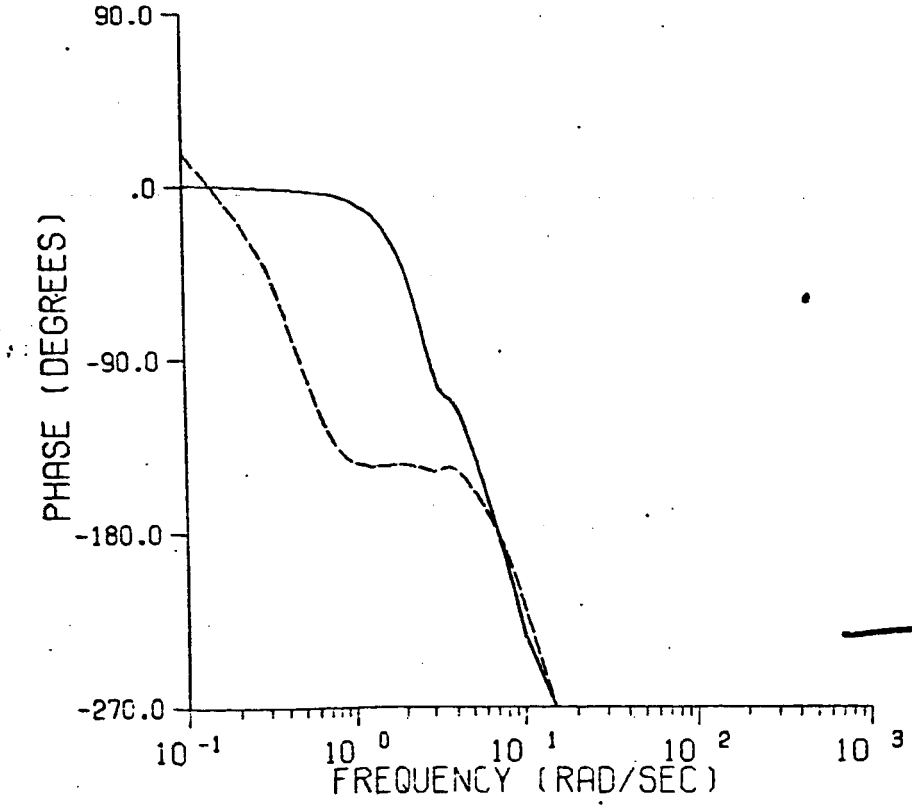

Fig. 8

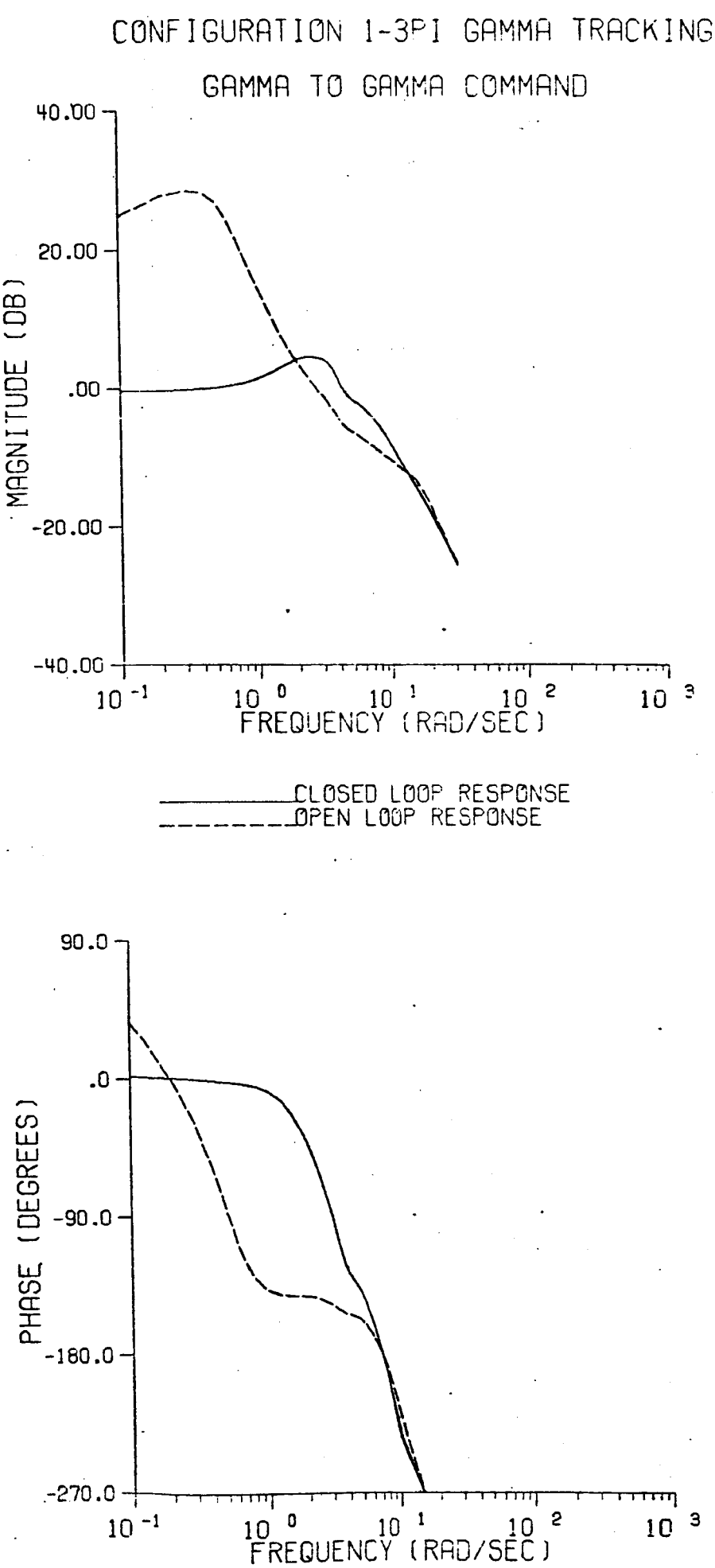
CONFIGURATION 1-3PI GAMMA TRACKING
GAMMA TO GAMMA COMMAND
40.00
20.00
.00
-20.00
-40.00
MAGNITUDE (DB)
10 -1
10 0
10 1
10 2
10 3
FREQUENCY (RAD/SEC)
CLOSED LOOP RESPONSE
OPEN LOOP RESPONSE
90.0
.0
-90.0
-180.0
-270.0
PHASE (DEGREES)
10 -1
10 0
10 1
10 2
10 3
FREQUENCY (RAD/SEC)

POR: 3, 4/7

Fig. 9

CONFIGURATION 4-1PI GAMMA TRACKING

GAMMA TO GAMMA COMMAND

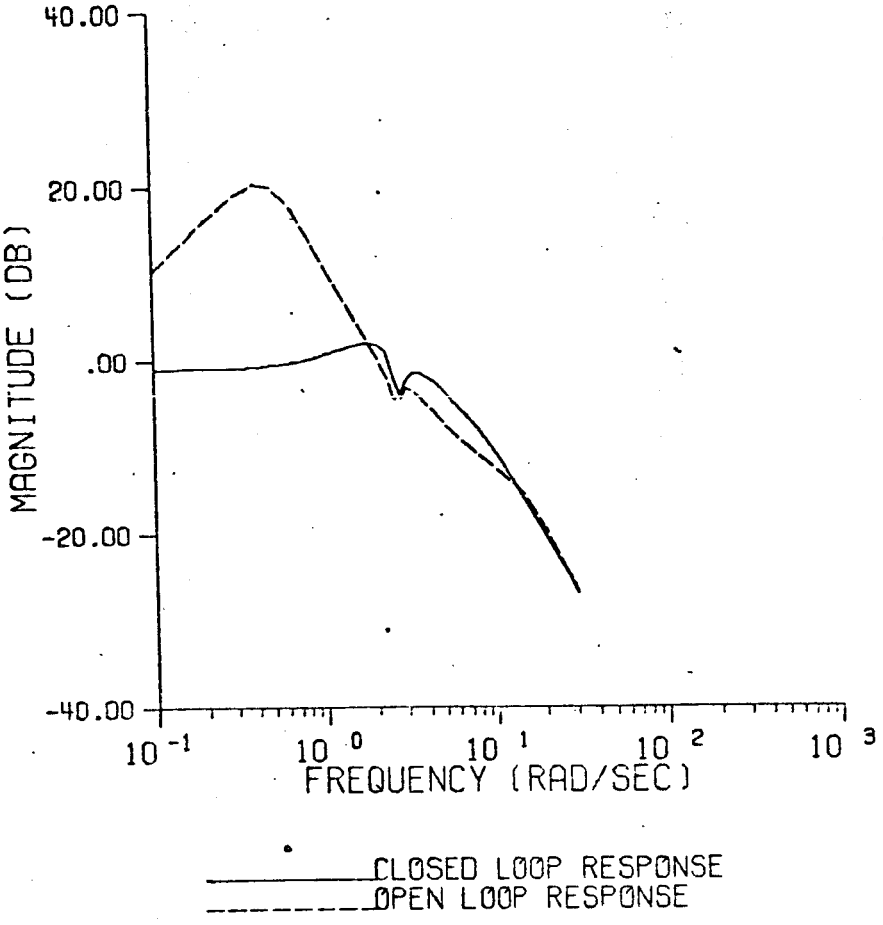

POR: 2.5/5.

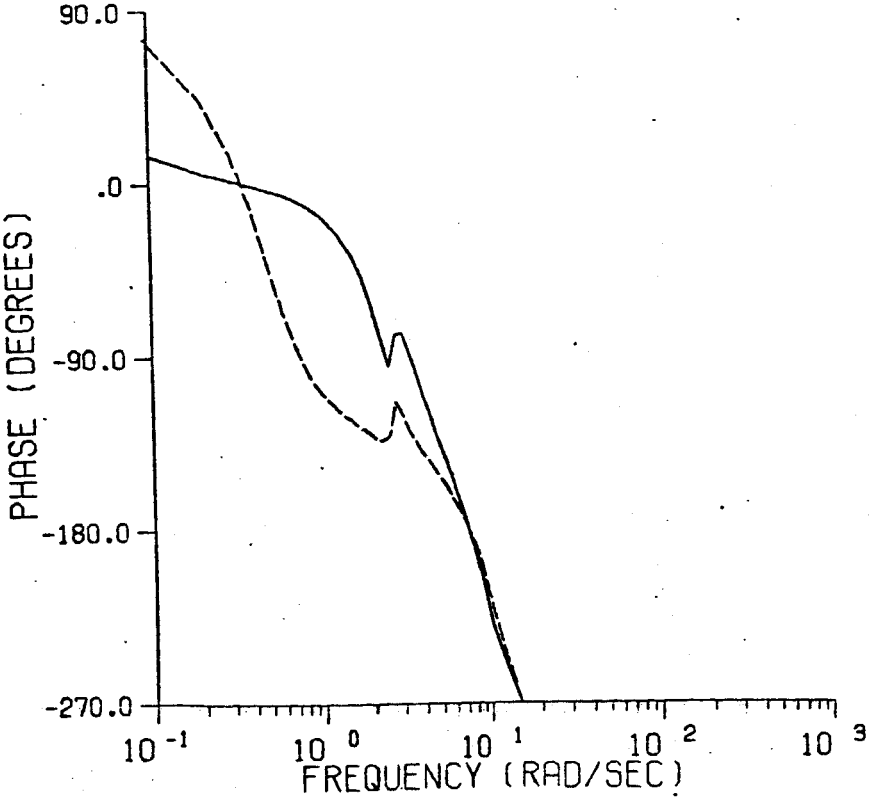

Fig. 10

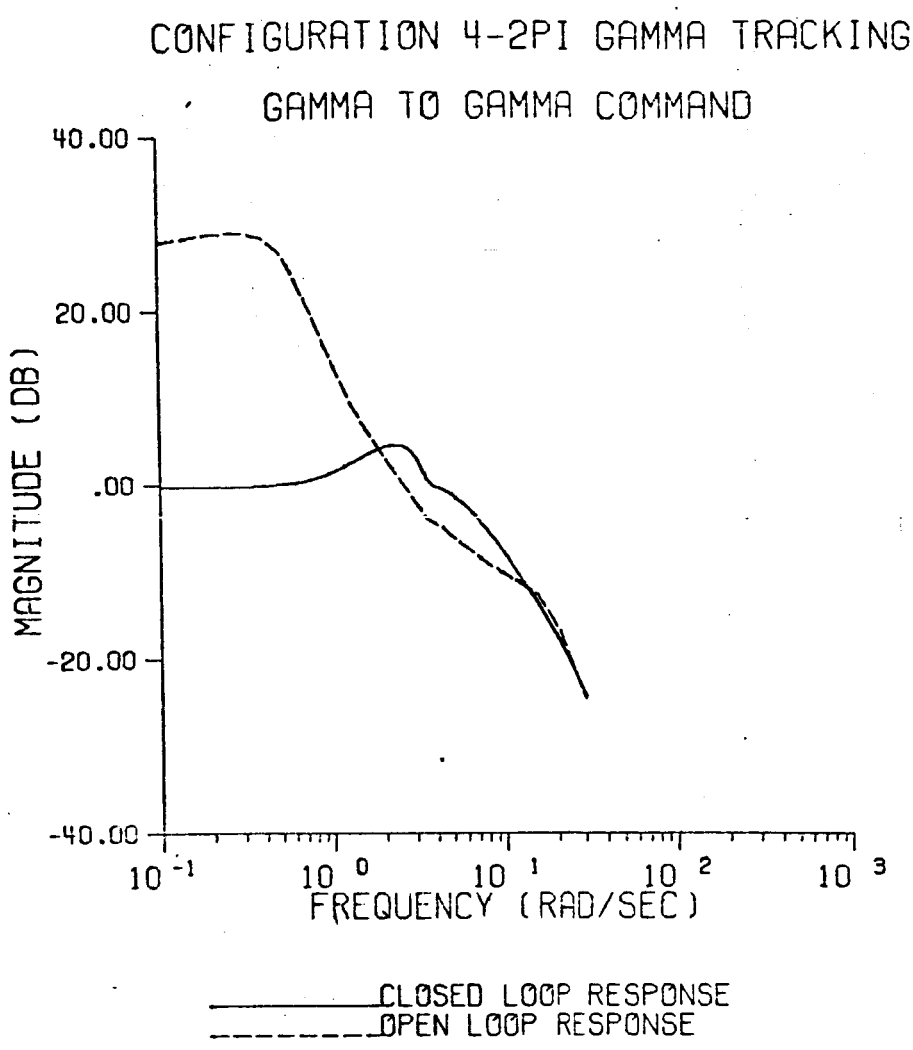
CONFIGURATION 4-2PI GAMMA TRACKING
GAMMA TO GAMMA COMMAND
40.00
20.00
.00
-20.00
-40.00
MAGNITUDE (DB)
10 -1
10 0
10 1
10 2
10 3
FREQUENCY (RAD/SEC)
CLOSED LOOP RESPONSE
OPEN LOOP RESPONSE

POR: 2/3

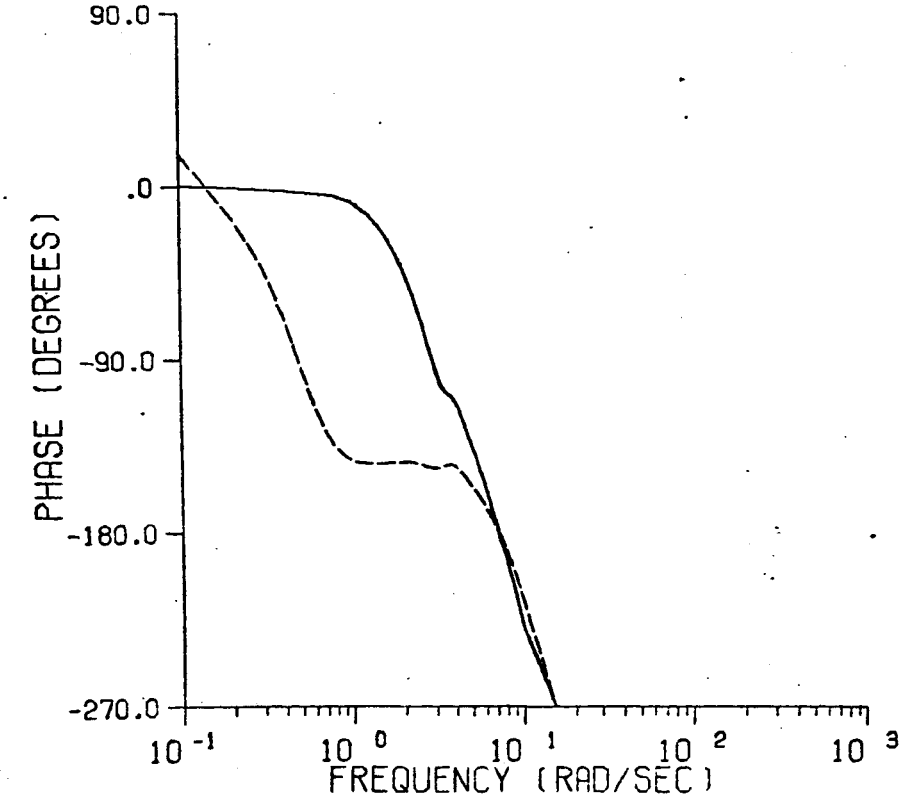
90.0
.0
-90.0
-180.0
-270.0
PHASE (DEGREES)
10 -1
10 0
10 1
10 2
10 3
FREQUENCY (RAD/SEC)

Fig. 11

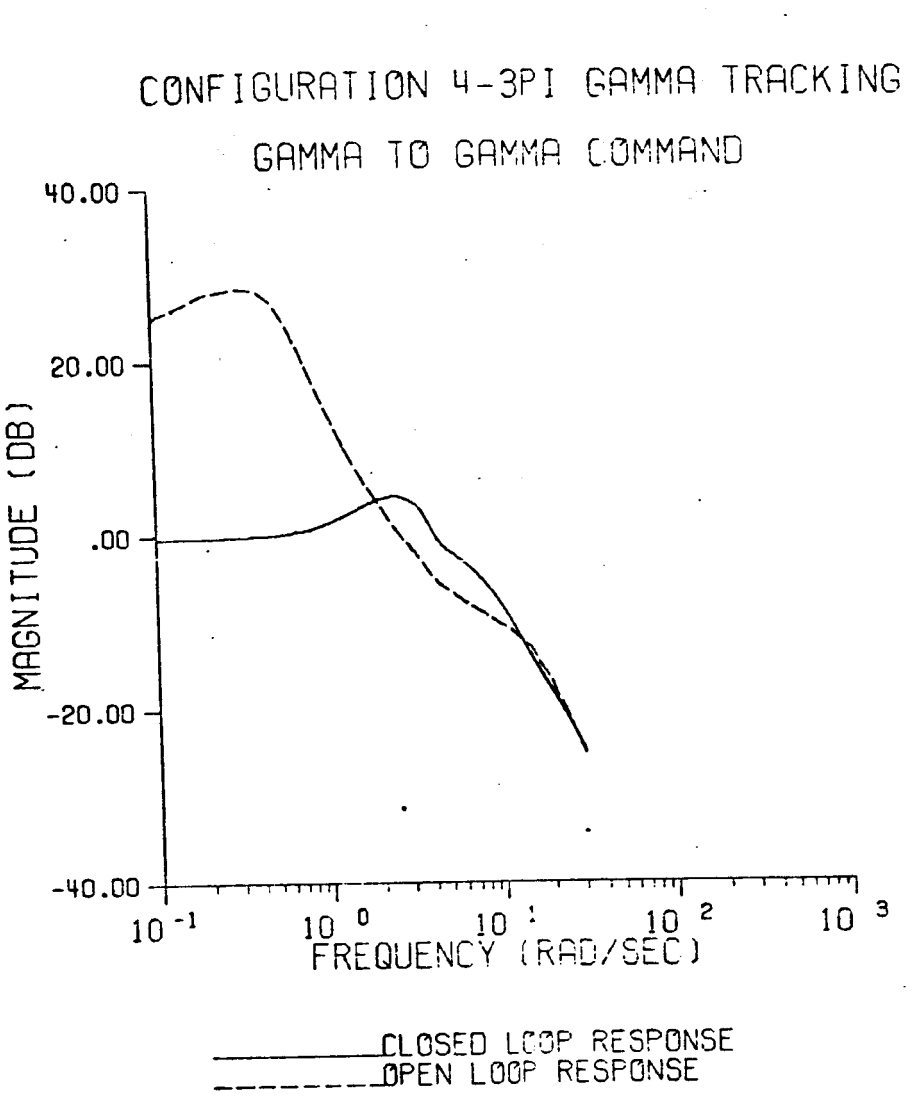
CONFIGURATION 4-3PI GAMMA TRACKING
GAMMA TO GAMMA COMMAND
40.00
20.00
.00
-20.00
-40.00
MAGNITUDE (DB)
10 -1
10 0
10 1
10 2
10 3
FREQUENCY (RAD/SEC)
CLOSED LOOP RESPONSE
OPEN LOOP RESPONSE

POR: - /7

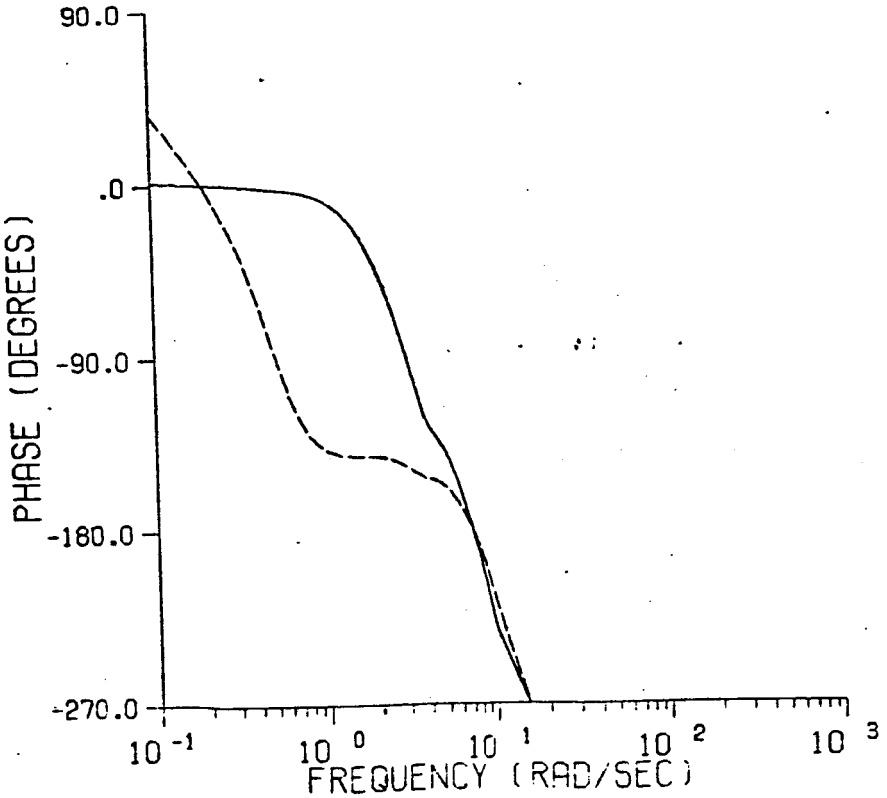
90.0
.0
-90.0
-180.0
-270.0
PHASE (DEGREES)
10 -1
10 0
10 1
10 2
10 3
FREQUENCY (RAD/SEC)

Fig. 12

CONFIGURATION 4-3-1PI GAMMA TRACKING

GAMMA TO GAMMA COMMAND

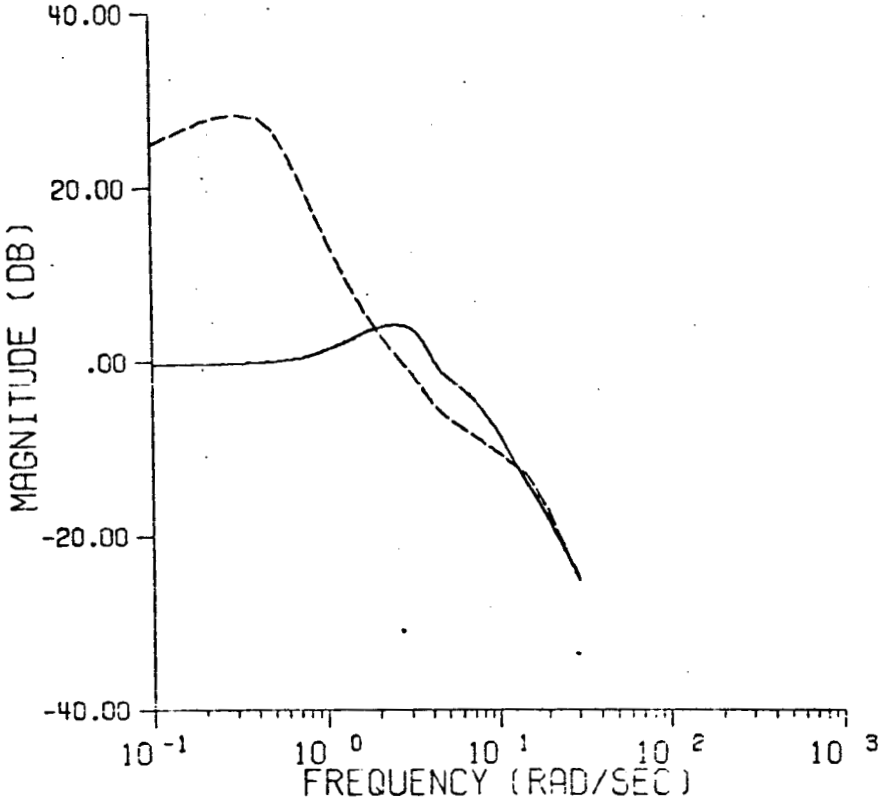

POR: 4/-

CLOSED LOOP RESPONSE

OPEN LOOP RESPONSE

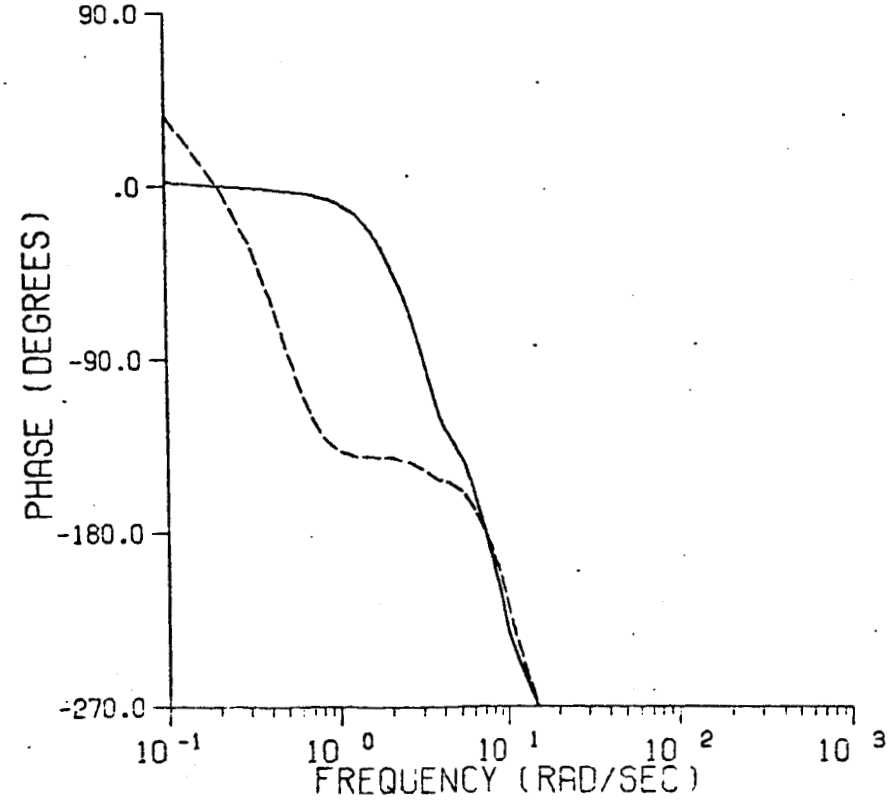

Fig. 13

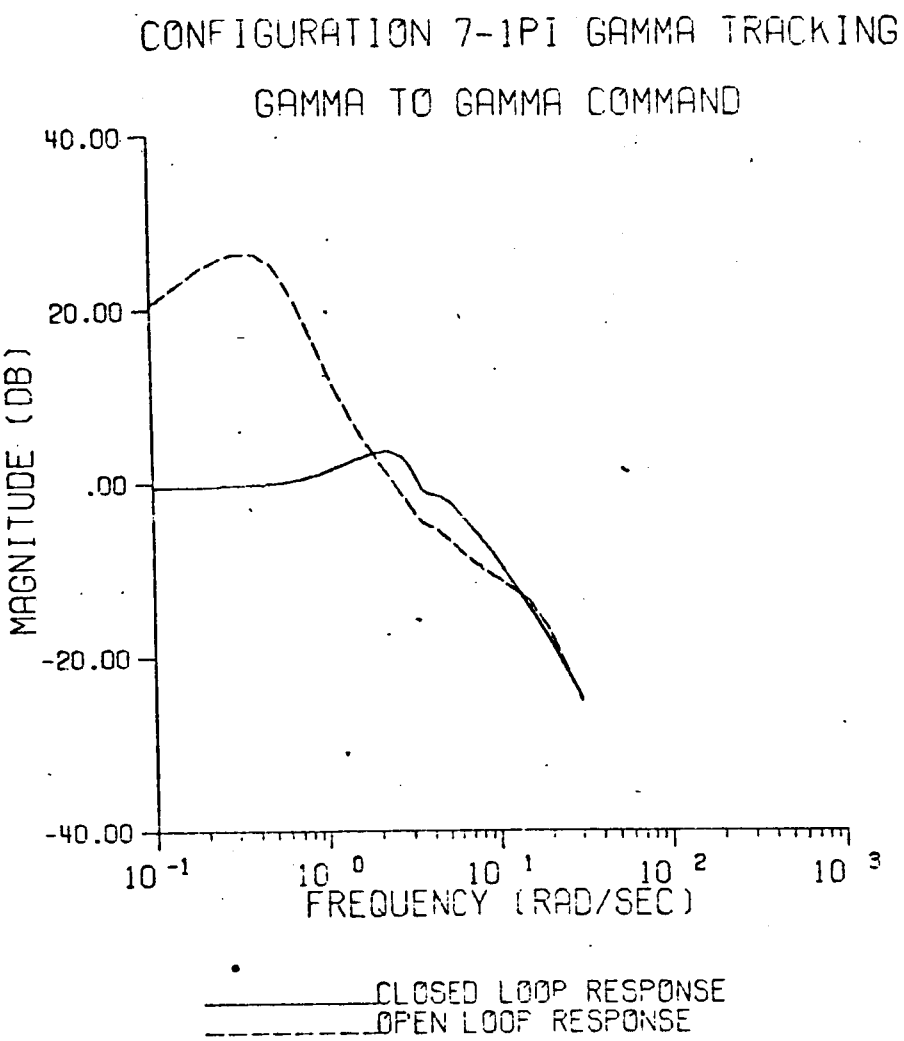

POR: 3/2.5

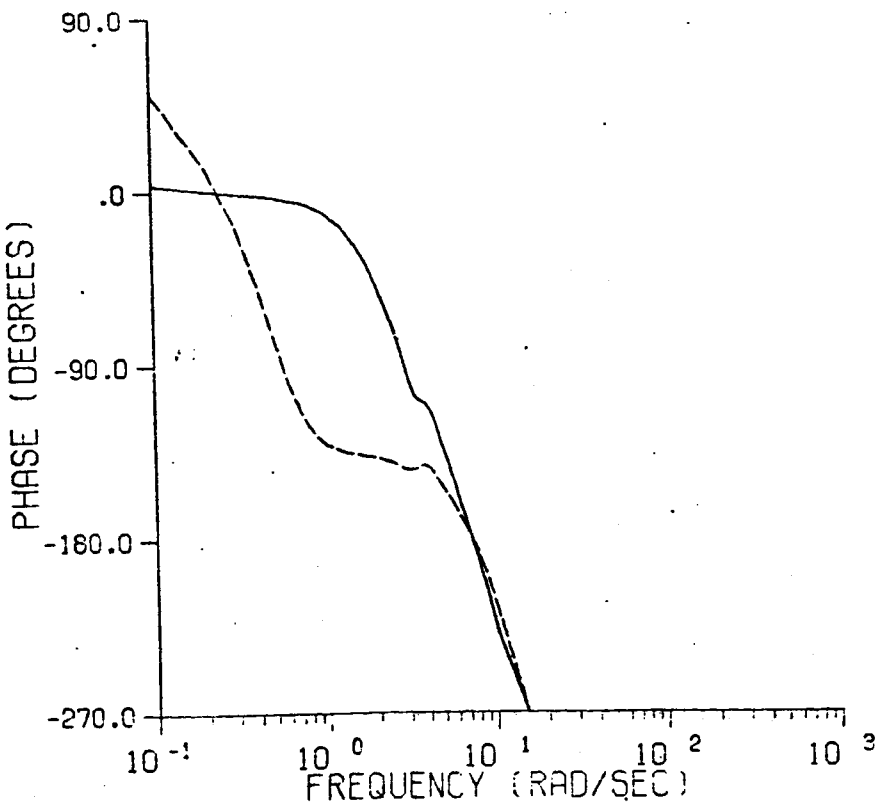

Fig. 14

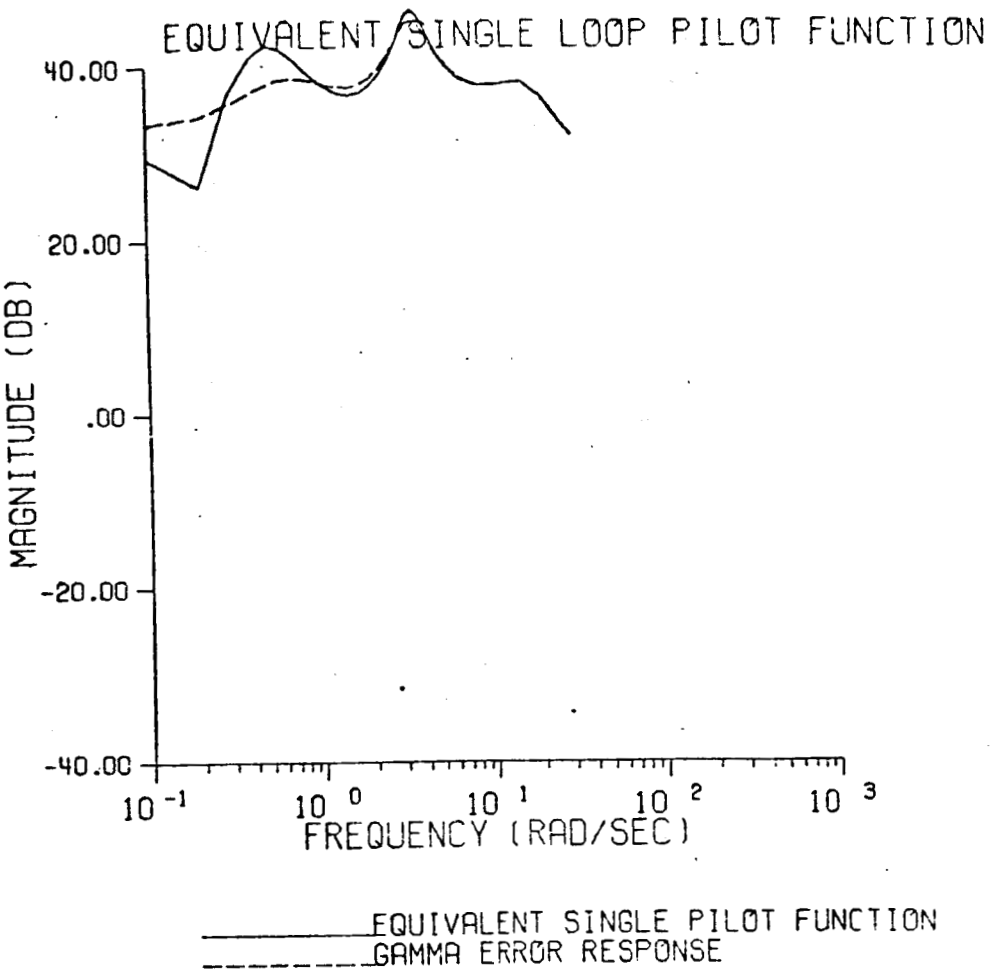

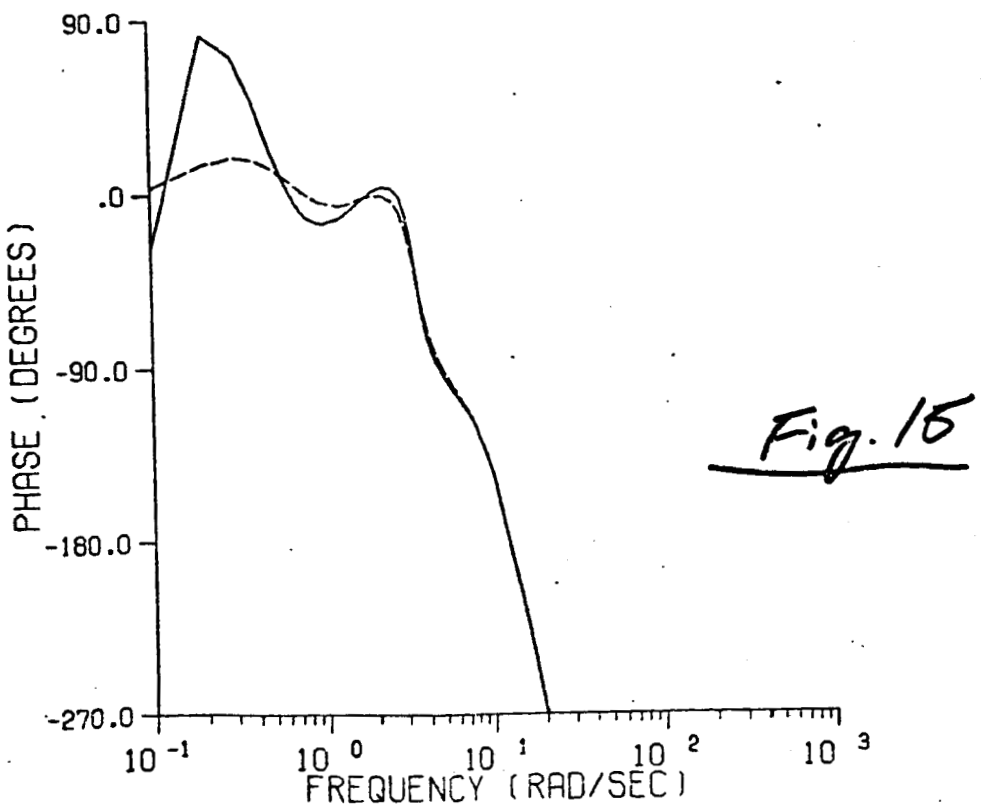

Fig. 15

4 FT. IDSO MATH.

BA40071.

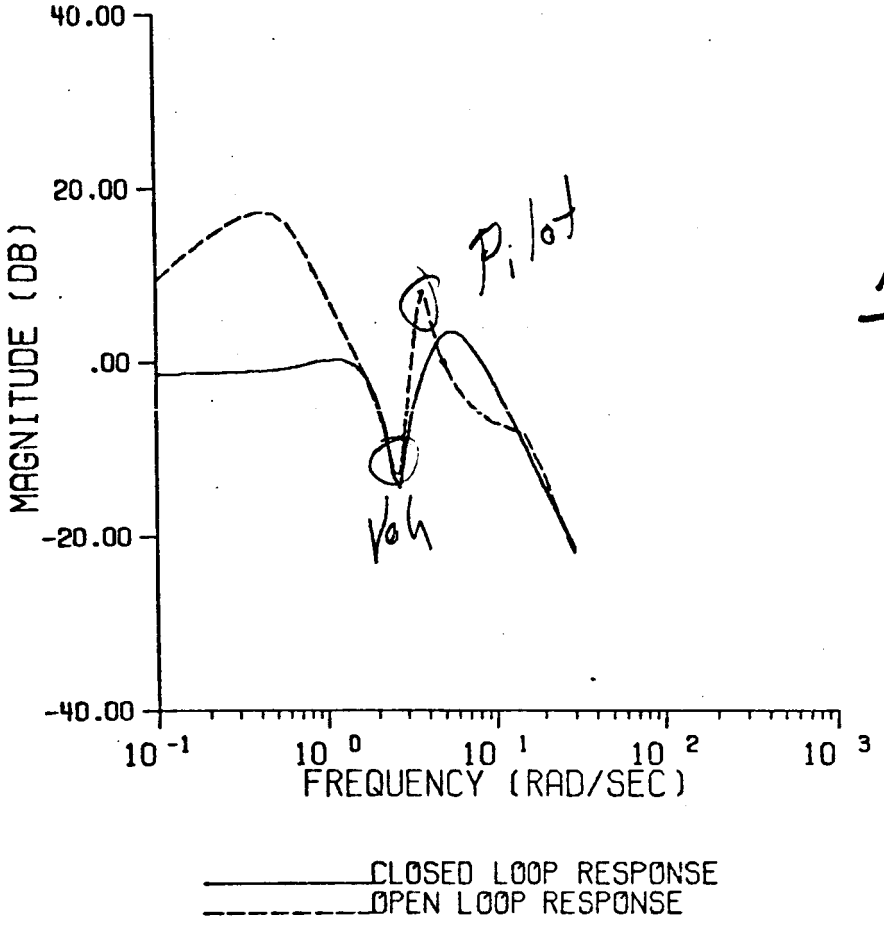
CONFIGURATION 1-1R GAMMA TRACKING
GAMMA TO GAMMA COMMAND AT C.P.
40.00
20.00
.00
-20.00
-40.00
MAGNITUDE (DB)
Pilot
Voh
10 -1
10 0
10 1
10 2
10 3
FREQUENCY (RAD/SEC)
CLOSED LOOP RESPONSE
OPEN LOOP RESPONSE

P.O.R: 5/7

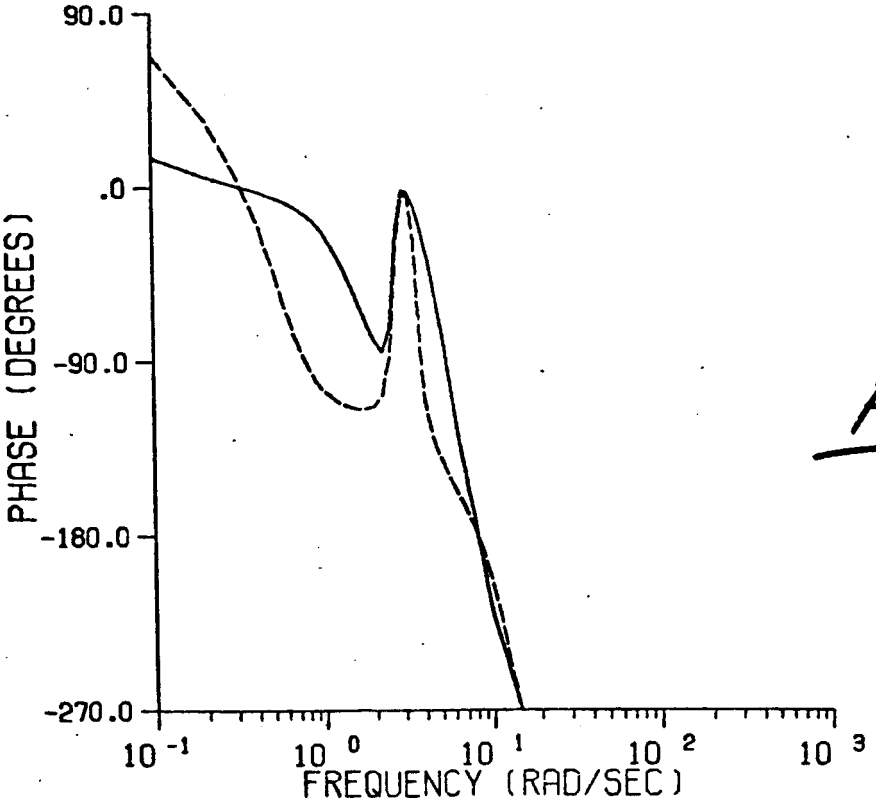
90.0
.0
-90.0
-180.0
-270.0
PHASE (DEGREES)
10 -1
10 0
10 1
10 2
10 3
FREQUENCY (RAD/SEC)

Fig. 16

CONFIGURATION 1-2R GAMMA TRACKING

GAMMA TO GAMMA COMMAND AT C.P.

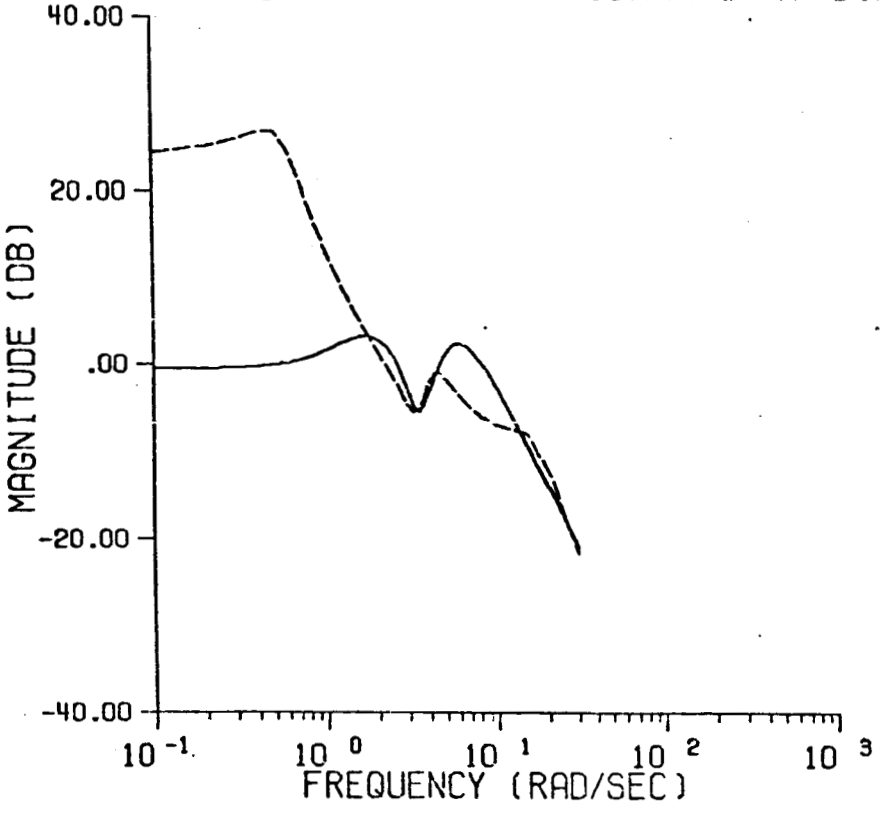

CLOSED LOOP RESPONSE
OPEN LOOP RESPONSE

POR: 8,7/5.5

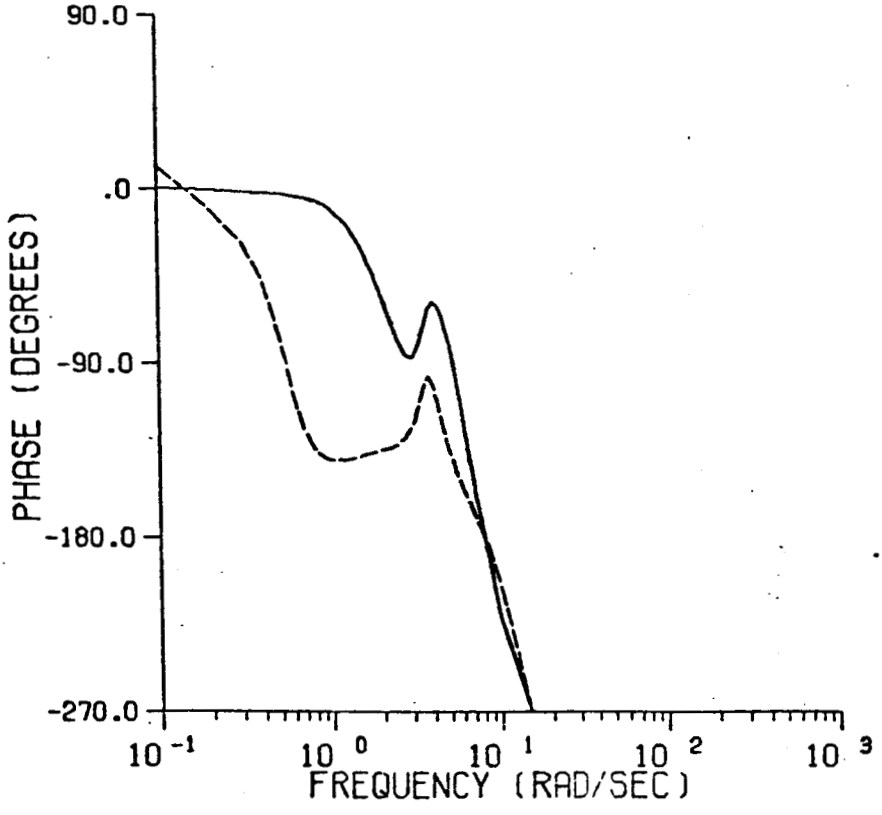

Fig. 17

CONFIGURATION 1-3R GAMMA TRACKING

GAMMA TO GAMMA COMMAND AT C.P.

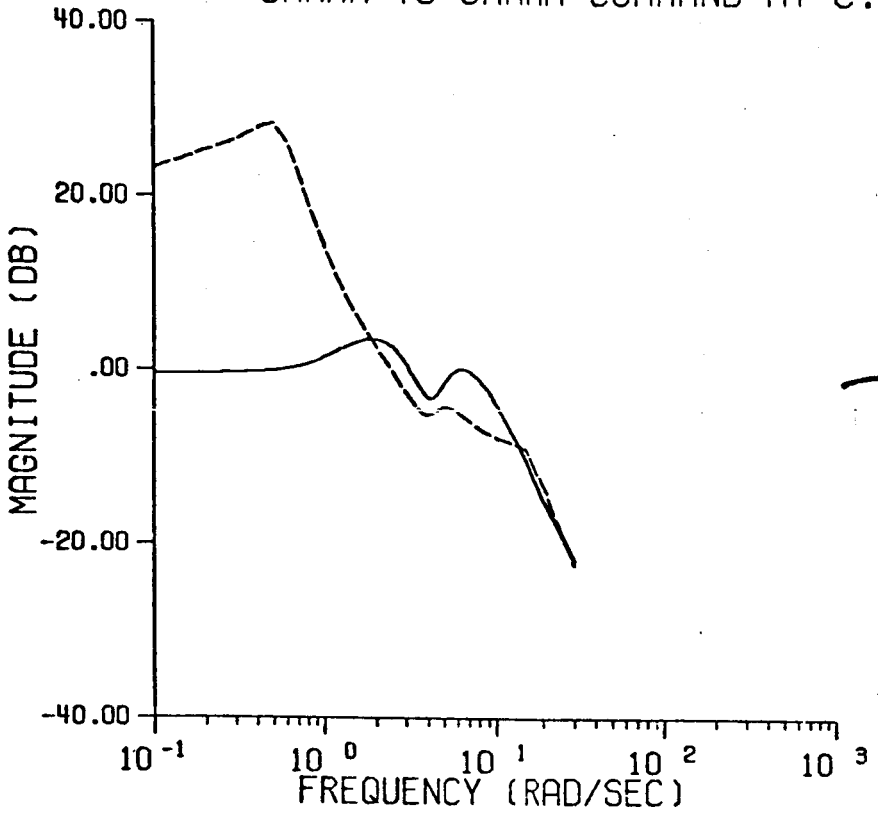

POR: 3, 4/7

CLOSED LOOP RESPONSE

OPEN LOOP RESPONSE

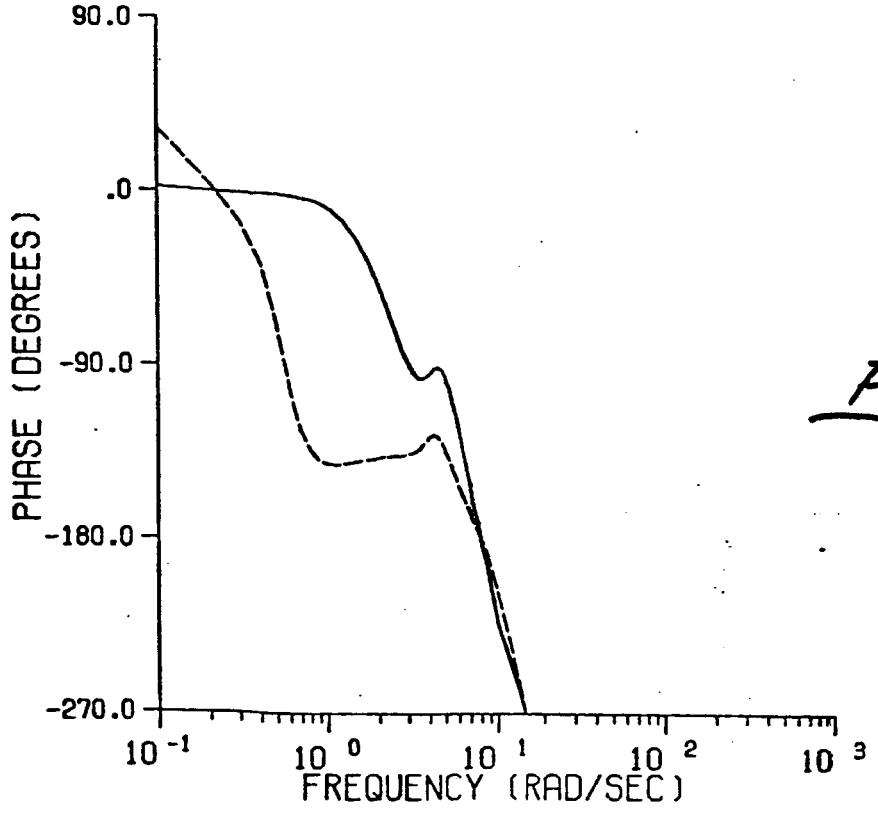

Fig. 18

CONFIGURATION 4-1R GAMMA TRACKING

GAMMA TO GAMMA COMMAND AT C.P.

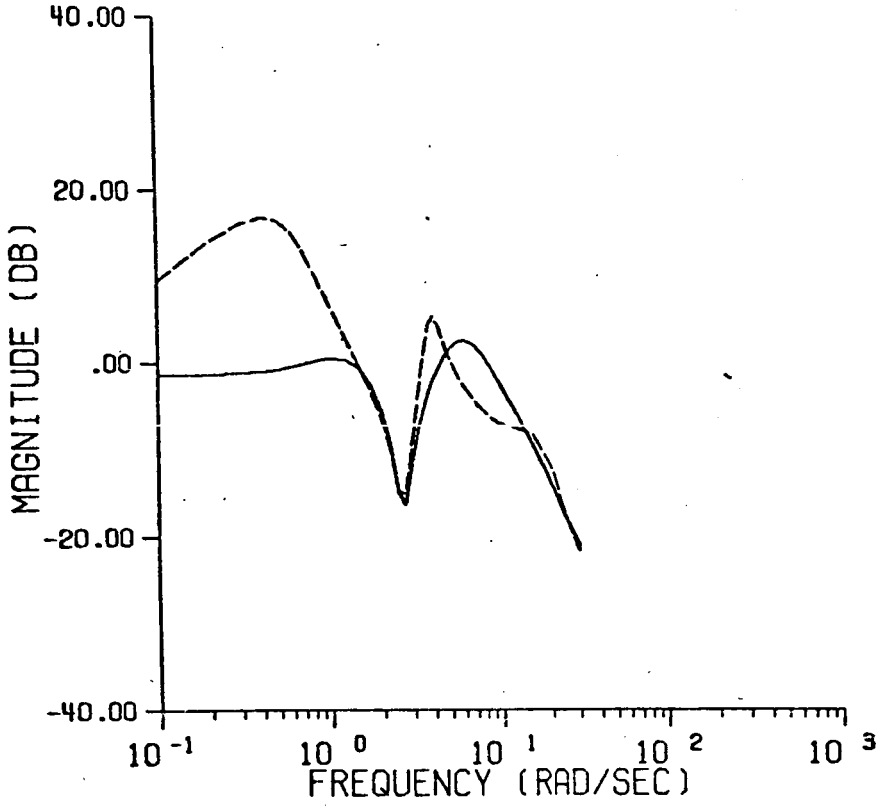

POR: 2.5/5

CLOSED LOOP RESPONSE

OPEN LOOP RESPONSE

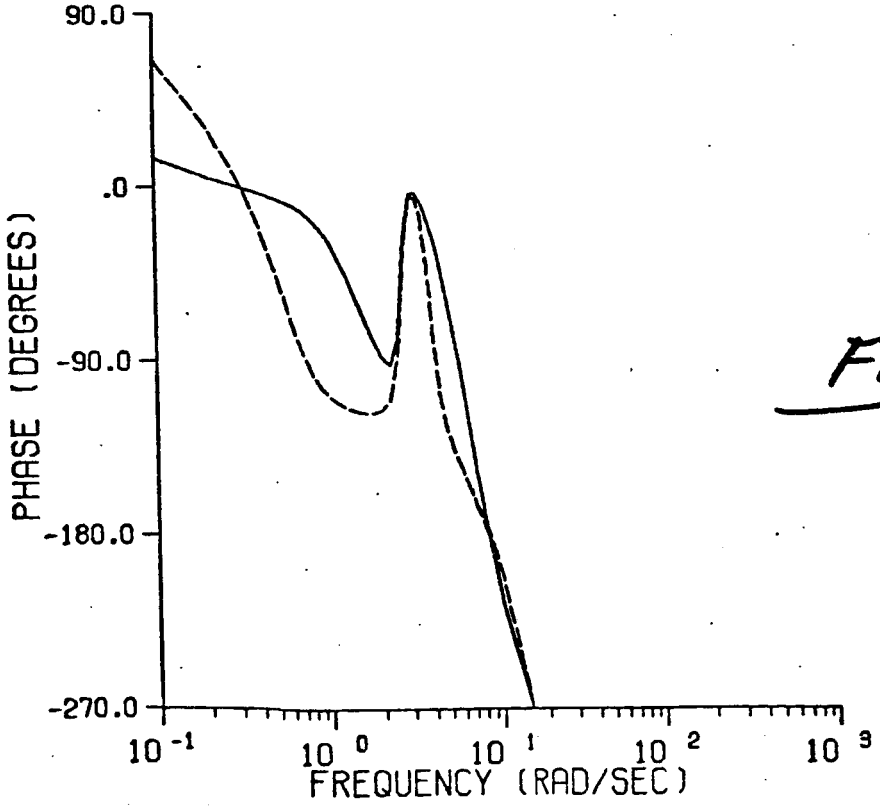

Fig. 19

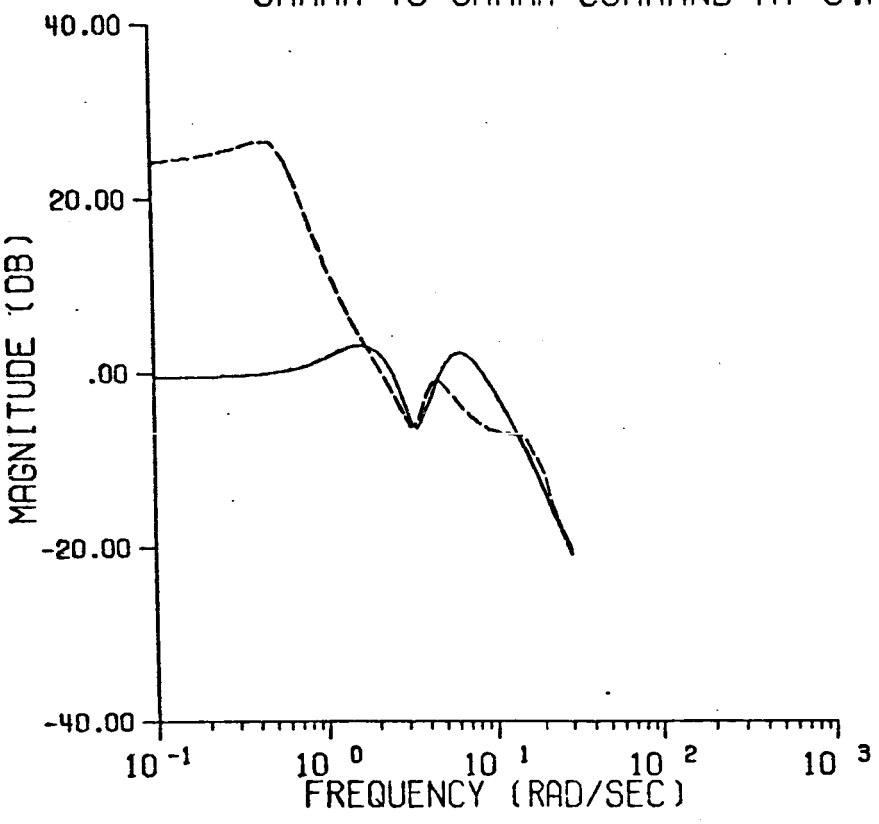
CONFIGURATION 4-2R GAMMA TRACKING
GAMMA TO GAMMA COMMAND AT C.P.
40.00
20.00
.00
-20.00
-40.00
MAGNITUDE (DB)
10 -1
10 0
10 1
10 2
10 3
FREQUENCY (RAD/SEC)
CLOSED LOOP RESPONSE
OPEN LOOP RESPONSE

POR: 2/3

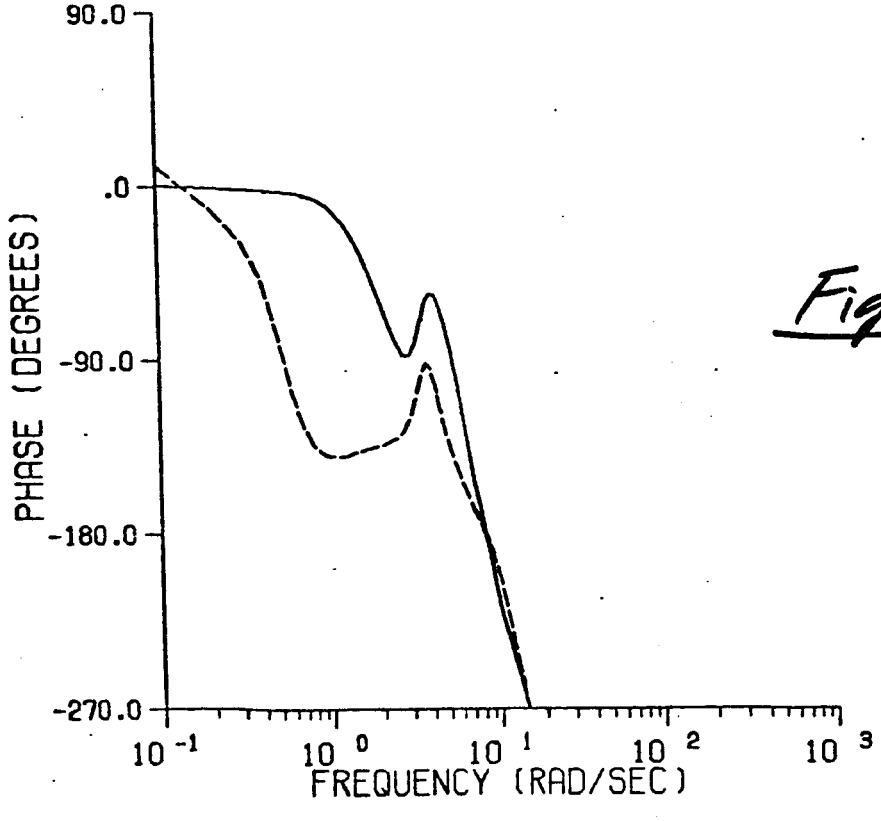
90.0
.0
-90.0
-180.0
-270.0
PHASE (DEGREES)
10 -1
10 0
10 1
10 2
10 3
FREQUENCY (RAD/SEC)

Fig. 20

CONFIGURATION 4-3R GAMMA TRACKING

GAMMA TO GAMMA COMMAND AT C.P.

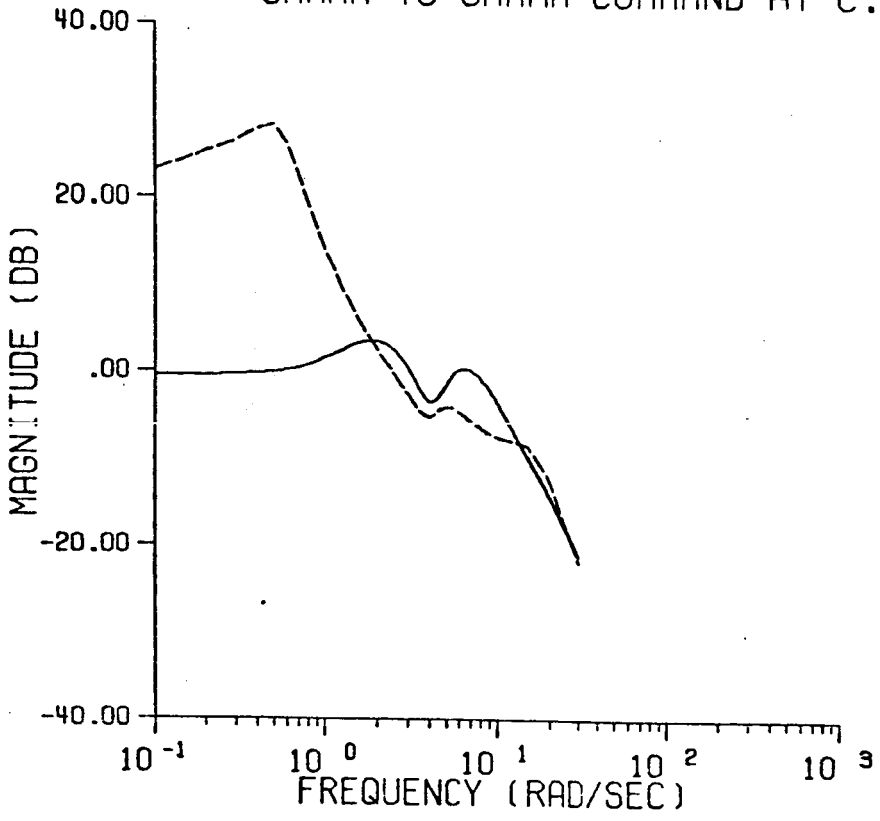

POR: -/7

CLOSED LOOP RESPONSE

OPEN LOOP RESPONSE

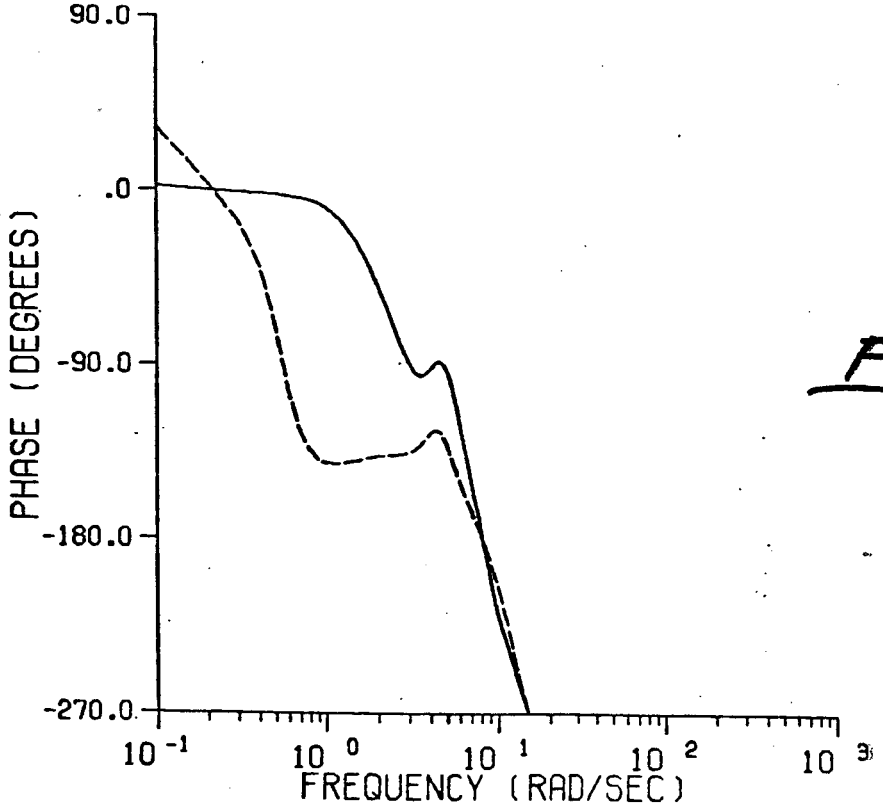

Fig. 21

CONFIGURATION 4-3-1R GAMMA TRACKING

GAMMA TO GAMMA COMMAND AT C.P.

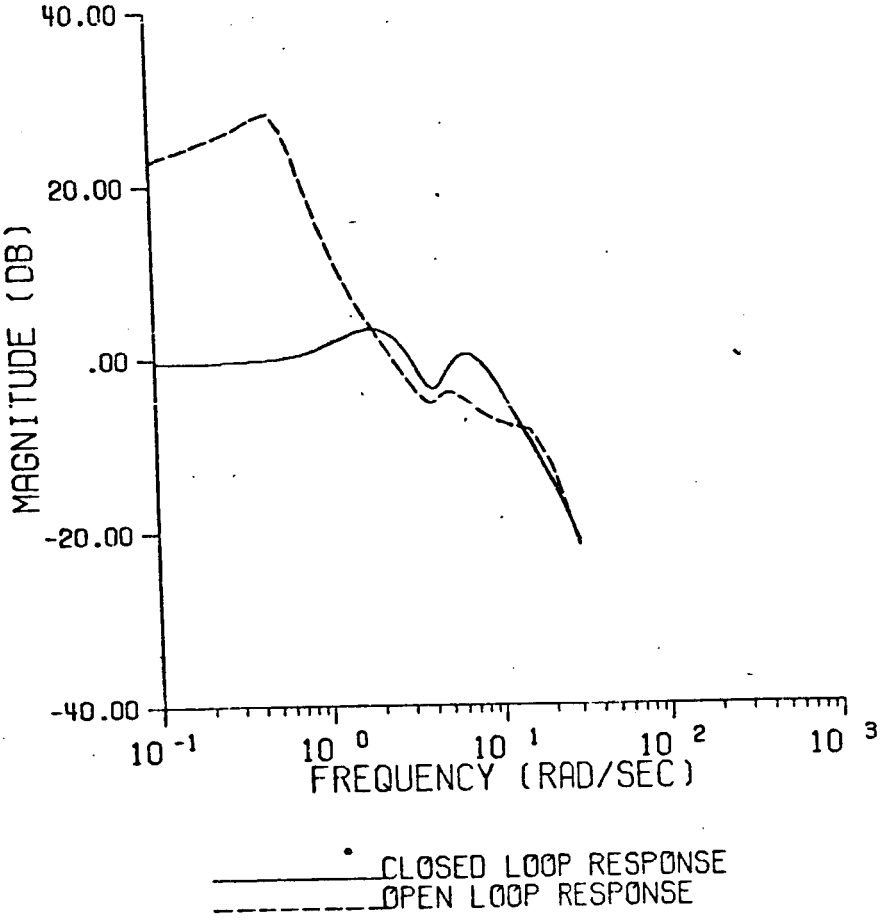

POR: 4/-

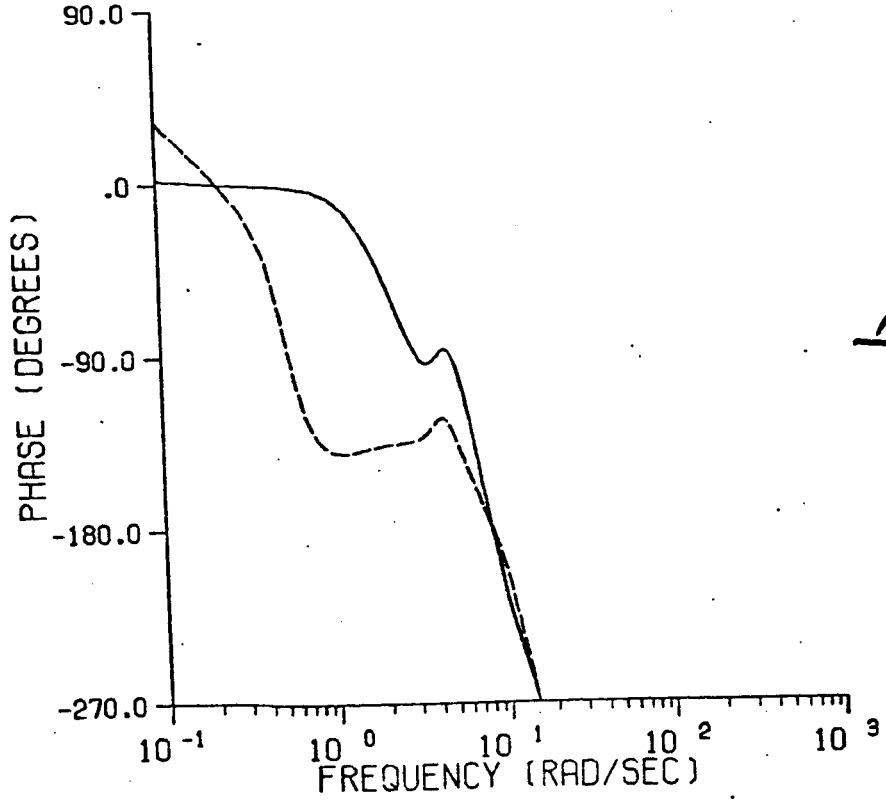

Fig. 22

CONFIGURATION 7-1R GAMMA TRACKING

GAMMA TO GAMMA COMMAND AT C.P.

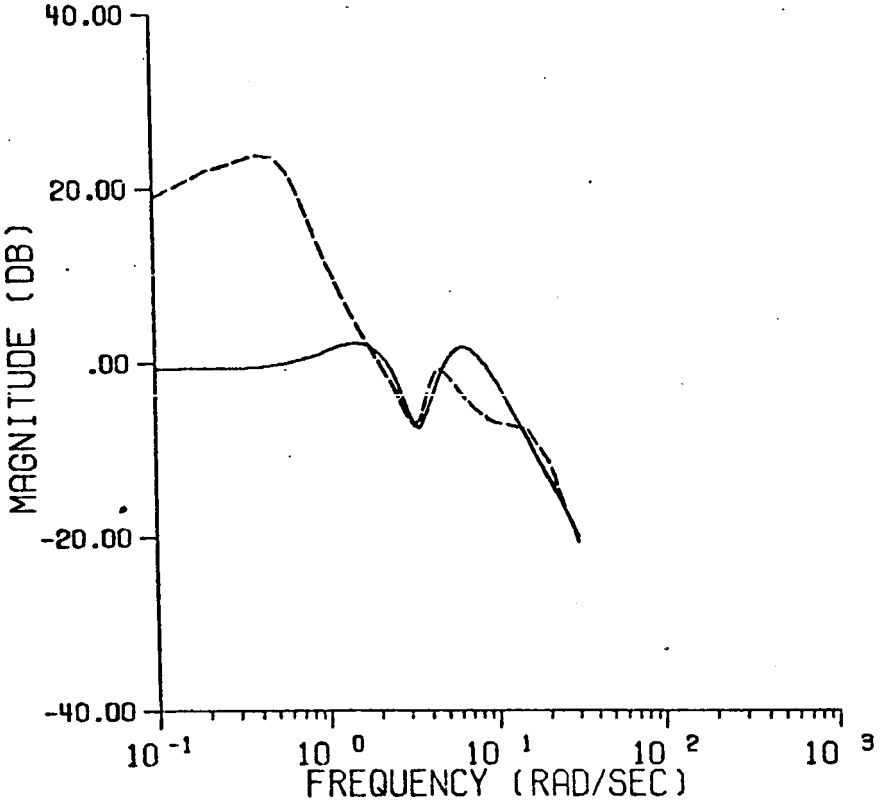

CLOSED LOOP RESPONSE
OPEN LOOP RESPONSE

POR: 3/2.5

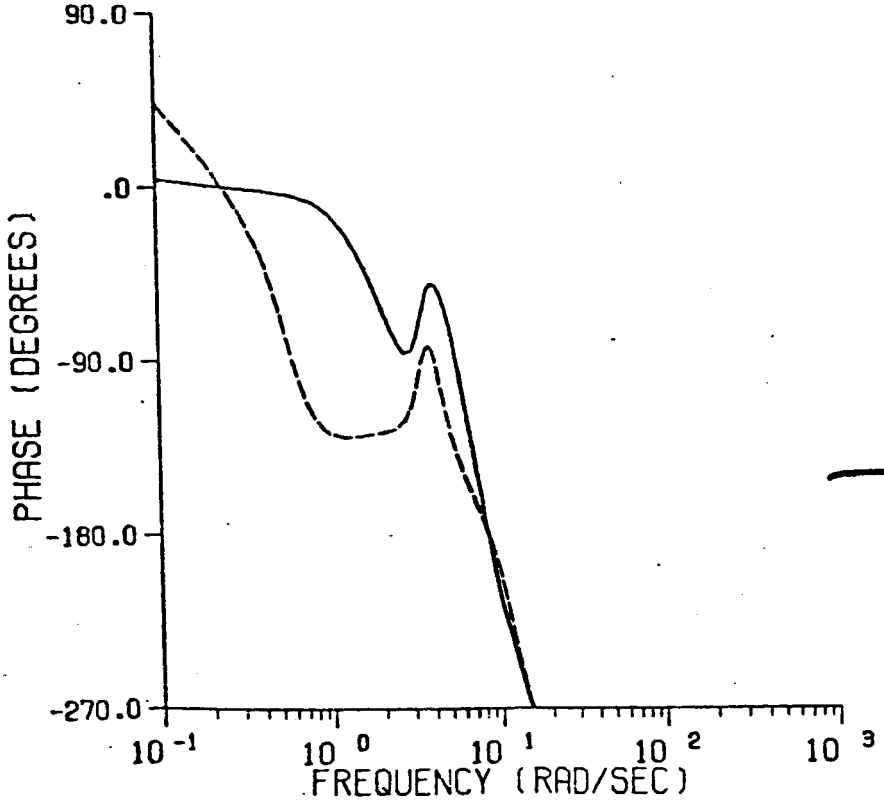

Fig. 23

COMPLEX CONTROL OBJECTIVE

BLOCK DIAGRAMS

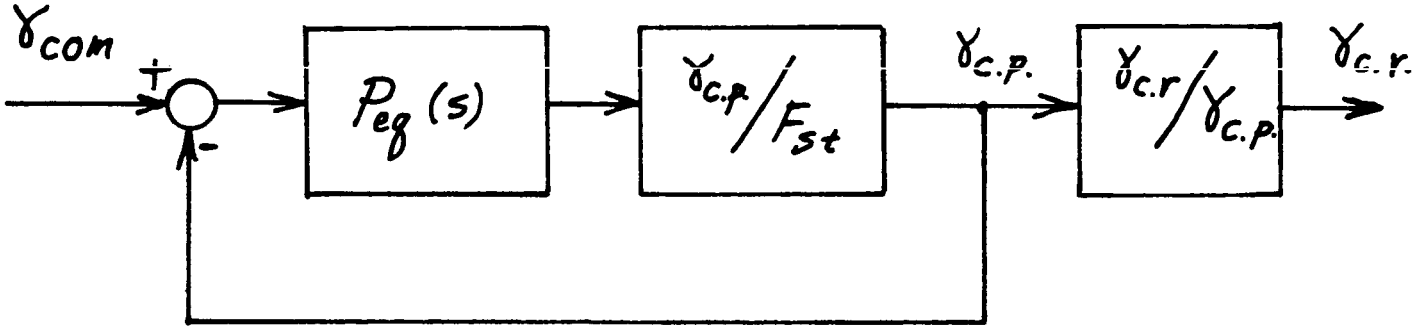

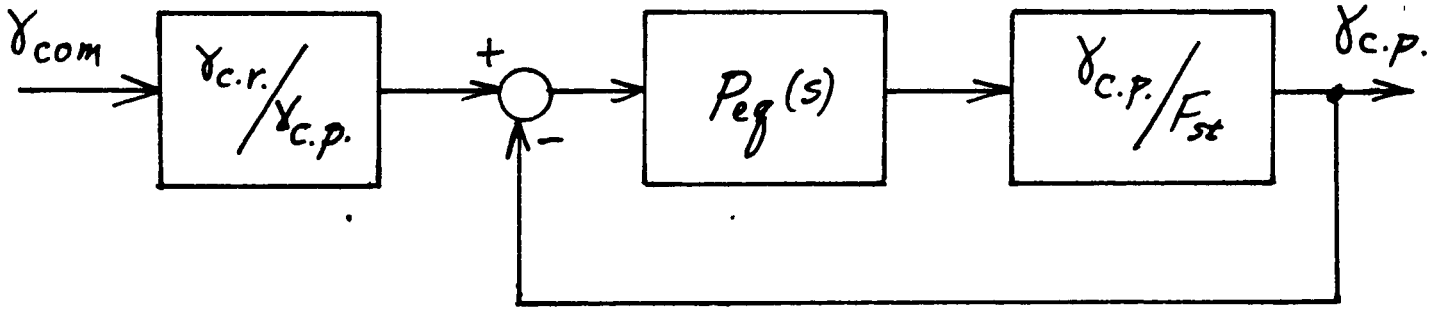

Fig. 24

OC/FD $\gamma_{c.p.} - \gamma_{c.r.}$ FLIGHT PATH ANALYSIS - TIFS Data

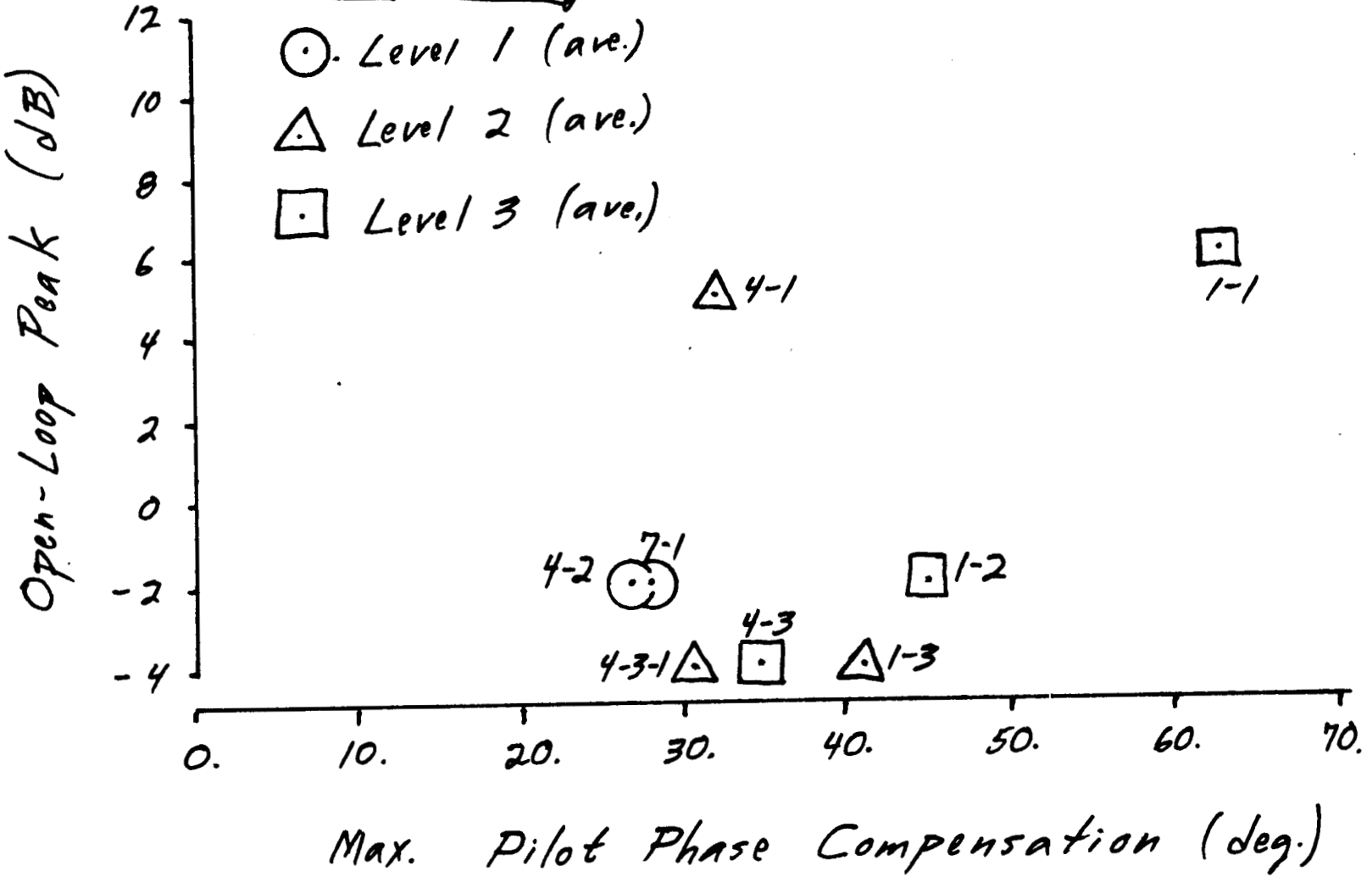

Fig. 25

APPENDIX A

CLOSED-LOOP, PILOT/VEHICLE ANALYSIS OF THE APPROACH AND LANDING TASK

by

Mark R. Anderson* and David K. Schmidt†

School of Aeronautics and Astronautics
Purdue University
West Lafayette, IN 47906

Extended Abstract

Recently, Bacon and Schmidt[1] presented an integrated optimal-control, frequency-domain approach for pilot/vehicle analysis of the precision attitude control task. When applied to the flight test results of Neal and Smith[2], the optimal control approach was shown, not only to agree extremely well with the original technique developed by Neal and Smith, but also to yield additional information on the achieveable closed-loop bandwidth in the task. This task was essentially modeled as a single-input, single-output, closed-loop task.

In the case of approach and landing, however, it is universally accepted that the pilot uses more than one vehicle response, or output, to close his control loops. Therefore, to model this task, a multi-loop analysis technique is required. The analysis problem has been in obtaining reasonable analytic estimates of the describing functions representing the pilot's loop compensation. Once these pilot describing functions are obtained, appropriate performance and workload metrics must then be developed for the landing task.

The optimal control approach[1,3] provides a powerful technique for obtaining the necessary describing functions, once the appropriate task objective is defined in terms of a quadratic objective function. In this paper, we will present such an approach through the use of a simple, reasonable

---

* Graduate Student.
† Professor, Associate Fellow, AIAA.

objective function and model-based metrics to evaluate loop performance and pilot workload. We will also present the results of an analysis of the LAHOS (Landing and Approach of Higher Order Systems) study performed by R.E. Smith[4].

In flare or near touchdown, precision flight-path control is required. Assuming a "frontside" landing technique is used, the pilot can control flight path or sink rate through elevator commands. Including inner pitch-attitude and flight-path-angle feedback loops, this situation leads to a block diagram of the approach and landing task shown in Figure (1). A reasonable task objective function, J_p, would then reflect the pilot's desire to minimize flight-path error, γ_{error}, by using pitch-attitude, flight-path, and flight-path-error information.

The pilot describing functions, $P_{(\cdot)}$, shown in the closed-loop structure of Figure (1) can then be obtained using the optimal-control approach. These describing functions represent those required to achieve the best loop performance, subject to the task definition and inherent pilot limitations modeled. Once determined, they can also be manipulated using block diagram algebra to obtain, for example, an equivalent unity feedback single-loop structure shown in Figure (2).

Neal and Smith, as well as Bacon and Schmidt, described the pilot/vehicle handling-quality criteria problem as a trade-off between the pilot workload required to achieve acceptable task performance and a subsequent measure of the pilot/vehicle closed-loop performance. The most important aspect of closed-loop performance, furthermore, is stability and robustness (or insensitivity to small changes in pilot compensation). These loop characteristics are clearly reflected in the open-loop, γ/γ_{error}, frequency response. In fact, the desirable "shape" of this frequency response for good closed-loop stability is well-known (i.e. constant -20 dB/decade slope in the crossover region). Any deviation from the desirable frequency response is defined herein as a reduction in *loop quality*.

A model-based measure of the "loop quality" has been developed and is entitled the "open loop peak", obtainable from the open-loop frequency response plots after the pilot/vehicle system has been modeled. Also a model-based metric has been identified that reflects the pilot workload necessary to achieve closed-loop stability. This workload metric is expressed in terms of a pilot phase compensation angle.

When thirty-two of the aircraft configurations flight tested in the LAHOS study were modeled and analyzed, the results are as shown in Figure (3).

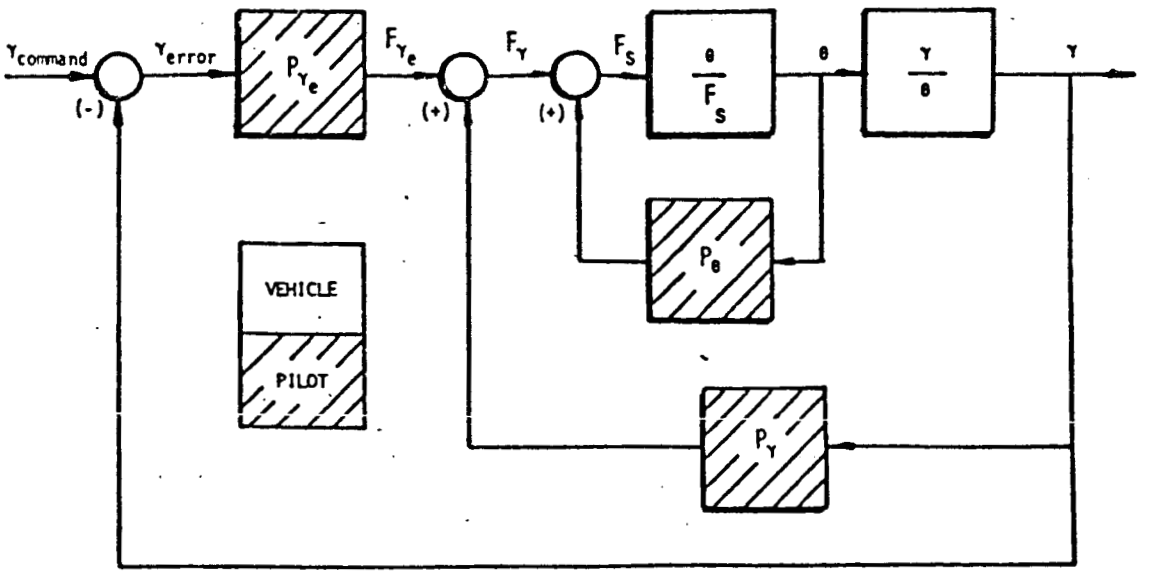

Figure 1 The Multi-Loop Flight Path Tracking Task

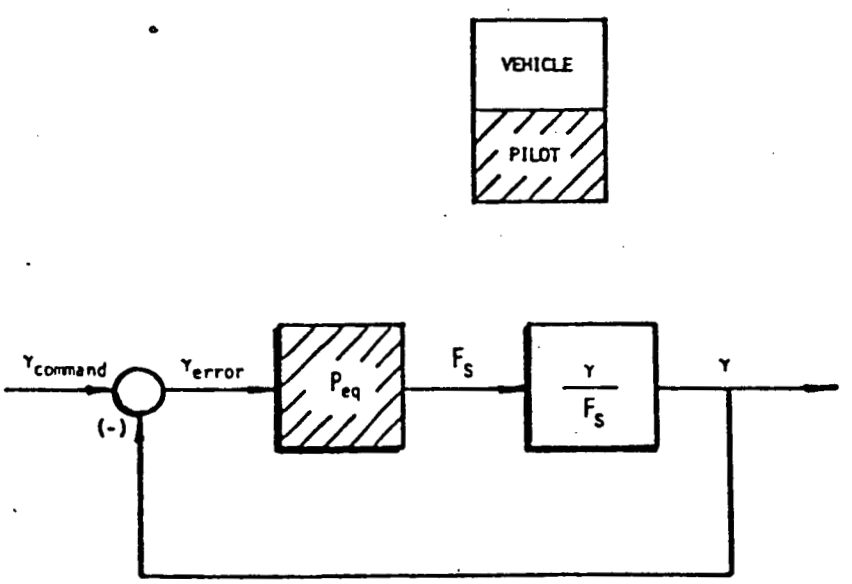

Figure 2 Flight Path Tracking with
Equivalent Pilot Function

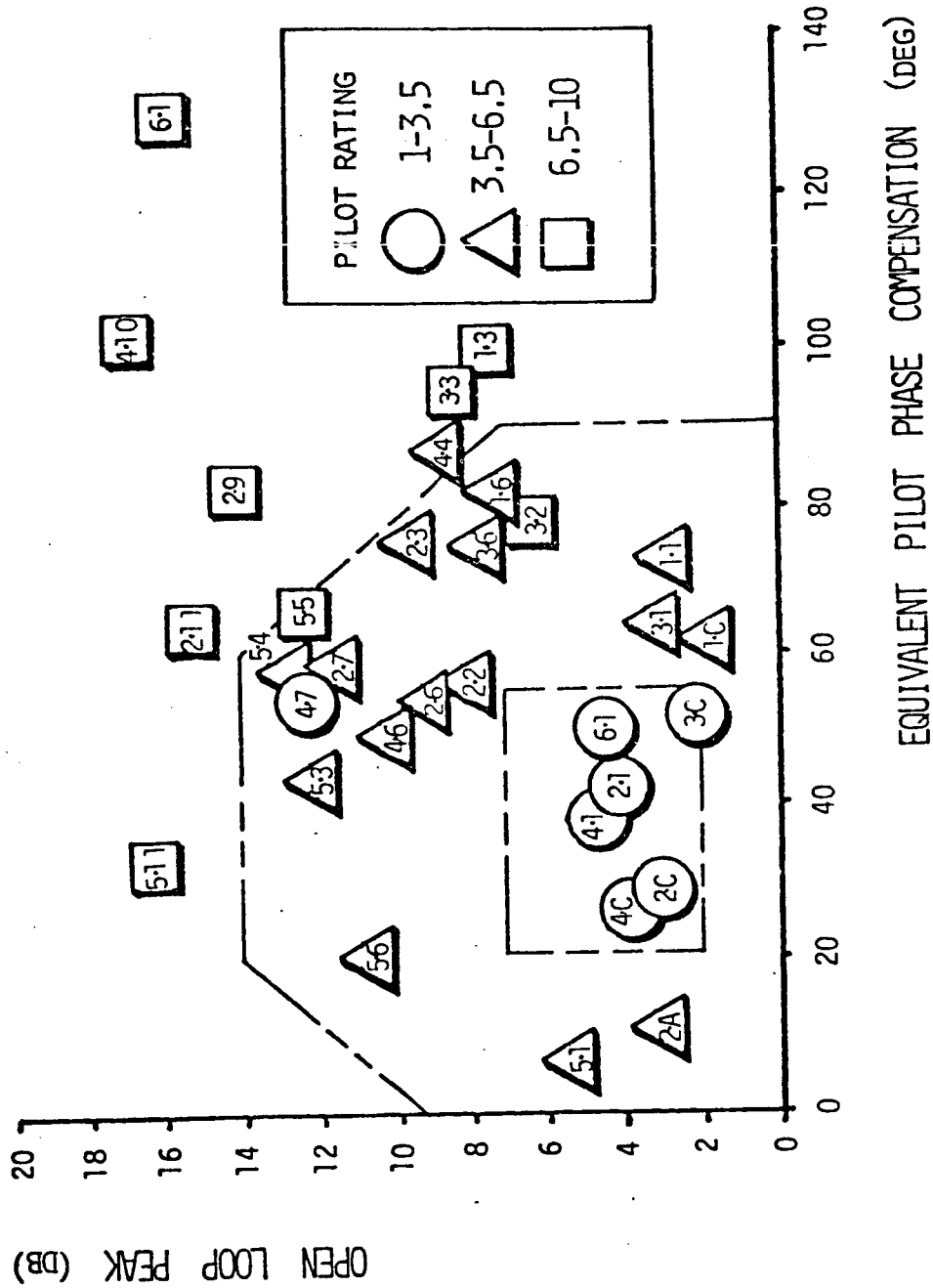

Figure 3 OCM Results for the Flight Path Tracking Task

Recalling that the " open-loop peak" is a measure of stability robustness, and the "pilot compensation" is a measure of workload, we see a characteristic grouping of the results not unlike that presented in References [1] and [2]. However, in these references, the task modeled was precision attitude control, and two different (though similar) model-based metrics were used in the related plots.

It is also noted from Figure (3), that those configurations rated best (level 1) in the *approach and landling task* were appropriately grouped together, in terms of "performance" and "workload". Those rated worse were the result of excessive pilot phase lead or lag conpensation required or a reduction in "loop quality". Other results concerning loop characteristics such as achieveable loop bandwidths, pilot comments, and pilot behavior will be presented in the complete paper.

Acknowledgement

This work has been sponsered by the NASA Dryden Flight Research Facility/Ames Research Center under Grant No. NAG4-1. Mr. Donald T. Berry is the technical monitor. This support is greatly appreciated.

References

[1] Bacon, B.J. and Schmidt, D.K., "An Optimal Control Approach to Pilot/Vehicle Analysis and the Neal-Smith Criteria", *Journal of Guidance, Control, and Dynamics*, Vol. 6, No. 5, Sept-Oct., 1983, pp. 339-347.

[2] Neal, T.P. and Smith, R.E., *An In-Flight Investigation to Develop Control System Design Criteria for Fighter Airplanes.* AFFDL-TR-70-74, Vol. I, December, 1970.

[3] Kleinman, D.L., Baron, S., and Levison, W.H., "An Optimal Control Model of Human Response Part I: Theory and Validation", *Automatica*, Vol. 6, 1970, pp. 357-369.

[4] Smith, R.E., *Effects of Control System Dynamics on Fighter Approach and Landing Longitudinal Flying Qualities*, AFFDL-TR-78-122, Vol. 1, March, 1978.

APPENDIX B

Theta Tracking Results

CONFIGURATION 1-1U THETA TRACKING

PILOT TRANSFER FUNCTIONS

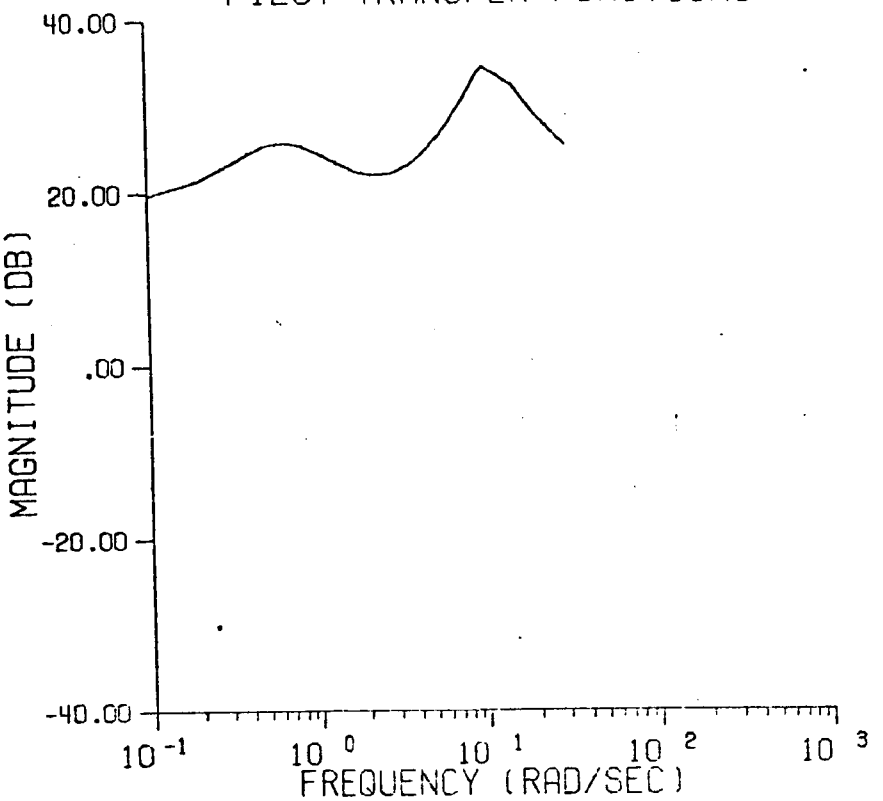

PILOT RESPONSE TO THETA ERROR

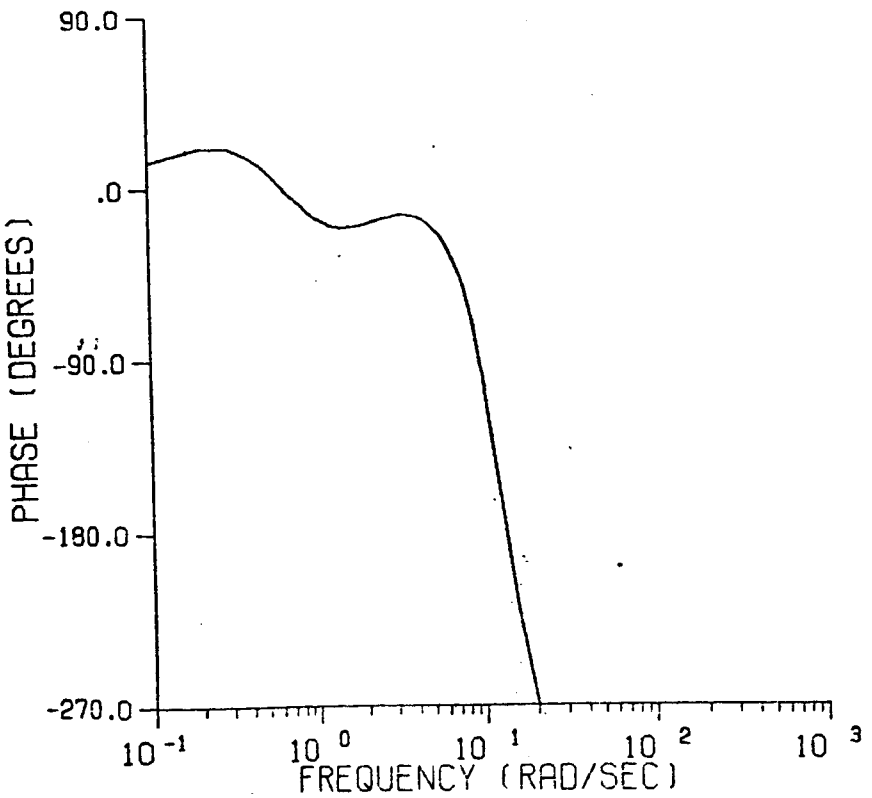

CONFIGURATION 1-1U THETA TRACKING

THETA TO THETA COMMAND

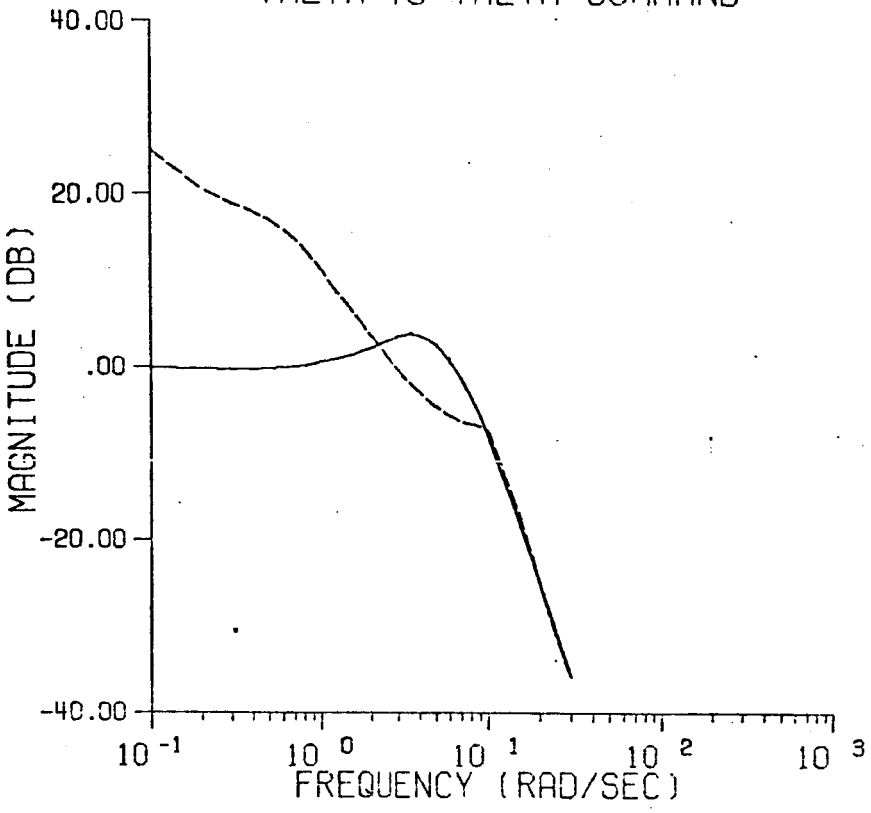

CLOSED LOOP

OPEN LOOP

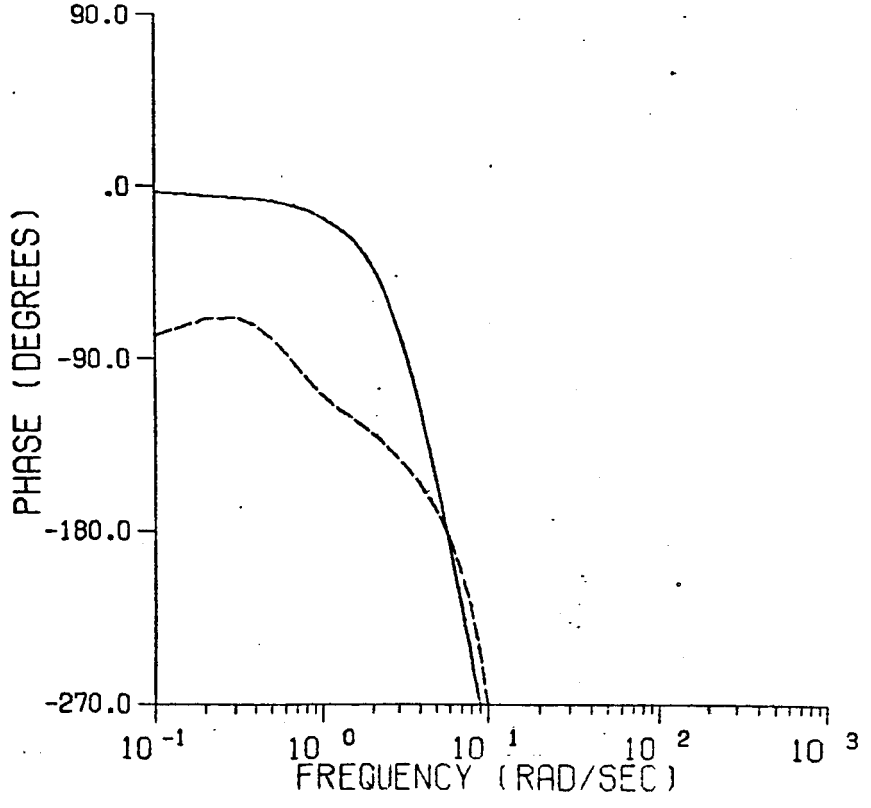

CONFIGURATION 4-1U THETA TRACKING

PILOT TRANSFER FUNCTIONS

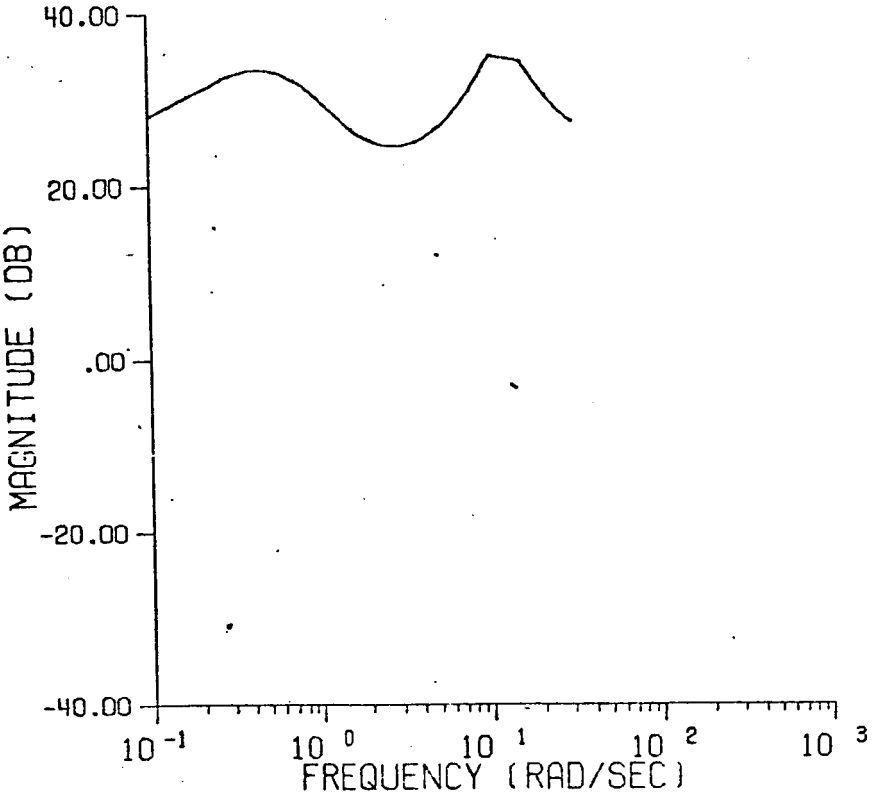

PILOT RESPONSE TO THETA ERROR

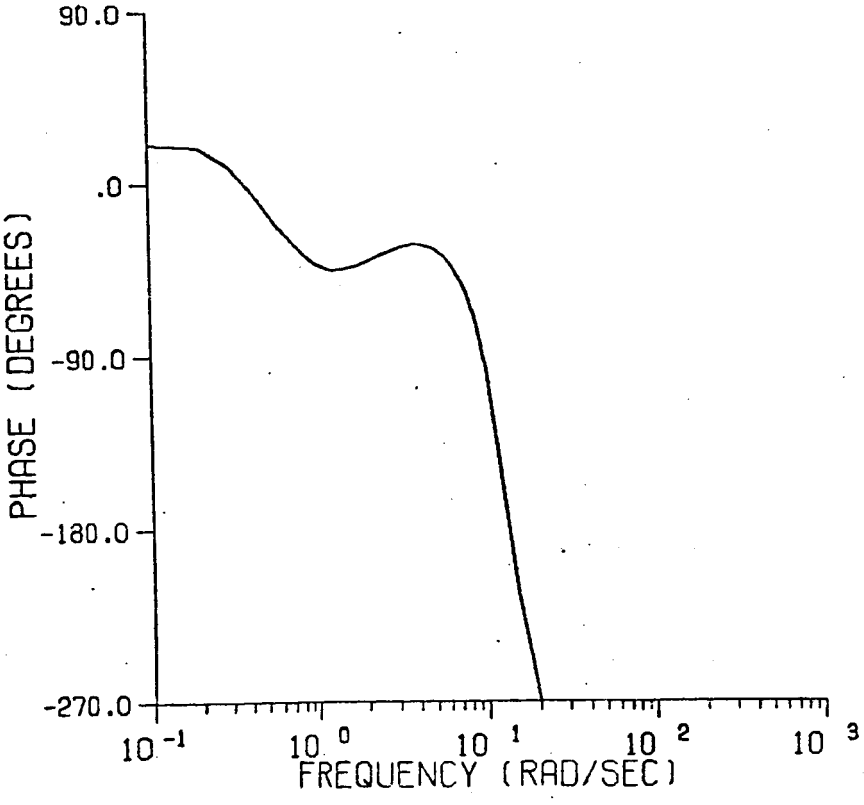

CONFIGURATION 4-1U THETA TRACKING

THETA TO THETA COMMAND

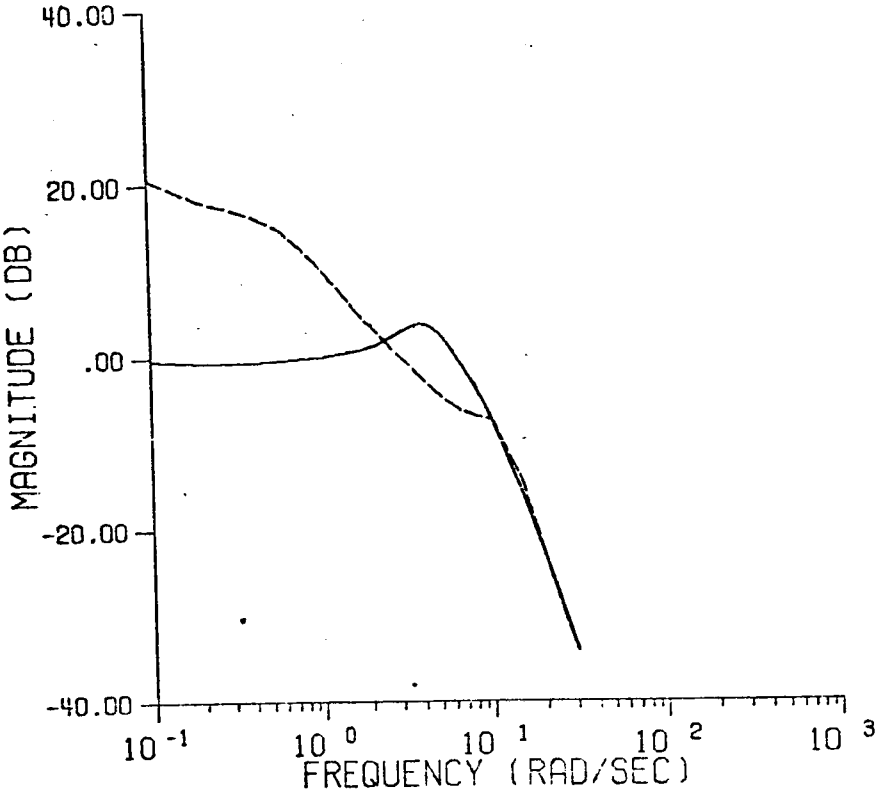

CLOSED LOOP

OPEN LOOP

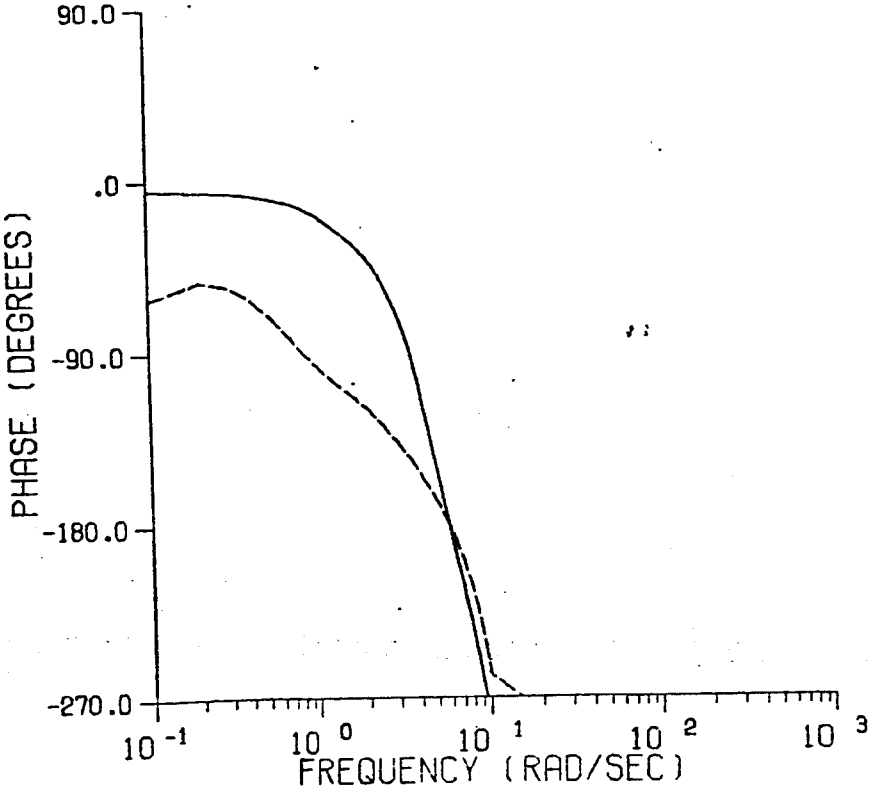

CONFIGURATION 1-2U THETA TRACKING

PILOT TRANSFER FUNCTIONS

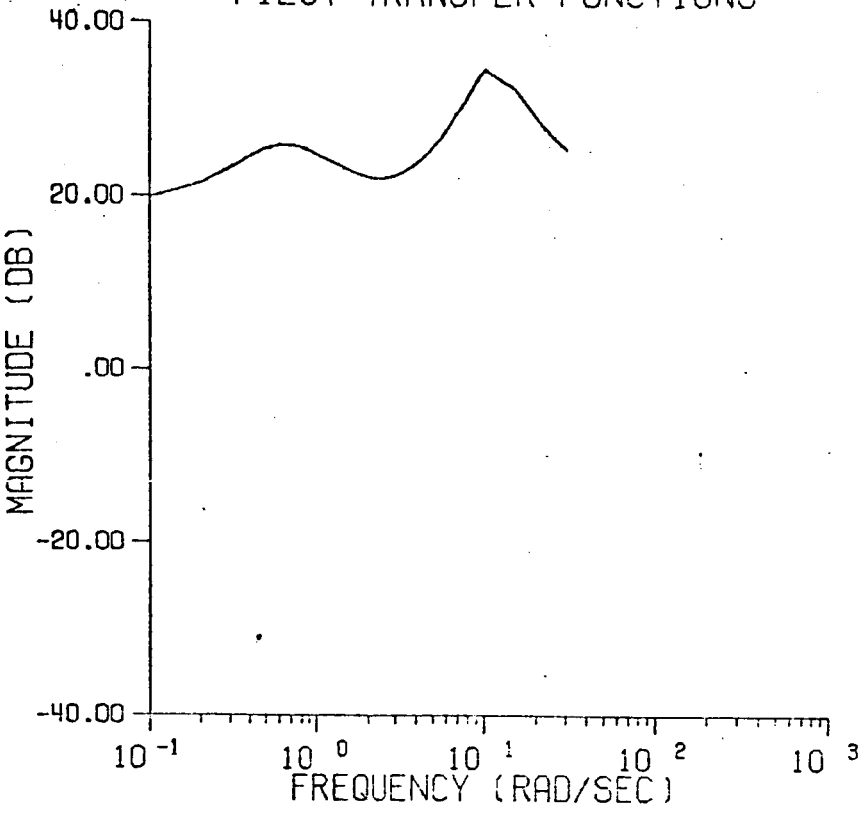

PILOT RESPONSE TO THETA ERROR

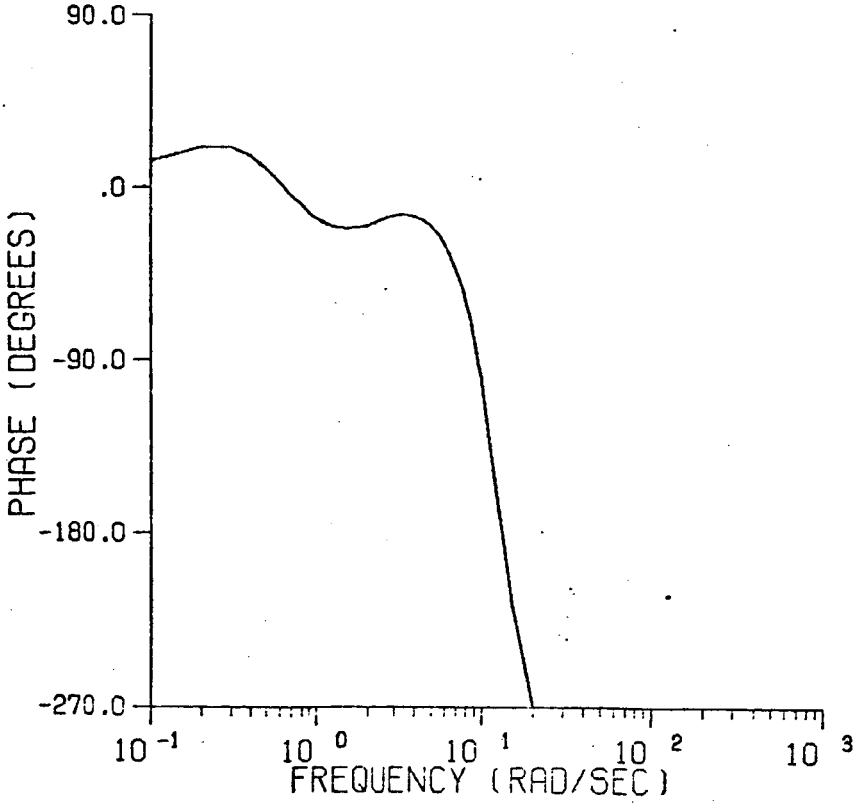

CONFIGURATION 1-2U THETA TRACKING

THETA TO THETA COMMAND

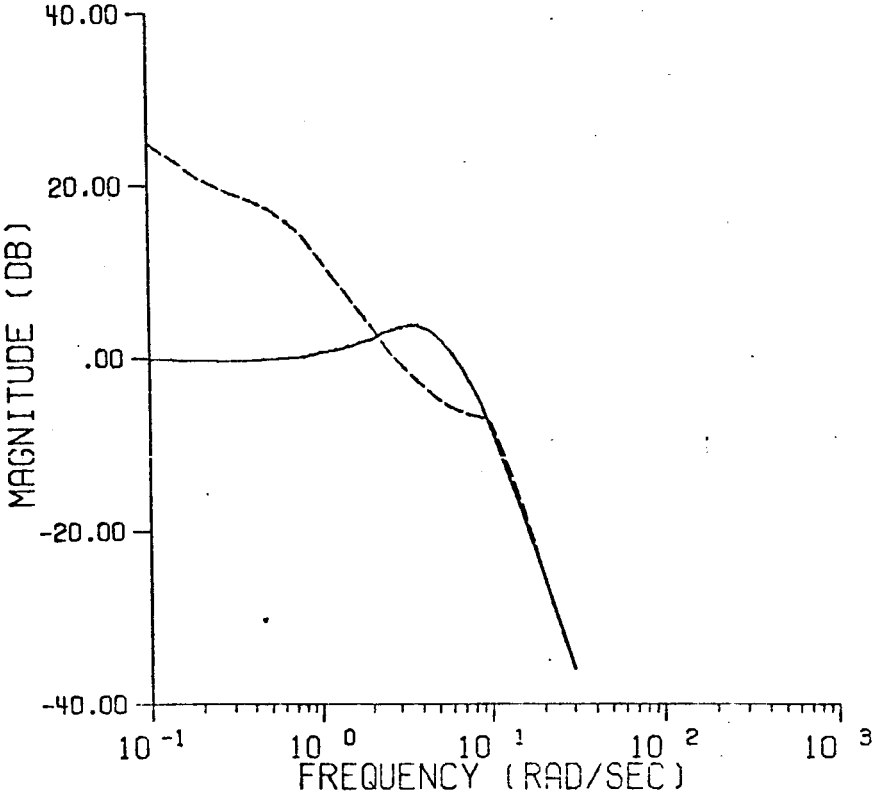

CLOSED LOOP

OPEN LOOP

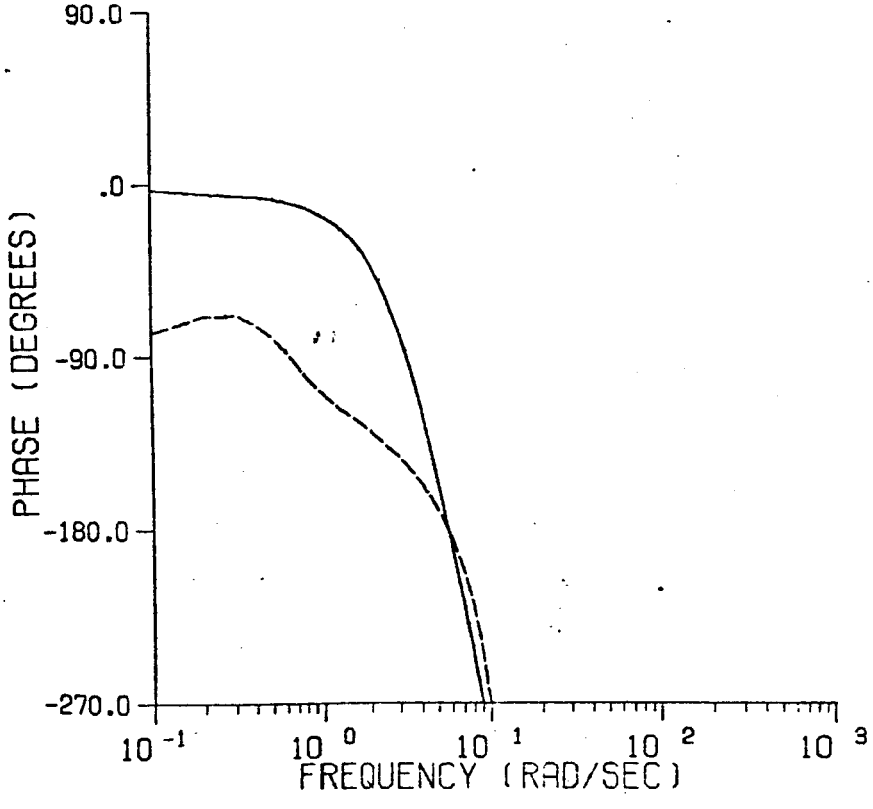

CONFIGURATION 4-2U THETA TRACKING

PILOT TRANSFER FUNCTIONS

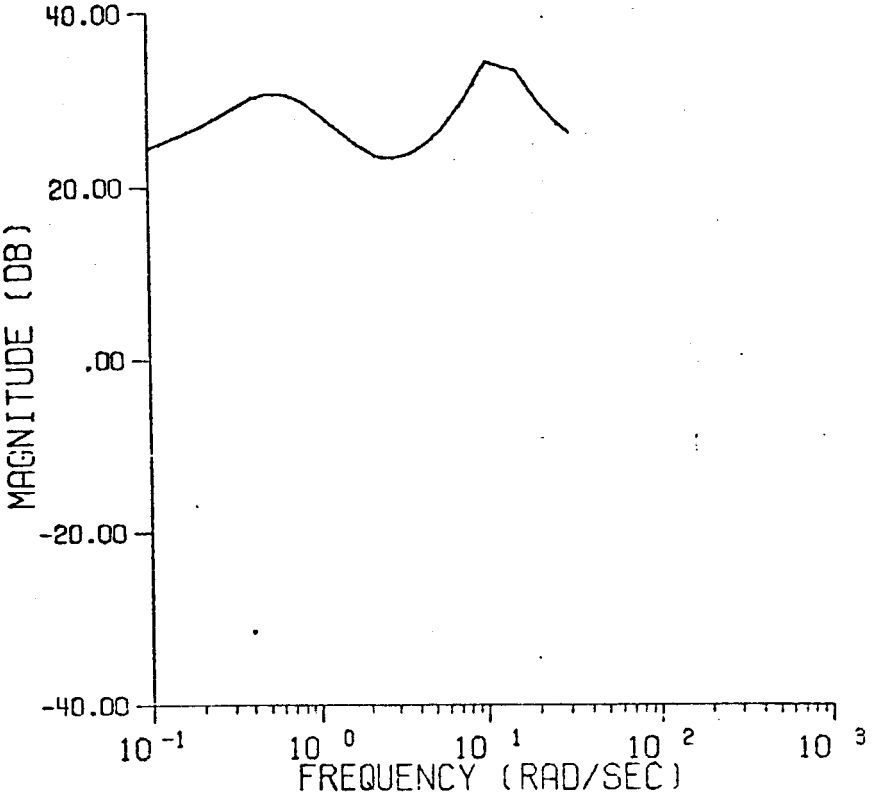

PILOT RESPONSE TO THETA ERROR

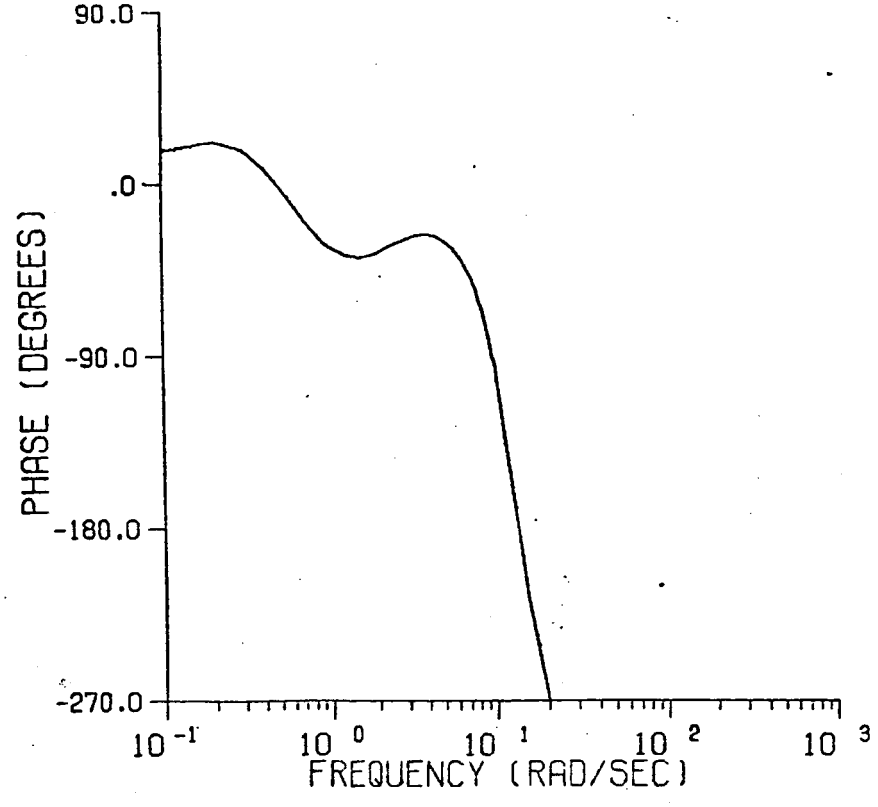

CONFIGURATION 4-2U THETA TRACKING

THETA TO THETA COMMAND

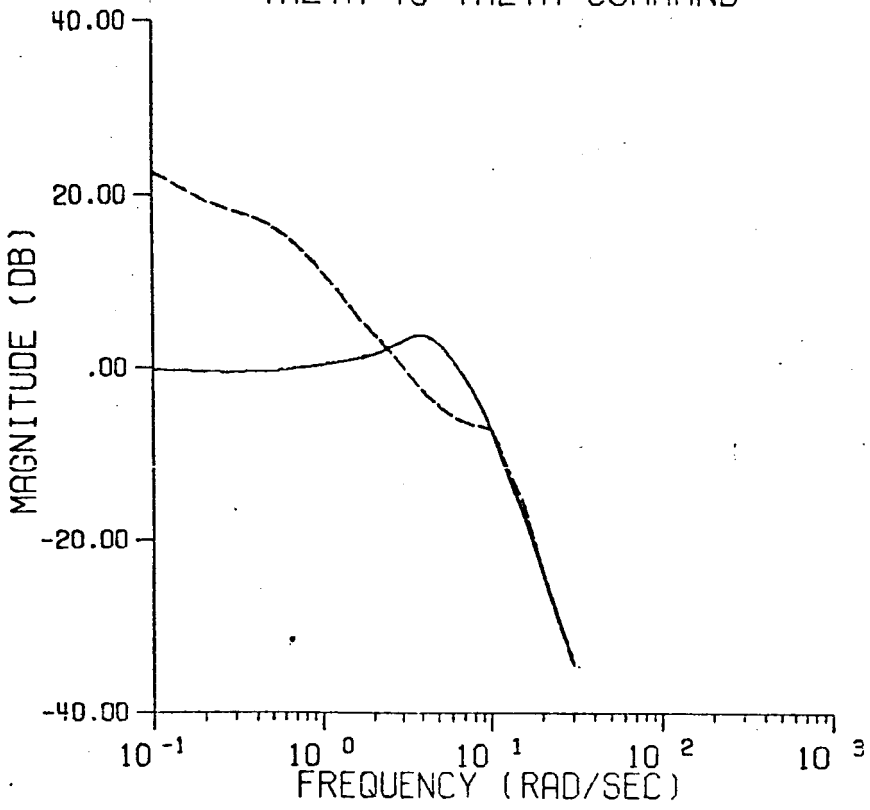

CLOSED LOOP

OPEN LOOP

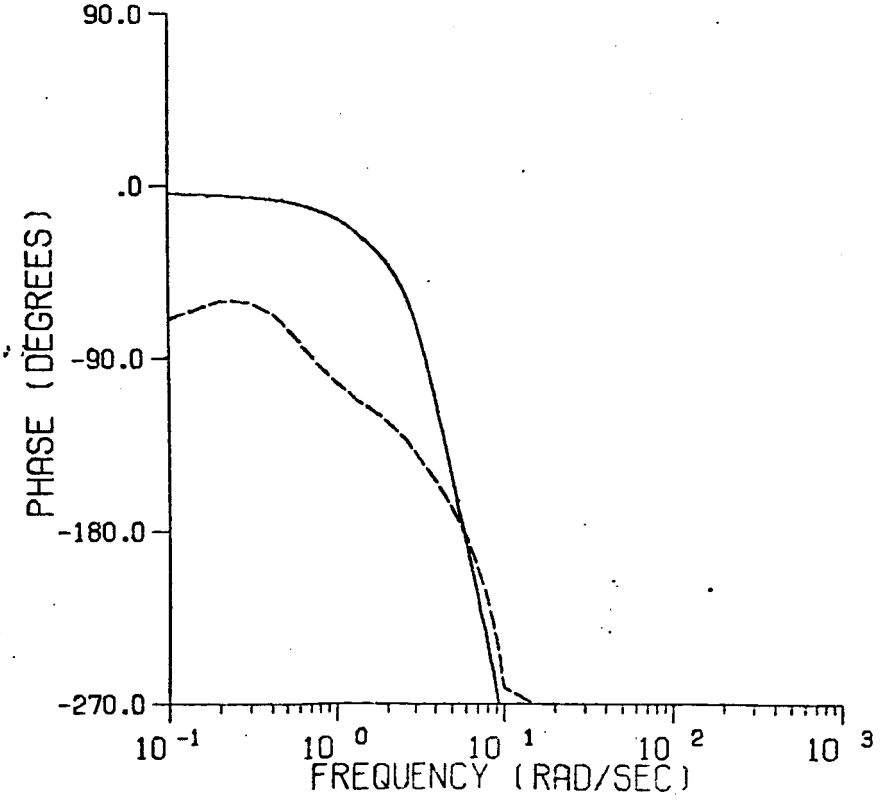

CONFIGURATION 1-3U THETA TRACKING

PILOT TRANSFER FUNCTIONS

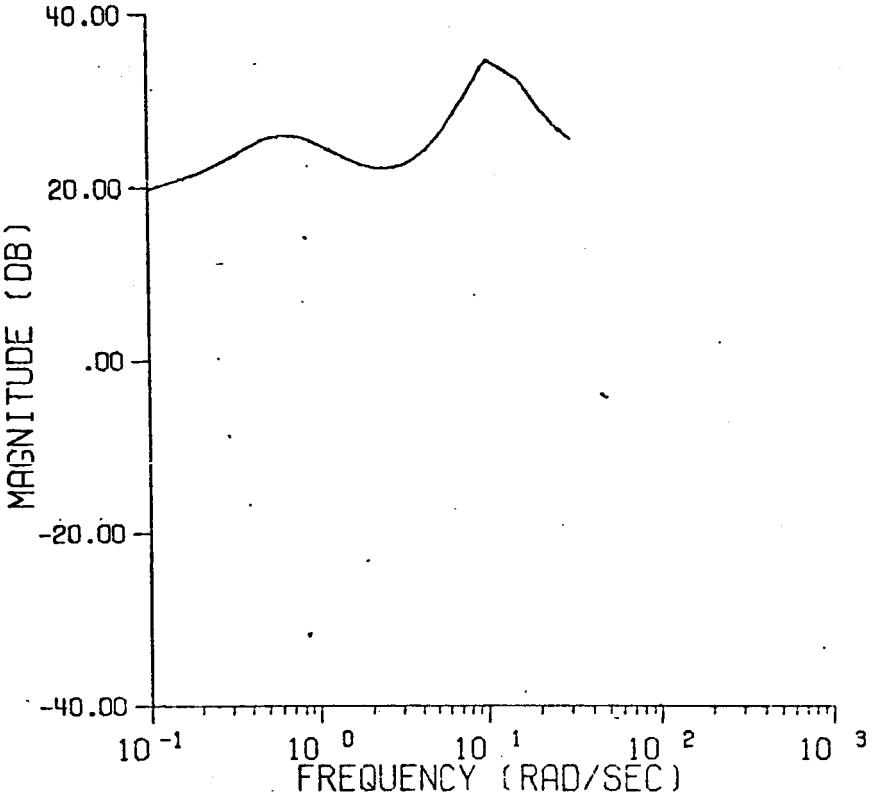

PILOT RESPONSE TO THETA ERROR

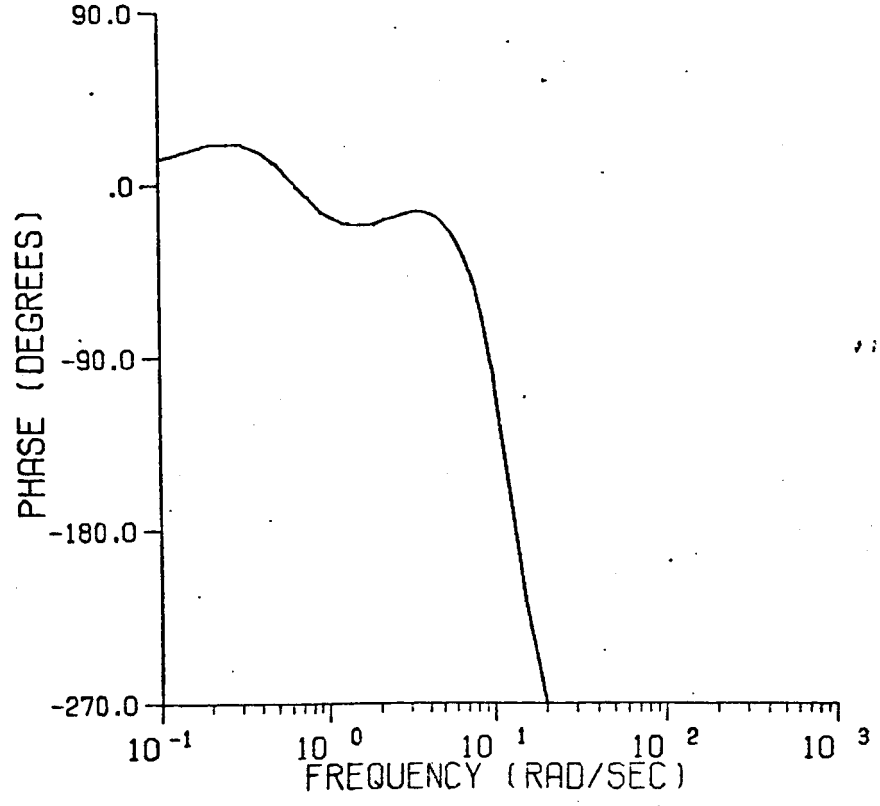

CONFIGURATION 1-3U THETA TRACKING

THETA TO THETA COMMAND

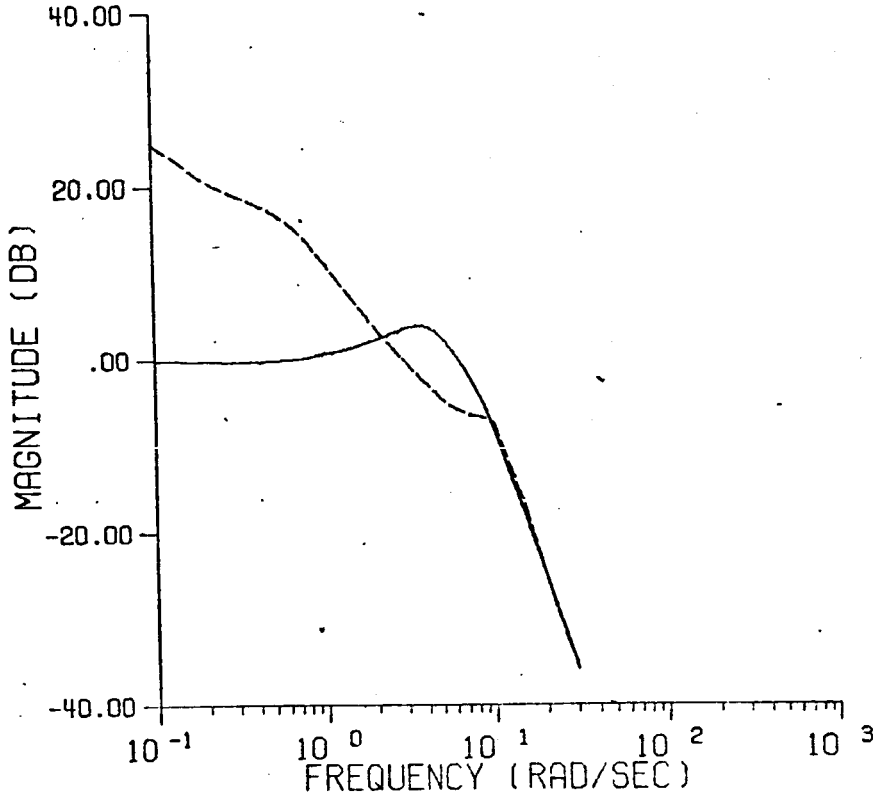

CLOSED LOOP

OPEN LOOP

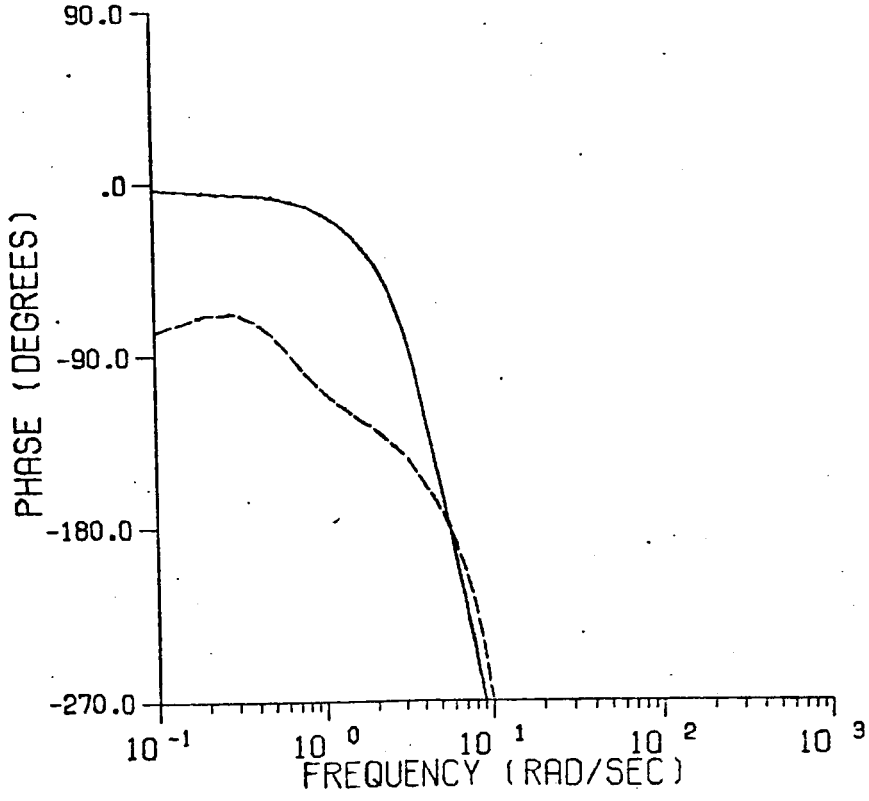

CONFIGURATION 4-3U THETA TRACKING

PILOT TRANSFER FUNCTIONS

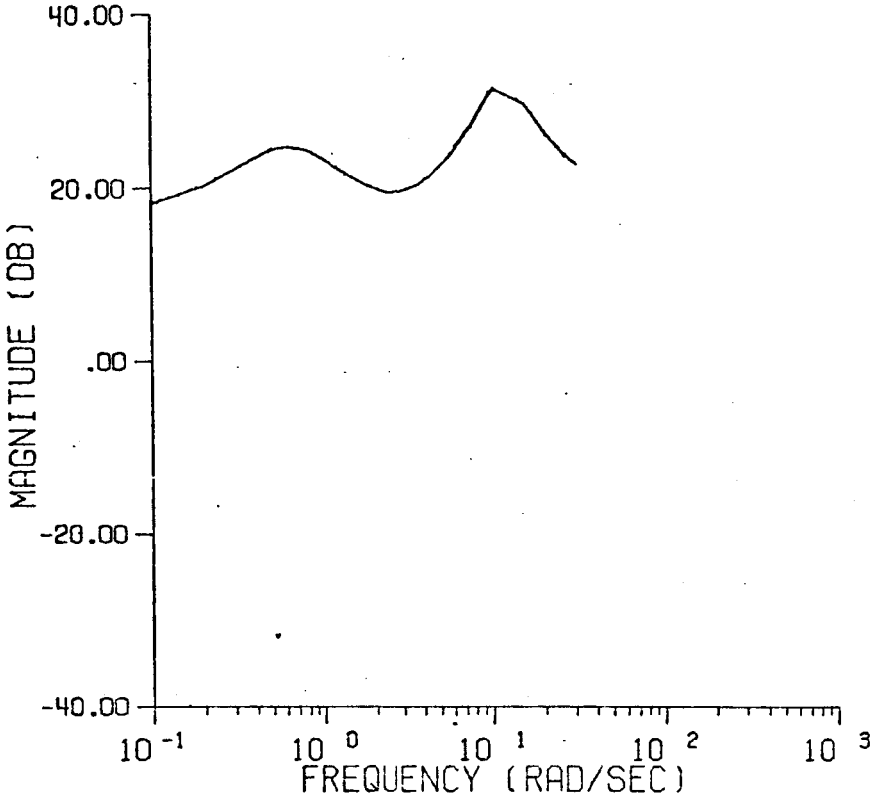

PILOT RESPONSE TO THETA ERROR

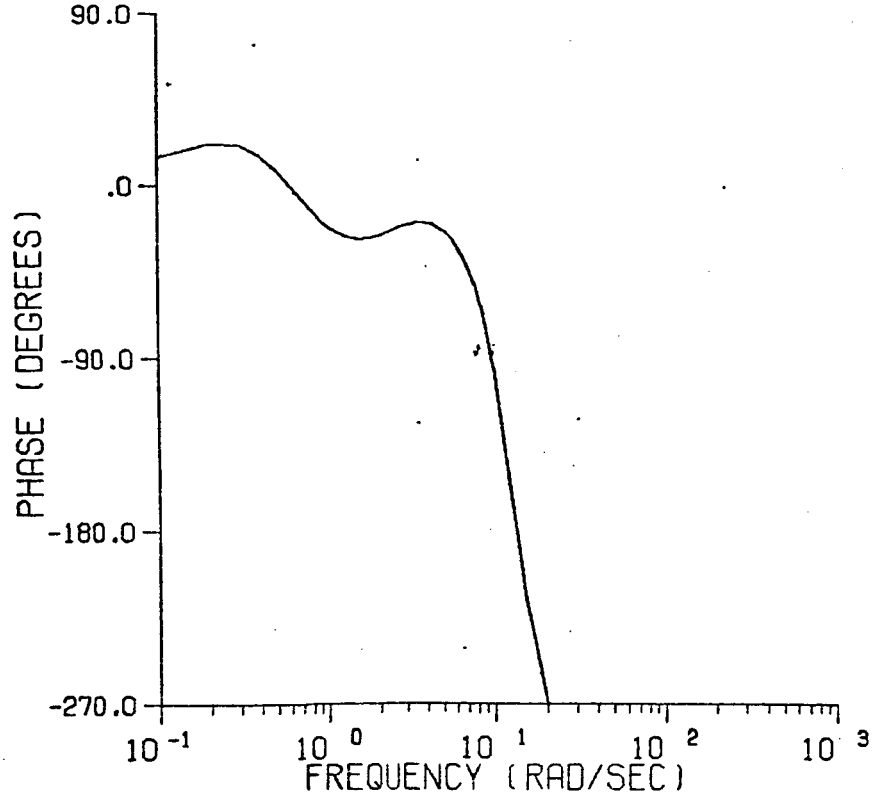

CONFIGURATION 4-3U THETA TRACKING

THETA TO THETA COMMAND

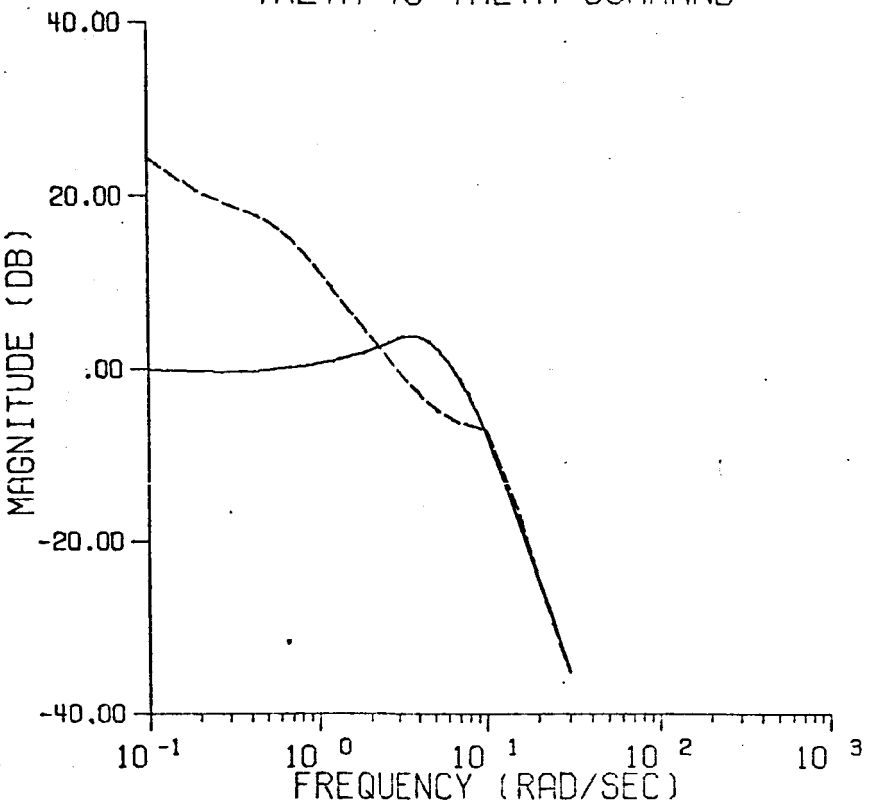

CLOSED LOOP
OPEN LOOP

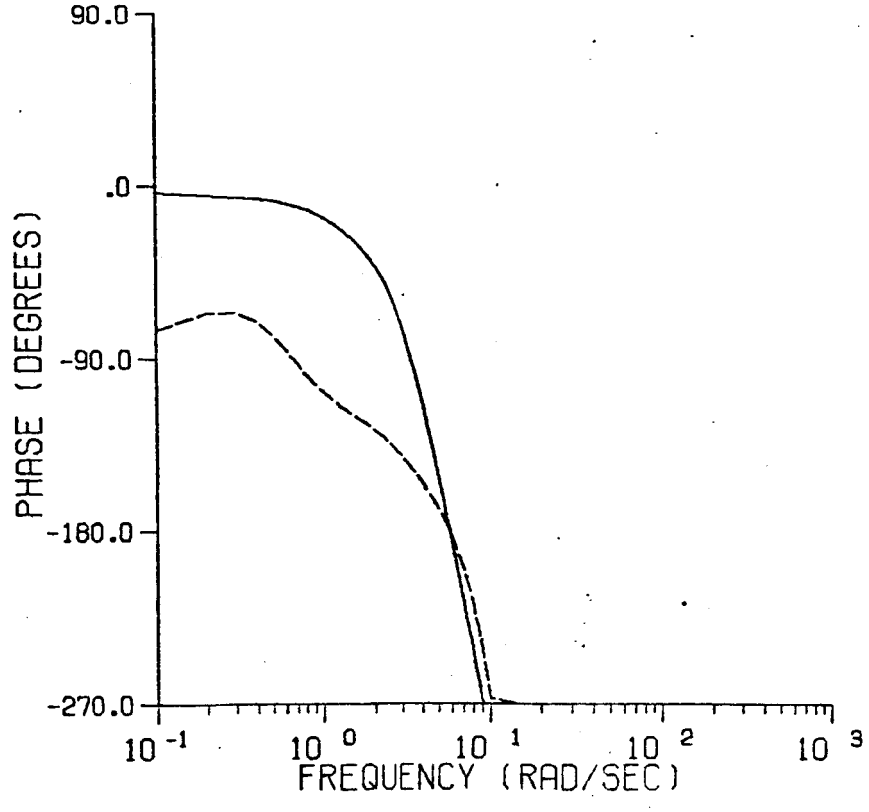

CONFIGURATION 4-3-1U THETA TRACKING

PILOT TRANSFER FUNCTIONS

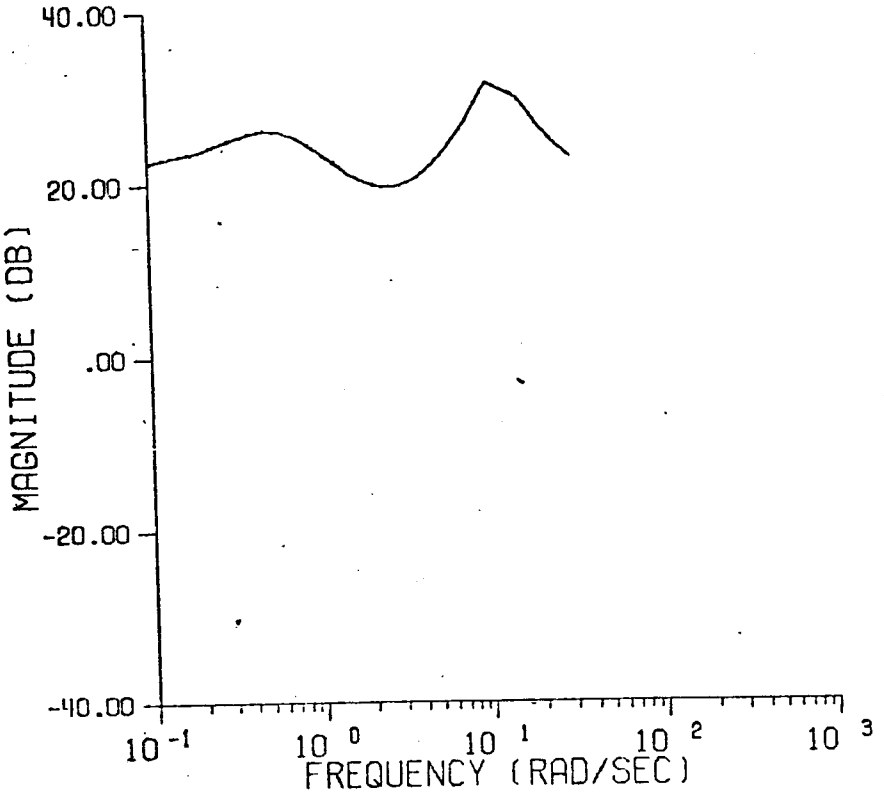

PILOT RESPONSE TO THETA ERROR

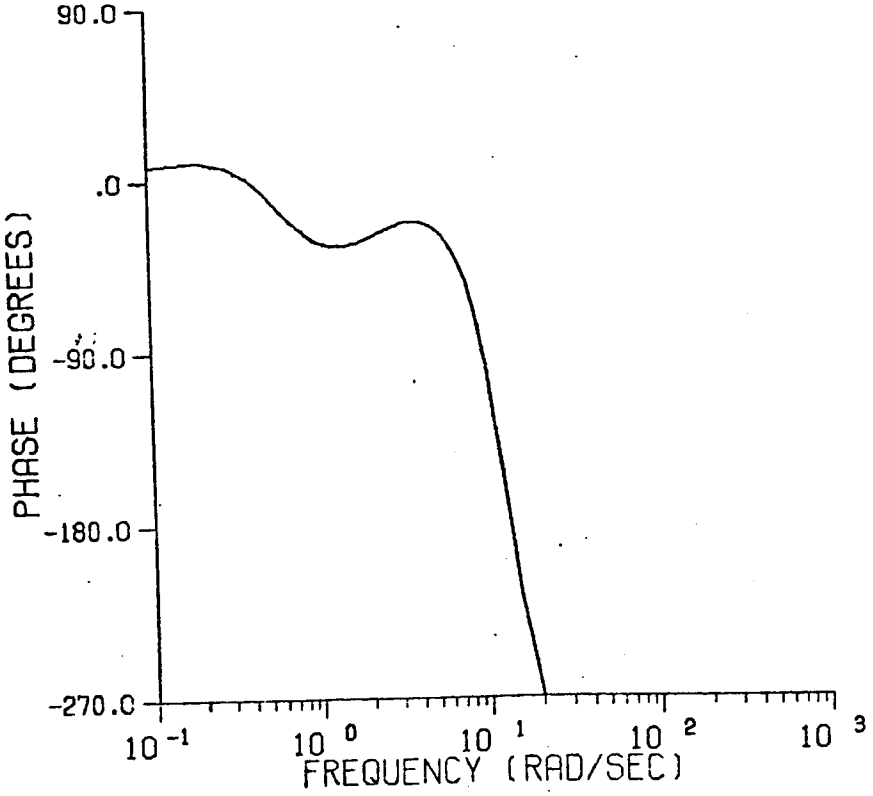

CONFIGURATION 4-3-1U THETA TRACKING

THETA TO THETA COMMAND

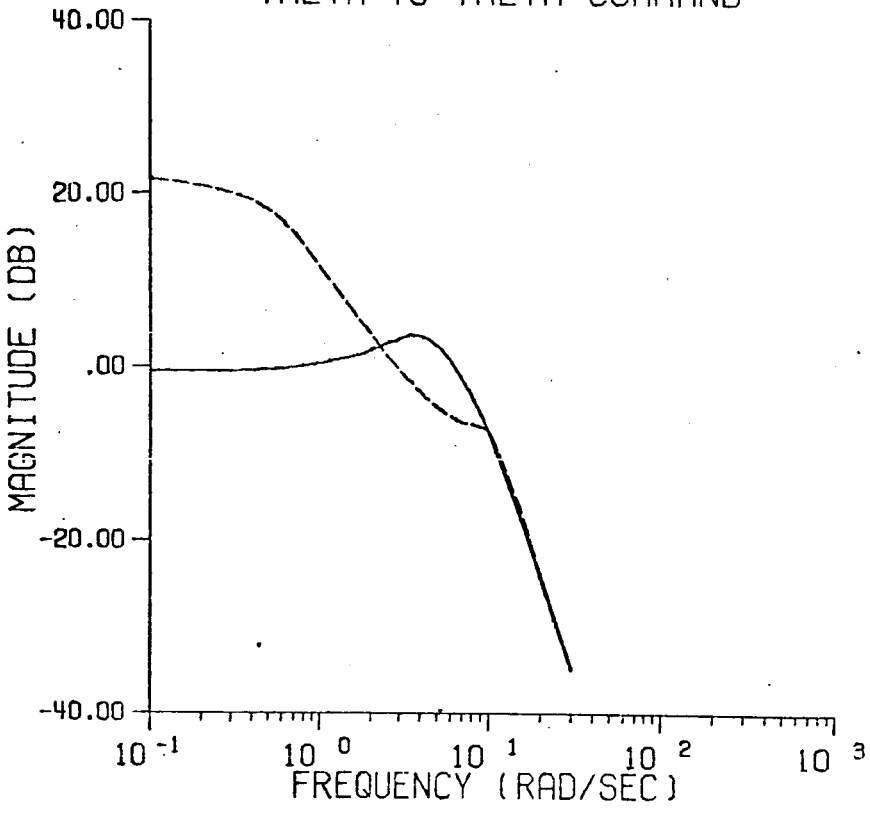

CLOSED LOOP
OPEN LOOP

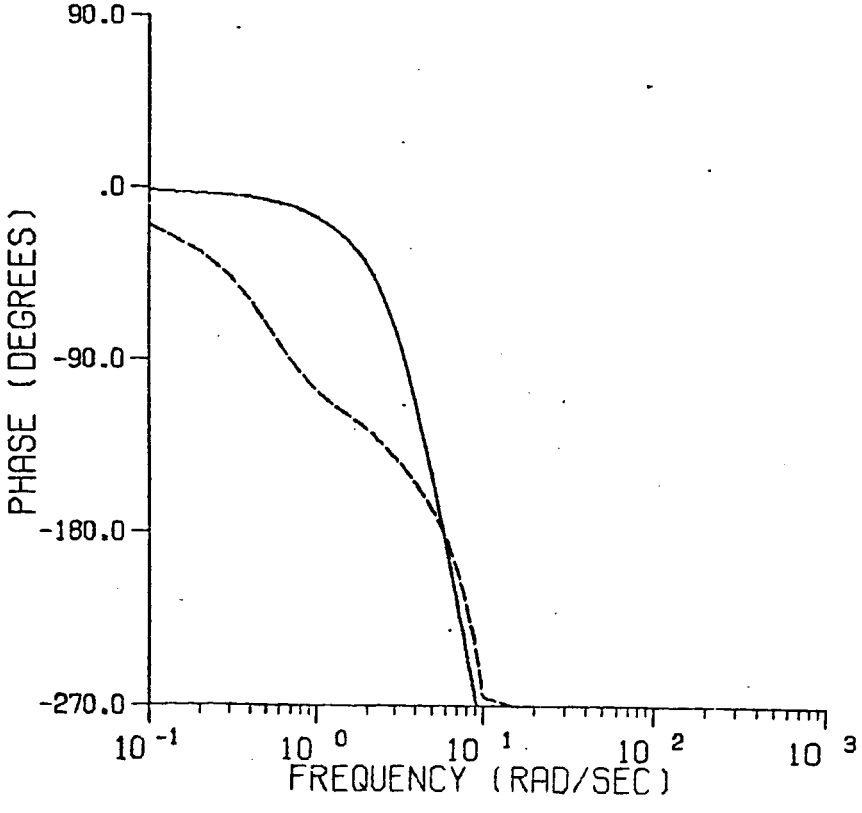

CONFIGURATION 7-1U THETA TRACKING

PILOT TRANSFER FUNCTIONS

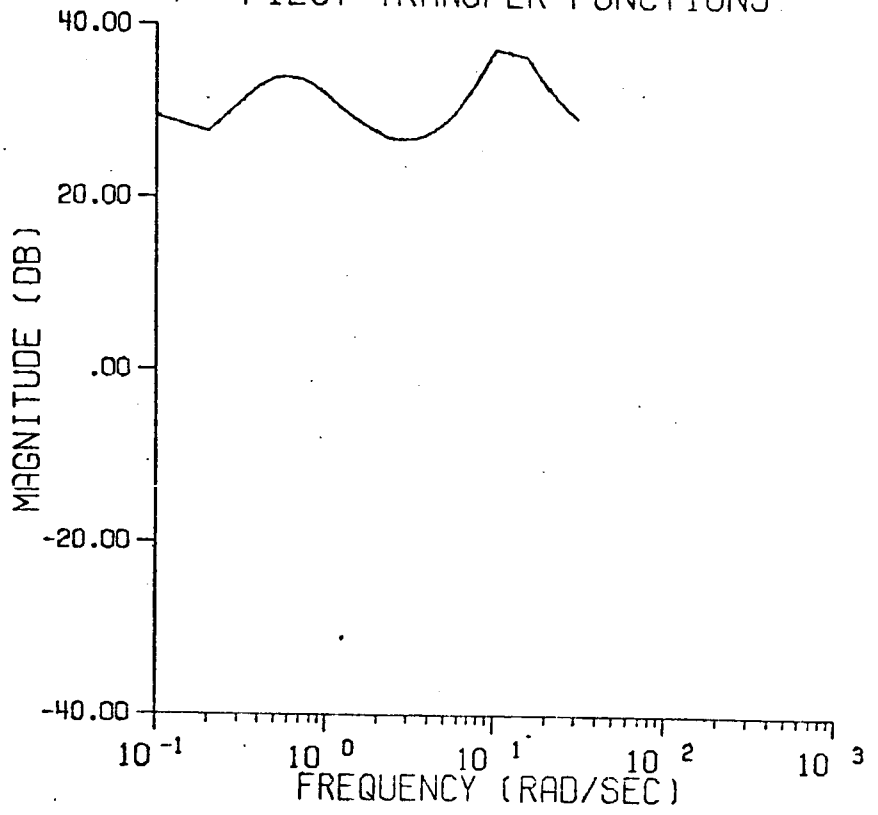

PILOT RESPONSE TO THETA ERROR

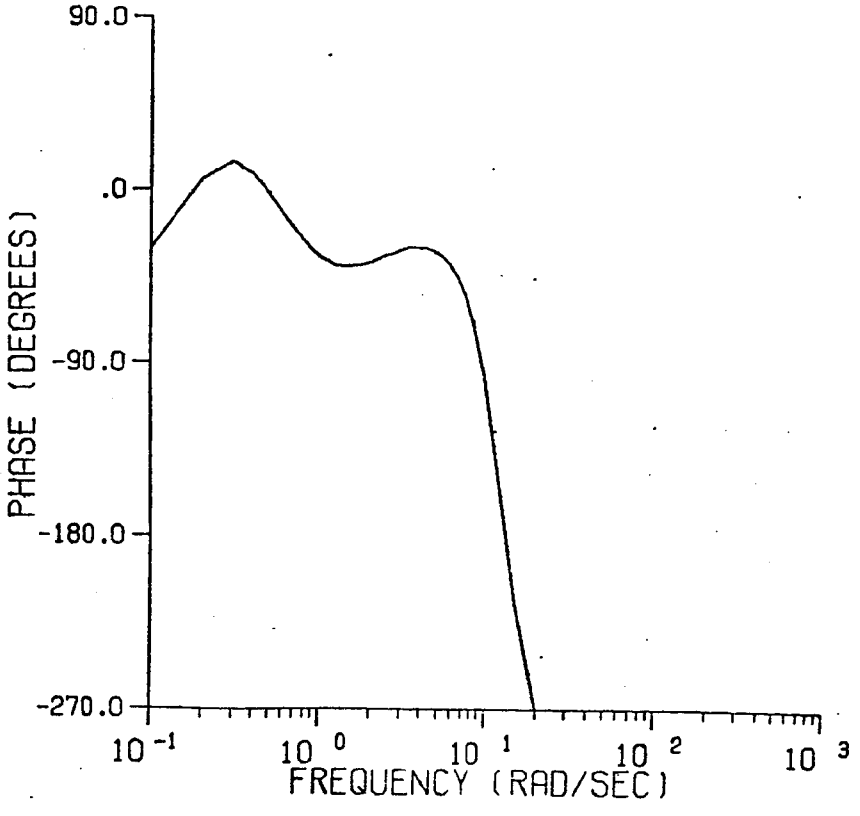

CONFIGURATION 7-1U THETA TRACKING

THETA TO THETA COMMAND

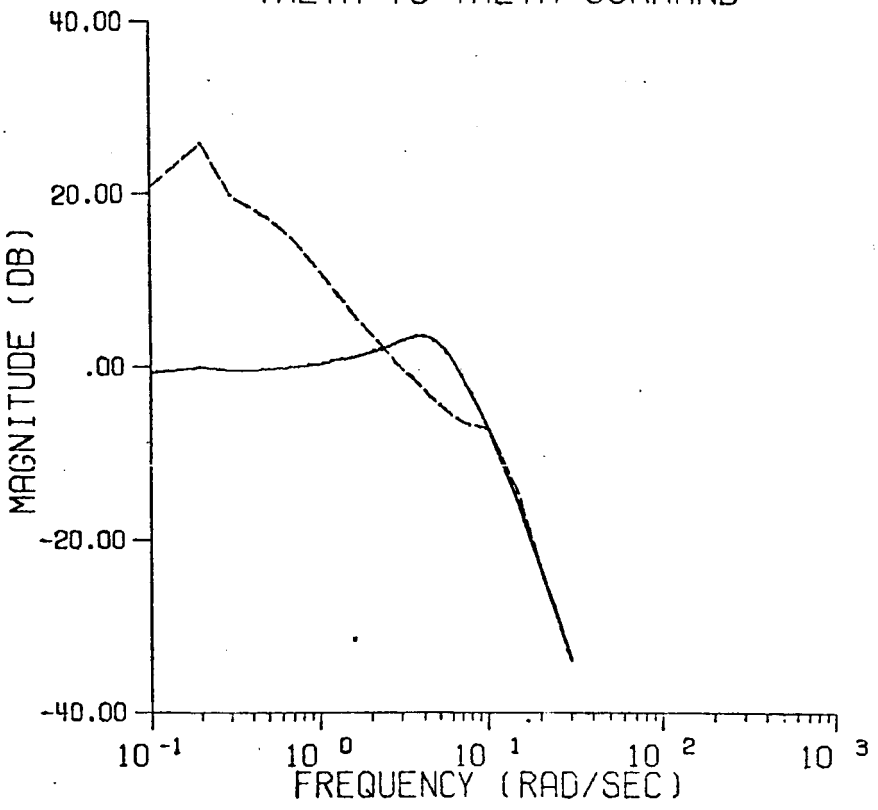

CLOSED LOOP

OPEN LOOP